INVESTIGATION OF TIDAL STREAM ENERGY IN THE STRAITS OF MALACCA

CHANDRA BHUSHAN ROY

DISSERTATION SUBMITTED IN FULFILMENT OF THE REQUIREMENTS FOR THE DEGREE OF MASTER OF ENGINEERING SCIENCE

FACULTY OF ENGINEERING

UNIVERSITY OF MALAYA

KUALA LUMPUR

2016

UNIVERSITY OF MALAYA

ORIGINAL LITERARY WORK DECLARATION

Name of Candidate: Chandra Bhushan Roy

Registration/Matric No: KGA 120084

Name of Degree: Master of Engineering Science (Dissertation)

Title of Dissertation ("this Work"): Investigation of Tidal Stream Energy in The Straits of Malacca.

Field of Study: Marine Renewable Energy.

I do solemnly and sincerely declare that:

(1) I am the sole author/writer of this Work;
(2) This Work is original;
(3) Any use of any work in which copyright exists was done by way of fair dealing and for permitted purposes and any excerpt or extract from or reference to or reproduction of any copyright work has been disclosed expressly and sufficiently and the title of the Work and its authorship have been acknowledged in this work;
(4) I do not have any actual knowledge nor I ought reasonably to know that the making of this work constitutes an infringement of any copyright work;

(5) I hereby assign all and every rights in the copyright to this Work to the University of Malaya ("UM"), who henceforth shall be owner of the copyright in this Work and that any reproduction or use in any form or by any means whatsoever is prohibited without the written consent of UM having been first had and obtained;

(6) I hereby declare that the Work is based on my original work except for quotations and citation, which have been duly acknowledged;

(7) I also declare that it has not been previously or concurrently submitted for any other degree at UM or other institutes.

Candidate's Signature Date 15/01/2016

Subscribed and solemnly declared before,

Witness's Signature Date

Name:

Designation:

ABSTRACT

Tidal stream energy is a type of marine renewable energy. Malaysia being maritime country with long coastline has potential to harness tidal stream energy. Therefore, it is crucial to investigate tidal stream energy and its potential for Malaysia.

This study investigates tidal stream energy in the Straits of Malacca. This work focus on the Straits of Malacca since its vicinity to highly populated west coast of Peninsular Malaysia. In addition, the Straits provide narrow passage to sea water, which converge tidal flows. Literature review found limited information on distribution of tidal flow and energy in the Straits of Malacca. Therefore, first this study gives information on distribution of tidal flow in the Straits of Malacca. Second, it identifies sites and their potential for harnessing tidal stream energy.

A three-dimensional finite-difference numerical model was used to model flow in the Straits of Malacca. The flow in the Straits of Malacca is governed by sea surface wind, semi-diurnal tide and stratification along continental shelf. This study carried out statistical analysis and found good correlation between the model results and field data at the tidal stations. Further model results were also compared with previous research works.

The Straits of Malacca receives semi-diurnal tide with two high and two lows on each day. Tidal flow speed varies from 0.1 m/s to 1.7 m/s across the Straits of Malacca. Four zones were considered for analysing distribution of tidal stream energy in the Straits of Malacca. Investigation identified that the southern and central part of the Straits have suitable sea depth, flow speed and tidal stream energy. Extractable tidal stream energy in the Straits of Malacca varies from 64 W/m^2 to 2516 W/m^2.

This study identified three sites for extracting tidal stream energy. The sites being off the coast of Pangkor Island, port Klang and Malacca. Site near coastline of the Pangkor

Island have depth of 35 m and receive peak tidal energy flux 1406 W/m^2. Port Klang provide depth of 25 m and receive 1406 W/m^2 of peak tidal energy flux. Malacca coastline provides depth of 20 m and receives 2516 W/m^2 of peak tidal energy flux. Further, this investigation calculated available and extractable power using two configurations of tidal current turbines. Single tidal current turbine configuration considered vertical axis Gorlov, and horizontal axis Open Hydro turbines. It found that the Gorlov turbine efficiently extracts available tidal stream energy. The Gorlov turbine perform with average capacity factor of 28%, while Open Hydro under performs with an average capacity factor of 2.25 per-cent. The study also estimates that a three-row configuration of tidal current farm with 500 units can produce 19610 Mwh, 18730 Mwh, and 17930 Mwh of electricity annually at Malacca city coastline, Port Klang, and Pangkor Island respectively.

This study successfully used numerical model to investigate tidal stream energy. This investigation finds that the Straits of Malacca is suitable for extracting tidal stream energy. At the identified sites Straits of Malacca provides suitable sea-depth, flow speed and tidal current energy.

ABSTRAK

Tenaga aliran pasang surut adalah sejenis tenaga yang boleh diperbaharui marin. Banyak negara melihat untuk memanfaatkan tenaga aliran pasang surut untuk meningkatkan bahagian daripada sumber yang boleh diperbaharui elektrik. Malaysia sebagai negara maritim dengan pantainya yang panjang mempunyai potensi untuk memanfaatkan tenaga aliran pasang surut. Oleh itu, adalah penting untuk menyiasat tenaga aliran pasang surut dan potensinya untuk Malaysia.

Kajian ini menyiasat aliran tenaga pasang surut di Selat Melaka. Fokus kerja di Selat Melaka sejak sekitar ke pantai barat berpenduduk padat di Semenanjung Malaysia. Tinjauan literatur mendapati maklumat terhad tentang taburan aliran pasang surut dan tenaga di Selat Melaka. Oleh itu, tujuan kajian ini adalah dua kali ganda. Pertama ia memberi maklumat tentang taburan aliran pasang surut di Selat Melaka. Kedua mengenal pasti tapak dan potensi mereka untuk memanfaatkan tenaga aliran pasang surut.

Satu perbezaan terhingga model berangka tiga dimensi digunakan untuk memodelkan aliran di Selat Melaka. Model berangka menggunakan terbuka data satelit sumber untuk keadaan awal dan sempadan. Perjanjian memuaskan didapati antara hasil model dan pemerhatian untuk kelajuan aliran pasang surut, ketinggian, suhu permukaan laut dan kemasinan. Pusat Hidrografi Nasional, Malaysia menyediakan data pengukuran dari stesen pasang surut untuk mengesahkan dan menentukur model berangka. Selain perjanjian cemerlang didapati antara model dan kerja-kerja penyelidikan sebelumnya.

Kajian ini dianalisis keputusan model untuk mendapatkan taburan kelajuan pasang surut, arah aliran, ketinggian dan tenaga pasang surut untuk musim bunga dan air pasang perbani. Kelajuan aliran pasang surut berbeza dari 0.1 m / s hingga 1.7 m / s

seberang Selat Melaka. Empat zon telah dipertimbangkan untuk menganalisis pengagihan tenaga aliran pasang surut di Selat Melaka. Siasatan mengenalpasti bahawa bahagian selatan dan tengah Selat mempunyai kedalaman laut sesuai, kelajuan aliran dan tenaga aliran pasang surut. Ekstrak tenaga aliran pasang surut di Selat Melaka berbeza dari 64 W/m^2 untuk 2516 W/m^2.

Kajian ini mengenal pasti tiga tapak untuk mengekstrak tenaga aliran pasang surut. Laman web yang di luar pantai Pulau Pangkor, pelabuhan Klang dan Melaka. Laman berhampiran persisiran pantai Pulau Pangkor mempunyai kedalaman 35 m dan menerima puncak pasang surut tenaga fluks 1406 W/m^2. Pelabuhan Klang menyediakan kedalaman 25 m dan menerima 1406 W/m^2 puncak fluks tenaga pasang surut. Pantai Melaka menyediakan kedalaman 20 m dan menerima 2516 W/m^2 puncak fluks tenaga pasang surut. Lagi siasatan ini dikira boleh didapati dan boleh diekstrak menggunakan kuasa dua konfigurasi turbin semasa pasang surut. Pasang surut konfigurasi turbin semasa Single dianggap paksi menegak Gorlov, dan mendatar turbin paksi Terbuka Hydro. Ia mendapati bahawa turbin Gorlov yang cekap ekstrak didapati tenaga aliran pasang surut daripada Hydro Buka. Kajian ini juga menganggarkan bahawa konfigurasi tiga deretan ladang semasa pasang surut dengan 500 unit boleh menghasilkan 19.610 MWh , 18730 MWh , dan 17.930 MWh elektrik setiap tahun di bandar pantai Melaka , Port Klang , dan Pulau Pangkor.

Melaka adalah sesuai untuk mengekstrak tenaga aliran pasang surut. Pada tapak yang dikenalpasti Selat Melaka menyediakan sesuai laut mendalam, kelajuan aliran dan tenaga semasa pasang surut.

ACKNOWLEDGEMENTS

I would like to express the deepest appreciation to the people who motivated and added to my Masters work like my supervisor, review committee members, and support staff.

In this regard first, I thank my supervisor, Professor. Ir. Dato' Dr. Roslan Bin Hashim for his guidance and support towards completion of my study. In addition, I like to thank my co-researchers for his/her feedbacks and patience throughout the thesis writing process. Also, I thank technical staff Mr Mohammad Termizi for his technical inputs during the research.

Last but not the least I hold high regards for the Department of Civil Engineering, Faculty of Engineering and University of Malaya for providing all the research support and infrastructure for conducting my research.

In addition, thank you to my wife Prerna for standing by me through tough times during the course of my research work.

TABLE OF CONTENT

CHAPTER 3 METHODOLOGY Page

LIST OF FIGURES

LIST OF TABLES

LIST OF SYMBOLS AND ABBREVIATIONS

MRE	Marine Renewable Energy
PV	Photo Voltaic
POM	Princeton Ocean Model
IPCC	Intergovernmental Panel on Climate Change
OTEC	Ocean Thermal Energy Converters
MCT	Marine Current Turbine
EPRI	Electric Power Research Institute
TCT	Tidal Current Turbine
ADCP	Acoustic Doppler Current profiler
SELFE	Semi implicit Euler Lagrange Finite Element
GIS	Geographical Information System
ROMS	Regional Ocean Modelling System
FVCOM	Finite Volume Coastal Ocean Model
FERN	Fundy Energy Research Network
OHI	Ocean Health Index
EEZ	Exclusive Economic Zones
CFL	Courant Friedrichs Levy
NGDC	National Geophysical Data Centre
ECMRWF	European Centre for Medium-Range Weather Forecasts
EMEC	European Marine Energy Centre Ltd
SST	Sea Surface Temperature
SSS	Sea Surface Salinity
F	Form factor
P_o	Power (*Kw*)

C_p	Power coefficient
C_{pMax}	Maximum power coefficient
ρ	Density of fluid (kg/m^3)
A	Cross-sectional area of turbine rotor (m^2)
V	Speed of fluid (m/s)
P_{max}	Peak Power (kw)
C_F^{peak}	Optimal farm drag coefficient
U_o^{peak}	Transport amplitude at peak
B	Width (m)
H	Depth (m)
Δt	Infinitesimal time
F_h	Hydrostatic force per unit area (N/m^2)
F_d	Drag force
τ_o	Shear stress
P_{er}	Wetted perimeter (m)
Q	Discharge (m^3)
C_{te}	Depth-averaged bed roughness
T	Tidal cycle ($hours$)
H	Sea depth (m)
U	Tidal flow velocity (m/s)
S	Sea water salinity (ppt)
Elv	Sea water elevation (m)
Σ	Sigma level coordinate
x, y, z	Cartesian coordinates
$\eta(x, y, t)$	Sea surface elevation (m)

ω	Mean velocity in the vertical (m/s)
D	Summation of η and H
G	Acceleration due to gravity (m/s^2)
R	Short wave radiation flux
K_H	Vertical turbulent flux coefficients
l	Turbulence length scale
K_M	Vertical turbulent flux coefficients
K_q	Vertical turbulent flux coefficients
$\widetilde{W}$	Wall proximity function
q^2	Turbulence energy
A_M	Horizontal turbulence coefficients
K	von Karman constant
z_0	Roughness parameter
B_1	Turbulence closure constant
u_τ	Friction velocity at the top or bottom
El	Sea surface elevation (m)
ua, va	Vertically averaged velocities in x and y direction (m/s)
t^{n-1} ,t^n	Time step at n-1 and n.
U_{max}	Maximum velocity (m/s)
C_T	Maximum internal gravity wave speed (m/s)
F	Nodal corrections for amplitude
u	Nodal corrections for phase
R^2	Coefficient of determination
P_i	Observed data
O_i	Estimated data
N	Number of data points

P_{avl}	Available Power (*Watt*)
A_T	Swept area (m^2)
V(t)	Instantaneous flow speed (*m/s*)
P(t)	Power (*Watt*)
$\eta_{Turbine}$	Efficiency of turbine (%)
$\eta_{Drive\ Train}$	Drive train efficiency (%)
$\eta_{Generator}$	Generator efficiency (%)
$\eta_{PowerConditioning}$	Power conditioning efficiency (%)
$P_{ext}(t)$	Extractable Power (*Watt*)
V_{in}	Cut-in speed (*m/s*)
V_r	Rated speed (*m/s*)
C_{cs}	Cut-off speed (*m/s*)
$E(t)$	Available energy (Watt-hour)
E_e	Extractable energy (Watt-hour)
C_f	Capacity factor (%)

LIST OF APPENDICES

Page

CHAPTER 1

INTRODUCTION

1.1 Background of Study

Renewable energy addresses dual challenge of climate change and meeting energy needs (Armstrong et al., 2011; Lloyd & Subbarao, 2009; Shamshuddin, 2012). Renewable energy comprises of various sources such as, hydro-power, wind, marine renewable energy (MRE) solar photovoltaic (PV), and biomass (Dresselhaus & Thomas, 2001; Turner, 1999). The main sources of renewable energy from ocean are tides, waves, ocean thermal energy and salinity gradient (Bahaj, 2011; Isaacs & Schmitt, 1980; Scruggs & Jacob, 2009). Present study focuses to investigate the tidal stream energy resources in the Straits of Malacca. Tidal stream energy is kinetic energy stored in the tidal flows (Fraenkel, 2006).

Deployment of tidal current turbines requires huge funding. Tidal stream energy investigation or assessment helps in convincing the funding agencies on the profitability of the project. Investigation studies identify the site for installing tidal current turbine and quantify the power available at that site. Malaysia is a maritime country with long coastline along the Straits of Malacca and the South China Sea. Previous studies reviewed all type of marine renewable energy sources and propose that the tidal stream turbines are best suited for generating electricity in the Straits of Malacca (Chong & Lam, 2013; Sakmani et al., 2013). However, till date no study has conducted in depth investigation of tidal stream energy resources in the Straits of Malacca.

Tidal stream energy investigation needs major considerations on power potential, bathymetry (sea depth), flow speed, and environmental impact (Bahaj & Myers, 2004; Blunden & Bahaj, 2006; Garrett & Cunnins, 2005). Researchers have investigated tidal

stream energy in various coastal locations across the globe such as, in the Pentland Firth, Channel Islands and the Sounds off the Scottish west coast (Adcock et al., 2013; Iyser et al., 2013). On same ground this work investigates tidal stream energy resource in the Straits of Malacca. Researchers use the analytical and numerical approach for assessment of tidal streams (Bryden et al., 2007; Bryden & Couch, 2007; Garrett & Cummins, 2008). Example of theoretical approach can be found in the work of Garrett and Cummins (2007) and Vennell (2010). Much review leads to the conclusion that the numerical methods are cost effective and reliable than the theoretical approach (Blunden et al., 2013).

First this work created a numerically models of the Straits of Malacca and obtained the tidal flow speed. Results were used to select site and investigate potential of tidal streams energy of the Straits of Malacca. In this regard, we developed a high resolution numerical model for the Straits of Malacca. This study uses the Princeton Ocean Model (POM) to numerically model tidal flow in the Straits of Malacca. POM is well-validated and proven code used by many researchers for modeling oceanic flows (Ezer & Mellor, 2004).

1.2 Scope of Work

This study investigates tidal stream energy in the Straits of Malacca. Straits of Malacca is narrow passage between the west coast of Peninsular Malaysia and the Sumatra Island. The west coast of the Peninsular Malaysia being highly populated and has potential to get benefit by extracting tidal stream energy from the Straits of Malacca. This study investigated various parameters affecting tidal stream energy such as sea depth, flow speed, and available power. Assessing tidal stream energy resources requires investigating the sea depth, flow speed, power potential and environmental impact (Bahaj, 2011) . Initially, a literature review presents concept of tidal stream

energy, conversion technologies, material and method used in previous works which investigated tidal stream energy resources in various part of the world. This helped to identify cost effective and reliable methodology for this study. First a numerical model was developed and validated for determining the tidal flow speed in the Strait. Then this study analysed the results to identify site with high tidal stream energy. Later, analytical methods were used to estimate power potential of tidal stream energy at selected sites. This work uses design specification of commercial tidal current turbines for estimating power potential of selected site. This works used combination of numerical, analytical, observation and satellite data in order to give accurate estimation and findings.

1.3 Objectives

Various research studies propose the tidal stream energy as sustainable energy option for the future. This study focuses on investigating and assessing tidal stream energy in the Straits of Malacca, which is nearest water body to the west coast of Peninsular Malaysia.

Following are the main objectives of the study:

1. To model flow speed of tidal streams in the Straits of Malacca, numerically.
2. To select sites with higher concentration of tidal stream energy using the determined flow speed.
3. To estimate the available and extractable power at the selected sites in the Straits of Malacca.

1.4 Problem Statement and Significance of this Study

Research works blame increasing global CO_2 emissions for ongoing climate change and global warming (Bala et al., 2013; Gillett et al., 2011). Use of fossil fuel by developed and developing countries contribute to major shares of increasing greenhouse gases in the atmosphere. In order to counter these emissions, the Intergovernmental Panel on Climate Change (IPCC), in their report emphasized to all nations for increasing renewable energy shares for meeting global energy need (Mitigation, 2011). Tidal stream energy is renewable energy stored in tidal flows of seawater (Smith, 2013). Countries with coastline such as United Kingdom, Canada, USA, Spain, Portugal, South Korea, China and Australia start to look to harness tidal stream energy (Ali et al., 2012; Esteban & Leary, 2012; Sanz-Casado et al., 2013; Wang et al., 2011). Commercial use of conversion devices are at early stages with most devices in prototype testing state. Researchers are still in the process of optimizing tidal turbines and related technologies. It is apt time for assessing tidal stream energy, as it is first step towards generating electricity from tidal flows.

The Straits of Malacca is a candidate site as it is tidally driven channel (Rizal et al., 2010; Wyrtki, 1961). In Malaysia the west coast of Peninsular Malaysia houses most of the industry and human population. Initial studies have reviewed and propose that the Straits of Malacca is candidate site for harnessing tidal stream energy using tidal current turbines (Sakmani et al., 2013). However, research work remains to investigate tidal stream energy resources in the Straits of Malacca. Therefore, this study assesses tidal stream energy resource in the Straits of Malacca. The study identifies site for energy extraction and determines power potential.

This study conducted complete analysis for bathymetry (sea depth), flow conditions, and power potential of tidal stream energy in the Straits of Malacca. Off shore field

measurement of the tidal flow speed involves huge finance. Therefore, this study uses numerical model, and satellite data to estimate tidal flow speed in the Straits of Malacca. This study uses cost effective and reliable method for modelling and investigating tidal stream energy. In this regard, this work uses open source finite difference numerical model, satellite data and reliable analytical methods. The model uses open source satellite data for initialising major parameters such as tidal constituents, seabed topography, sea surface wind, sea surface salinity and temperature in the Straits. Tidal flows are periodic and predictable resource unlike wind and wave energy (Hassan et al., 2012). Predicting tidal flow speed and available energy requires few weeks of flow data. Results from the numerical model were validated with observations. In order to calculate extractable energy, this study considered design specifications of commercially conversion devices. This study shows that reliable and cost effective method can be used for assessing resources of tidal current turbine.

1.5 Thesis Outline

This work investigate various aspects of tidal stream energy such as distribution of tidal energy flux, bathymetry (sea depth), tidal flow speed, site selection and power potential of selected site in the Straits of Malacca. Chapter 2 presents literature review related to present study. It starts by introducing basic concepts in tidal stream energy such as, design of conversion devices, their classification, concept of tidal current farm, and project development issues. Later this chapter discusses previous research works from across the globe that investigated tidal stream energy resources in other parts of the world.

Chapter 3 presents methodology for achieving the objective of this work. Primarily it discusses numerical method used for obtaining tidal flow speed of the Straits of Malacca. Then, it introduces criteria for selecting site. Later it presents the analytical

method for computing available and extractable tidal stream energy at selected site under selected conditions. Chapter 4 presents in depth discussion on the results obtained from the numerical method. Results for all the objectives are presented in sequence. Figure 1.1 shows flow chart outlining flow of this thesis. At the end we summarise major findings from this study in Chapter 5 and discuss on limitations of this study. In addition, this work also provides suggestion for future work.

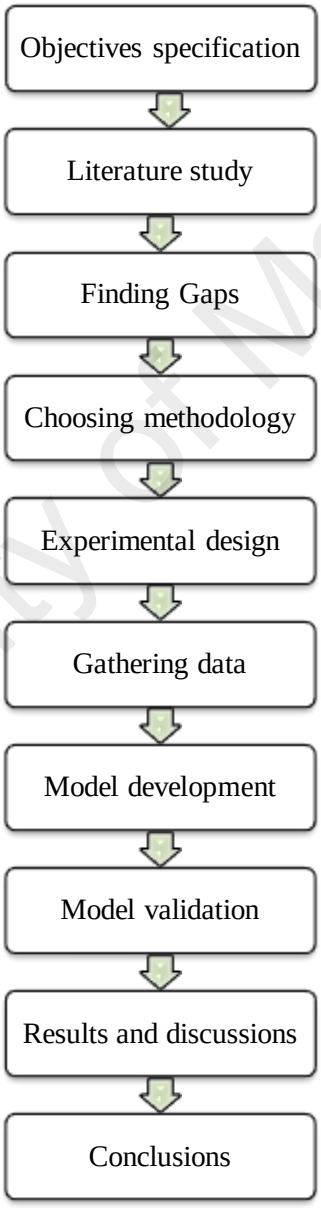

Figure 1.1 Flow chart showing thesis outline.

CHAPTER 2

LITERATURE REVIEW

2.1 Introduction

Kinetic energy stored in tidal flows is known as tidal stream energy. Flowing sea water is known as tidal stream or tidal current. Occurrence of tide generates difference in sea level between two points in the ocean. This variation in sea water level provides a potential head for water to flow from higher to lower head. Kinetic energy in tidal streams gets concentrated at sites with constraining topographies such as islands and straits. Such sites includes the waters in the Straits of Malacca, the Channel Islands, the Sounds off the Scottish west coast, in the Taiwan Strait, the Alas Straits and the Khowr-e Musa Bay (Adcock et al., 2013; Blunden et al., 2013; Draper et al., 2014; Iyser et al., 2013; Lam et al., 2013; Rashid, 2012). Researchers consider such sites appropriate for harnessing energy for generating electricity.

This review addresses topics related to investigation of tidal stream energy. This chapter first gives a general introduction to marine renewable energy (MRE) and tidal current energy in particular. It presents a list of world-wide commercial marine renewable power plant. Later this review presents research work which investigated power potential of tidal stream energy in the waters of USA, UK, China, and other part of world. Section 2.3 provides a brief introduction to scientific terminologies used for describing tide. Section 2.4 presents design components of tidal current turbines. Section 2.6 discusses key parameters for investigating tidal stream energy resource, such as sea-depth, tidal flow speed, and theoretical, experimental, and numerical tools

for computing power potentials. In the end this review presents environmental impact of tidal current turbine on ocean ecosystem.

2.2 Marine Renewable Energy

Interaction between the earth and planetary forces gives rise to tides in the ocean. The temperature difference produces wind, which produces surface waves in the sea (Brink, 1991). Ocean covers 70% of the earth surface and is largest receptor of thermal energy from sun. The evaporation from the ocean surface gives rise to salinity differences between the ocean water and river water. The sources of marine renewable energy (MRE) include tidal ranges, tidal currents, ocean waves, ocean thermal gradients and salinity gradients. A wide range of technologies can harness ocean energy to produces electricity. Major energy conversion techniques include the tidal barrage, tidal turbines, wave converters, Ocean Thermal Energy Converters (OTEC) and salinity gradient devices.

Researchers consider tidal barrage as the most established technology among the five types of MRE. Research and development for tidal current and wave energies made significant progress in the past decade. Today commercially installed MRE devices comprises of the tidal barrage, tidal current turbines, and wave converters. The Shihwa Lake tidal barrage in South Korea is the world's largest barrage with a capacity of 254 MW (Kim et al., 2012), as shown in Figure 2.1. La Rance is the oldest and the second largest tidal barrage with a capacity of 240 MW (Frau, 1993). Annapolis tidal barrage with a power capacity of 20 MW is the third largest tidal barrage (Dadswell et al., 1986). It is installed at the Bay of Fundy, Canada. Sea-Gen is the world's first commercial tidal current turbine in operation at Strangford Lough, Northern Ireland (Figure 2.2)(Douglas et al., 2008). The capacity of power generation for Sea-Gen is 1.2

MW. Wave Dragon is the first commercial wave power plant in the world (Figure 2.3)(Kofoed et al., 2006). It is located at the North Sea Demonstrator (Denmark) with a power capacity of 1.5 MW.

Table 2.1 lists commercial MRE plants presently in operation. OTEC and salinity gradient technology are catching up fast and likely to start operation at the commercial level in coming years. The IHI Plant Construction Corporation, Xenesys Incorporation and Yokogawa Electric Corporation are working together to build a trial OTEC plant in Japan.

Figure 2.1 Shihwa power plant (Kim et al., 2012).

Figure 2.2 SeaGen Tidal Turbine of MCT (Marine Current Turbine Ltd).

Figure 2.3 Wave-Dragon at the North Sea Demonstrator (Denmark).

Table 2.1 **C**ommercial MRE power plants.

MRE Power Plant	Capacity(MW)	Country	Year of Commission
Shihwa Lake Tidal barrage	254	South Korea	2011
WaveDragon	1.5	Denmark	2011
Uldolmok Tidal Station	1.5	South Korea	2009
SeaGen	1.2	Ireland	2008
Annapolis Royal Generating Station	20	Canada	1984
Jiangxia Tidal Power Station	3.2	China	1980
Kislaya Guba Tidal Power Station	1.7	Russia	1968
La Rance Tidal Power Station	240	France	1966

2.3 Tide and Tidal Flow

Tides are long waves; that causes rise and fall in level of seawater (Boersma & Terwindt, 1981). This difference in sea level generates tidal flow, also known as tidal currents. Tidal currents show change in flow speed and direction within a given time period. Tide generating forces are result of gravitational and centrifugal pull between the earth, the moon and the sun (Figure 2.4). Since moon is closer to earth than sun, its gravitational field varies strongly over earth surface than gravitational field of the sun

(Brans & Dicke, 1961). Qualitative analysis shows that the Sun's tide generating forces contribute only 46% as compared to the Moon (Christodoulidis et al., 1988).

This paragraph defines common terminologies associated with tides, such as high tide, low tide, mean sea level, tidal range, spring and neap tide. During *high tides* water level goes above mean sea level. During *low tides* water level goes below mean sea level. By averaging water levels over a long period, mean sea level is computed. Tidal-range is the difference of sea level between high and low tide. Spring tides occur when the Sun, the Moon and Earth orient in a straight line (full-moon and new-moon, Figure 2.4). Spring tides are associated with highest tidal range. Neap tides occur when the Sun, the Moon and Earth make right angle with each other. Neap tides are associated with minimum tidal range. Spring and neap tide occur in cyclic periods. One period of 14.77 day make for one spring and one neap tide (Kvale, 2006).

Tidal flow speed *V(t)* vary with time from the spring to neap tide (Figure 2.4). The Straits of Malacca receives semi-diurnal tide (Chen,Malanotte-Rizzoli, et al., 2014; Wyrtki, 1961). Semi-diurnal tide achieves two high and two low tides in a given day. Similar trend occurs for tidal flow speed. Figure 2.4 shows varying tidal flow speed from full moon to new moon (Matheson & Thomson, 1973; Wyrtki, 1961).

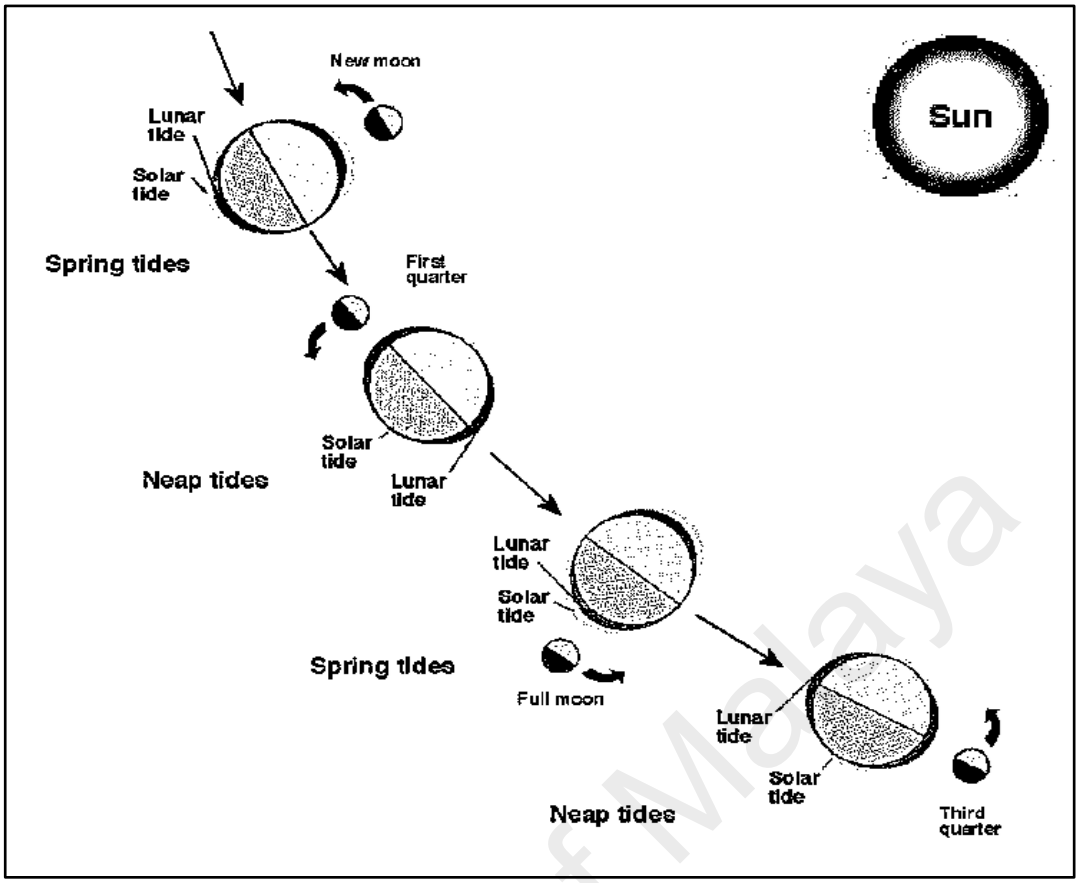

(a)

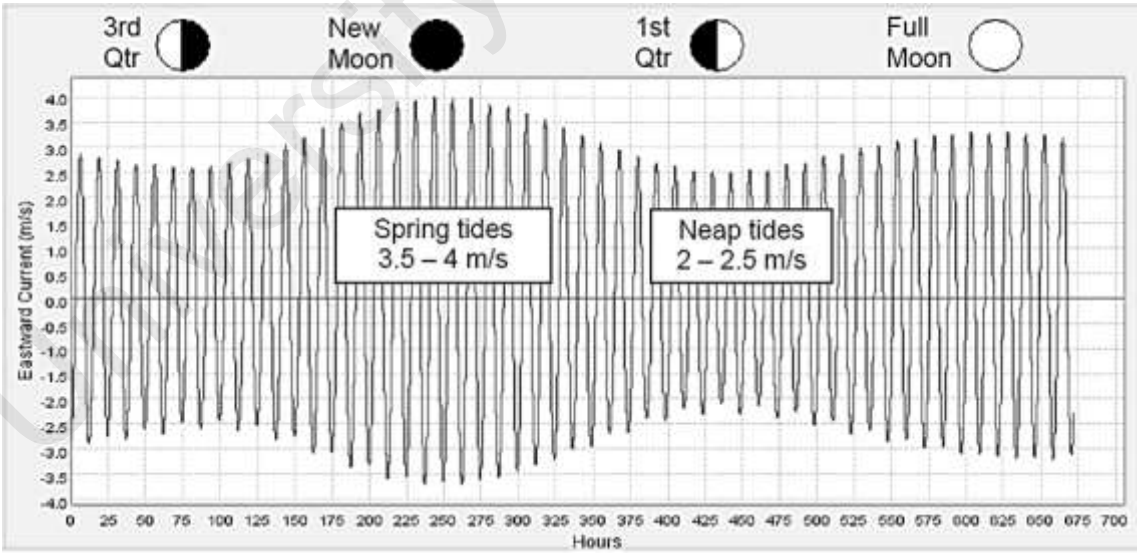

(b)

Figure 2.4 Corresponding change in (a) the phases of the moon and corresponding changes in (b) the tidal flow speed (Matheson & Thomson, 1973).

2.3.1 Tidal Periods

The summation of harmonic oscillations associated with a particular tidal periods represents tides mathematically. The harmonic oscillation consists of tidal constituent for the moon and the sun. Each tidal constituent have unique amplitude, period and phase.

The major tidal constituents of the moon and the sun are given below:

- M_2- Principal lunar semidiurnal constituent.
- N_2- Larger lunar elliptic semidiurnal constituent.
- S_2- Principal solar semidiurnal constituent.
- K_1- Luni-solar declinational diurnal constituent.
- O_1- Lunar declinational diurnal constituent.
- M_4- First over tide of M_2 constituent.
- M_6- Second over tide of M_2 constituent.
- S_4- First over tide of S_2 constituent.
- MS_4-A compound tide of M_2 and S_2 constituents.

Accuracy of tidal prediction depends on number of tidal constituent used in calculation. General prediction of tide for 15 days requires four tidal constituents i.e. M_2, S_2, K_1 and O_1 (Schwartz, 2006). However, a year of tidal prediction may require thirty seven tidal constituent (Schwartz, 2006). This study uses eight major tidal constituent in the numerical model of the Straits of Malacca. Most of the previous studies have used eight or less major constituent for predicting tidal flows and elevations; therefore, this study also used eight constituent for simulating the tidal flow covering sixty day for the Straits of Malacca.

2.3.2 Classification of tides

The form factor (F) is a dimensionless constant used for classifying tides (Williamson et al., 2015). It is defined as

$$F = \frac{(K_1+O_1)}{(M_2+S_2)} \quad (2.1)$$

where the tidal amplitudes are represented by tidal constituents M_2, S_2, K_1 and O_1.

Based on the form factor tides are classified into following categories:

1. Semidiurnal tides ('F' ranges from 0-0.25).
2. Mixed, mainly semidiurnal ('F' ranges from 0.25-1.5).
3. Mixed, mainly diurnal ('F' ranges from 1.5 -3.0).
4. Diurnal tides (F greater than 3.0).

Figure 2.5 shows amplitude and frequency of above tides for 24 hour duration.

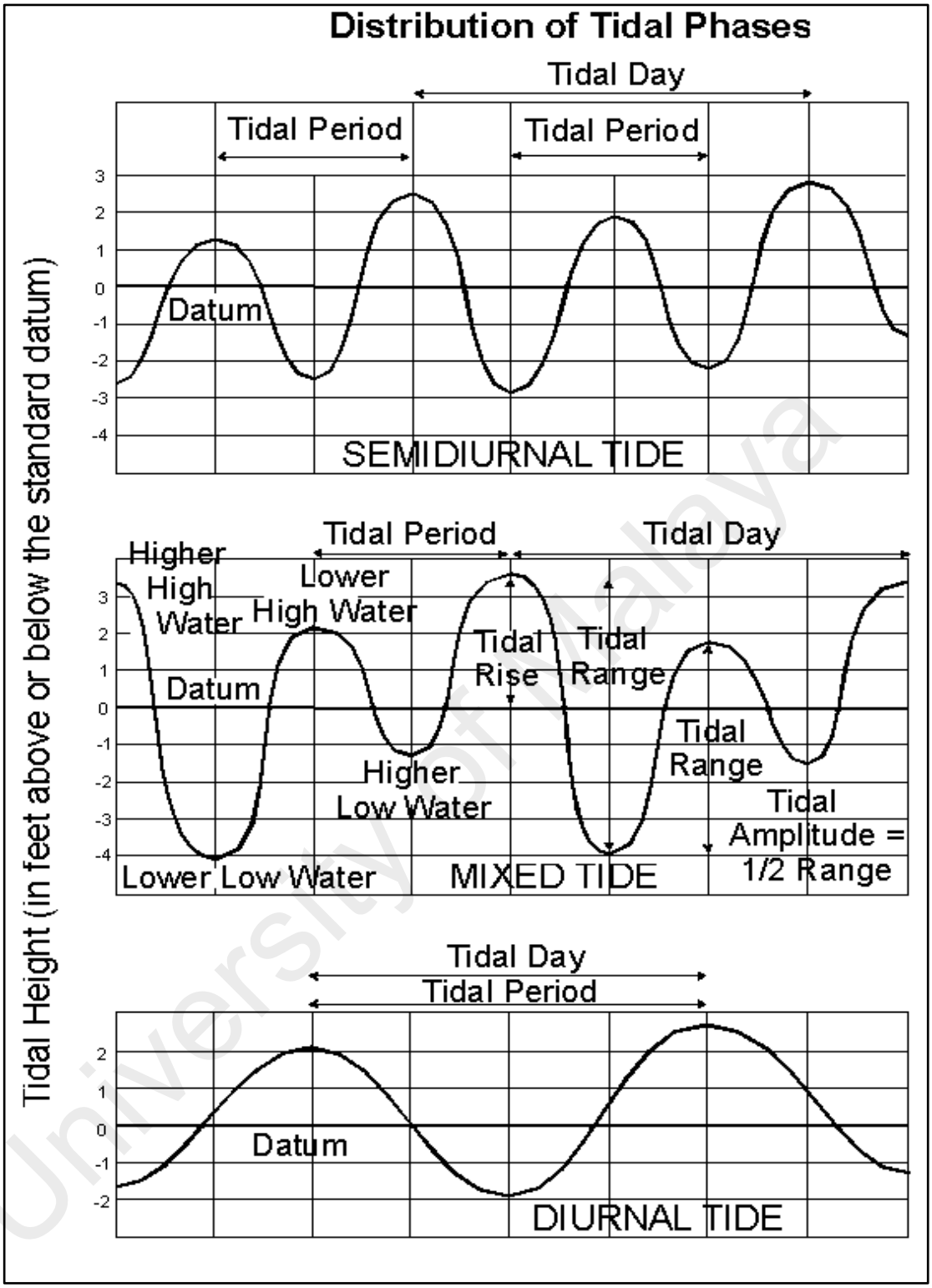

Figure 2.5 Tidal amplitude and frequency distribution of semidiurnal, mixed, and diurnal tide for a day.

2.3.3 Tidal Stream Energy Conversion Theory

Suitable turbine rotor extracts kinetic energy from the tidal flows. Tidal stream energy converter uses concept comparable to the wind turbine. Both tidal stream turbine and wind turbine harness kinetic energy from the moving fluids (Figure 2.6). Thus, power (P_o) available from tidal stream is given by:

$$P_o = \frac{1}{2}\rho A v^3 \qquad (W) \qquad (2.2)$$

where $\rho(kg/m^3)$ is the density of fluid, A (m^2) is the cross-sectional area of turbine rotor, and v (m/s) is the speed of fluid.

The above equation shows relationship between fluid density, flow speed and available power. Available power from moving fluid is directly proportional to its density. Water is 832 times denser than wind (air). Therefore, tidal stream turbine generates 832 times more power than wind turbine for the same flow speed. This implies tidal flow streams have higher power density or flux (W/m^2) than the wind (Bahaj, 2011).

At this point it is important to present the Bentz concept which puts limit to power extraction for a single turbine in an unconstrained flow. The Bentz limit is widely accepted in wind turbine technology and same goes true for the tidal stream turbine. The Bentz limit states that maximum extractable power from a turbine cannot exceed 16/27 or 59% of the available power at turbine rotors. This limit is called maximum rotor power coefficient C_{pMax} = 16/27 (Vennell, 2013).

$$C_{pMax} = {}^{P}/_{P_o} = \frac{P}{\frac{1}{2}\rho A v_0^3} \qquad (2.3)$$

where P is the power generated by turbine.

All operational current turbines have power coefficient (C_p) in the range of 0.3 to 0.5. However, better turbine design can achieve power coefficient closer to the Bentz limit. In practical applications, power coefficient represents effectiveness of turbine rotor in generating power.

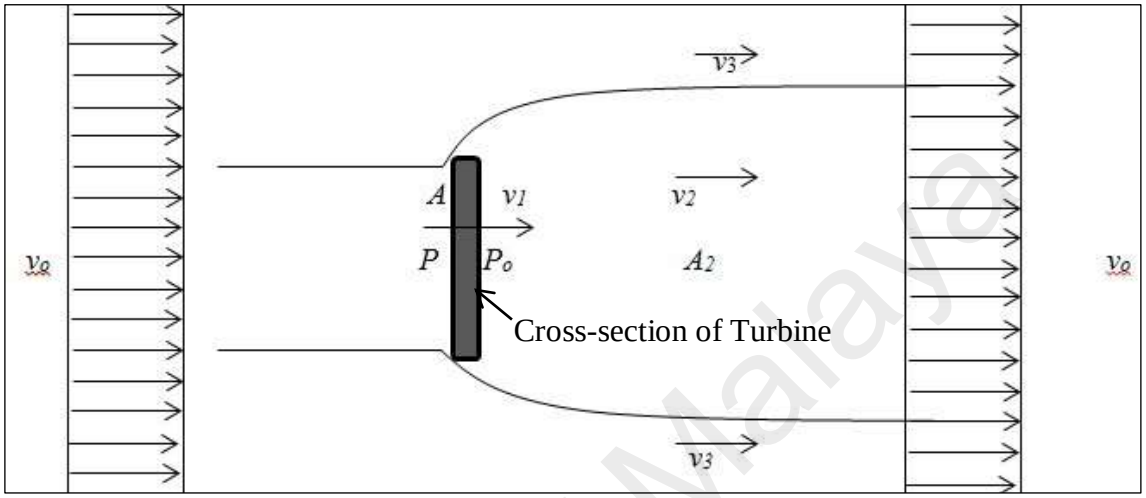

Figure 2.6 Diagram shows the theory behind converting tidal stream energy into useful power.

2.4 Tidal Stream Energy Conversion Devices

Tidal stream energy conversion devices are undergoing extensive research. These devices are called tidal current turbine (TCT) or tidal stream turbine. The technology is in its initial stages of development (Khan et al., 2009). New concepts for designing and testing conversion devices are being pursued by the researchers. Most conversion devices are at the proof-of-concept stage. Nevertheless, some devices have made it at commercial stage.

Harnessing tidal stream energy needs to consider site specific parameters and constraint. For example local flow speed, sea depth, environmental effects and conflict with other maritime activities (fishing, navigation and recreation). These factors make it difficult to design a single turbine that may work efficiently at every site. This is the primary reason for testing multiple design concepts at various sites around the world. Some of the devices are at research stage in academia, while some being tested as prototype and few are being commercially manufactured in industry.

A typical conversion system used for generating electricity from tidal currents consists of tidal current turbine (rotor), support structure, duct augmentation, drive system (gearbox), generator and electric cable for connection (Bahaj, 2011; Fraenkel, 2006; Khan et al., 2009; Rourke et al., 2010). Tidal stream energy converters use similar technology that being used in wind energy sector. However, water being 832 times denser than air; it applies sever loading on TCT structure. Thus, TCT requires several mandatory design changes for strengthening the overall structure. Following sub-sections present concept of tidal current turbine, support structure and duct augmentation.

2.4.1 Tidal Current Turbine

Tidal Current Turbines (TCTs), harness tidal stream energy to generate electricity. Technology of tidal current turbine is in early stages of development, unlike wind and solar technologies which is considered well developed. Therefore, tidal current turbines have enough scope for improvements.

A classic tidal current turbine consists of multiple blades mounted in a rotating hub and support structure (Rourke et al., 2010). They are classified into horizontal or vertical axis, based on orientation of rotating axis. At present stage industry favours the horizontal axis turbines over vertical axis (Rourke et al., 2010). Nevertheless, researchers still pursue the vertical axis turbine owing to its benefits for shallow water installation and lower capital cost (Coiro et al., 2005; Jing et al., 2014; Li & Calisal, 2010; Li et al., 2014).

Horizontal Axis Tidal Current Turbine: Rotation axis of horizontal axis tidal current turbine is along the direction of flow (Figure 2.7). It consists of multiple blades attached to central hub. It operates underwater and capable to self-start. Self-start capability comes from optimal design of hydrofoil blades (Khan et al., 2009).

Vertical axis marine current turbines: Rotation axis of vertical axis tidal current turbine is perpendicular to the direction of flow (Figure 2.8). Design of hydrofoil blades is simpler when compared to its counterpart. Vertical axis tidal current turbines produce less noise and cause lower blade tip losses (Khan et al., 2009).

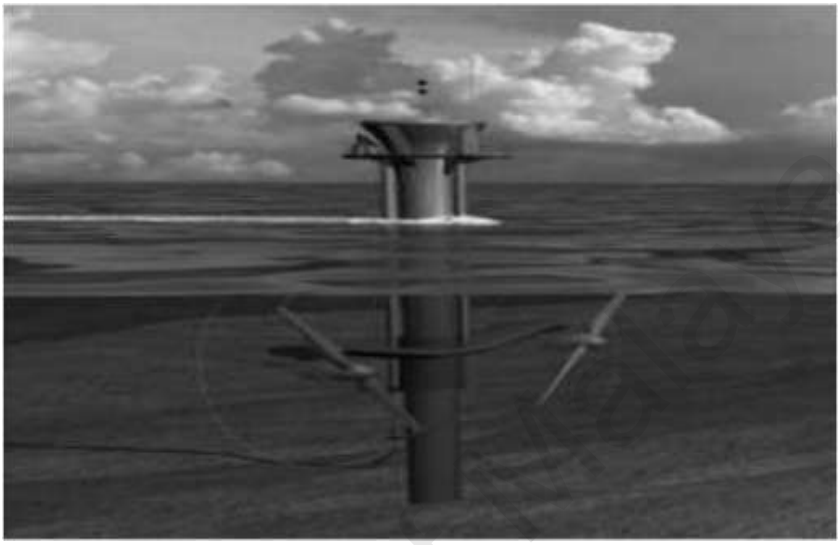

Figure 2.7 Horizontal axis tidal current turbine an artistic view of SeaGen(Fraenkel, 2007).

Figure 2.8 Vertical axis tidal current turbine (Gorlov & Rogers, 1997).

2.4.2 Duct Augmentation

Turbine with duct when placed in free stream, experiences higher flow at rotor blade than a turbine placed without duct(Alidadi & Calisal, 2014). Tidal current turbine when augmented with duct makes flow to pass in a constrained area and thereby increases the flow velocity (Alidadi & Calisal, 2014; Khan et al., 2009). This concept has long been used in wind turbines (Sarma et al., 2014). Duct is also called shroud, wind-lens, concentrator, diffusor, and augmentation channel (Ponta & Shankar Dutt, 2000). Khan et al. (2009), in their work conducted a survey on use of duct for hydrokinetic turbines. It can be concluded that half of vertical axis turbine and only one-third of horizontal axis turbines use duct augmentation. Ponta and Shankar Dutt (2000), in their work tested curvilinear duct and found that incoming flow velocity increase by a factor of 1.67. Thus, using tidal current turbine with duct will benefit regions with average tidal flows. Figure 2.9 shows design based categorization of various duct augmentation.

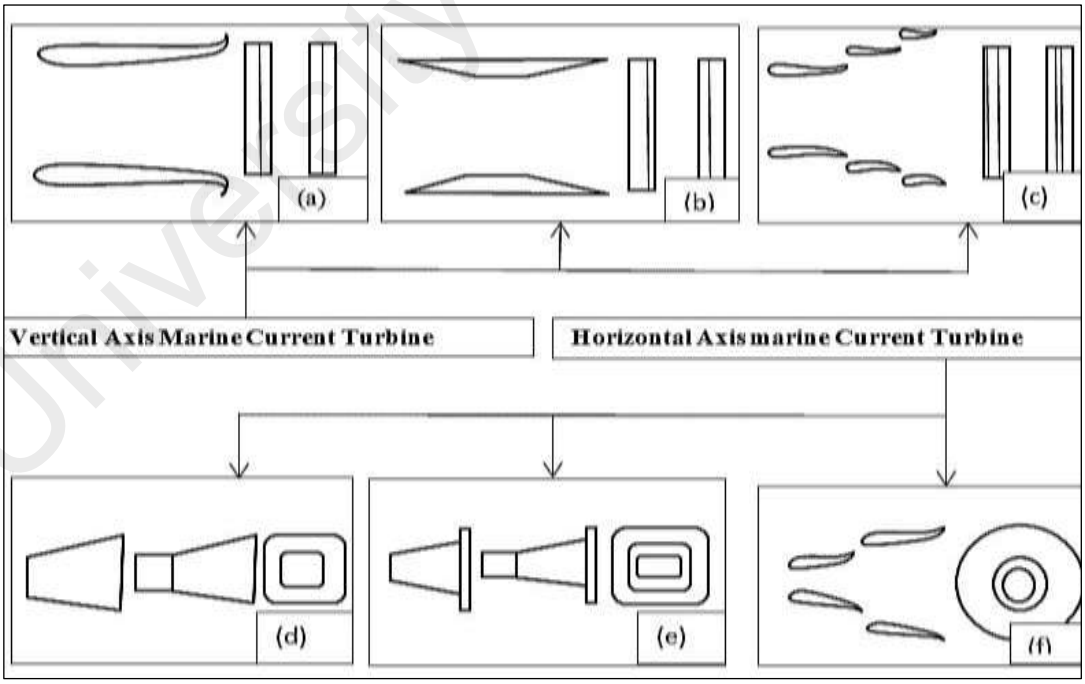

Figure 2.9 Schematic design of duct for vertical axis marine current turbine (a, b, and c) and horizontal axis marine current turbine (d, e, and f).

2.4.3 Support Structure and Rotor Placement

Support structure of a tidal current turbine is designed to with stand harsh weather of sea and operational loading (Fernandez-Rodriguez et al., 2014; Kong et al., 2014). As shown in Figure 2.10 the support structures can be broadly classified into following four types: (i) Gravity structures; (ii) monopile; (iii) Floating structures; and (iv) Tripod structures (Arany et al., 2014; Rourke et al., 2010).

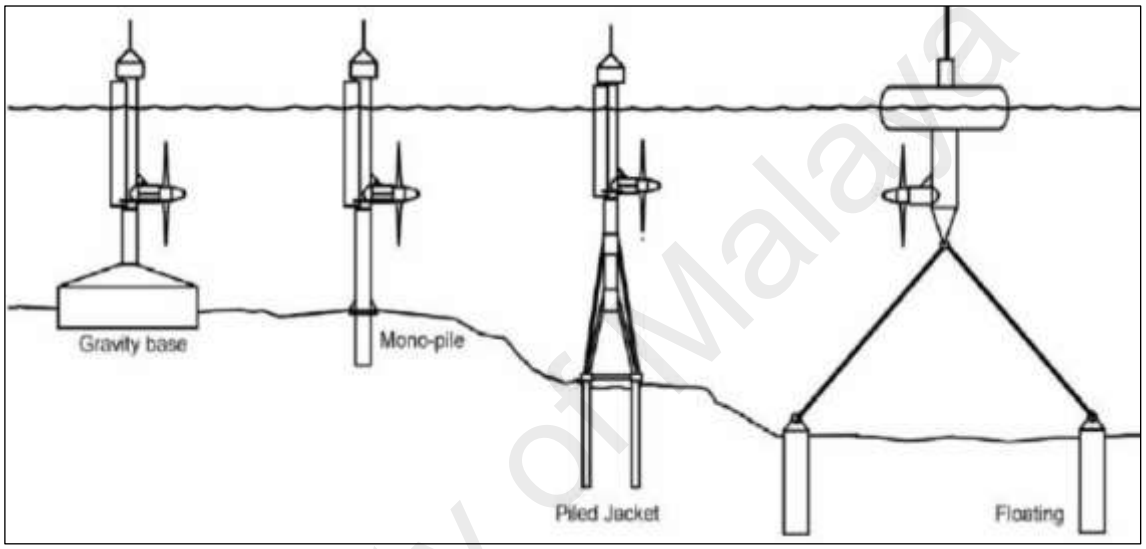

Figure 2.10 Tidal current turbine support structures.

Gravity structures are column based and use their own weight to overcome loading and harsh operating conditions(Yin et al., 2014). Therefore, huge amount of concrete and steel goes into making the gravity structures. They are scour prone due to their design. On the other hand the monopile structures have large hollow steel beam (Negro et al., 2014). The steel beams are driven deep inside seabed to give strength to these structures. Whereas, the floating structures are like floating vessel moored to seabed (Barbarelli et al., 2014). In deep water installations, floating type structures are considered economical. Tripod structures have three monopiles driven deep inside the seabed (Small et al., 2014). Thus, based on type of support structures the tidal current turbines can be supported either at the bottom or on the sea surface.

2.4.4 Tidal Current Farm

Only isolated and small communities can get benefit by the electricity generated from single devices (tidal current turbine). However, researchers propose installing the tidal current turbines in multiple row configurations in order to generate substantial electricity which could support larger communities. This design with multiple row of tidal stream turbine is called array or tidal current farm (Chen,Lin, et al., 2014; Myers & Bahaj, 2012).

Tidal current farm efficiently extract available power from tidal flow streams over larger area (Figure 2.11). Fishing, shipping lanes, tourism are important marine activities (Bahaj, 2013; Vennell, 2011b). Studies discourage full cross-sectional occupancy of a given channel by installing tidal current turbines. In addition larger blockage reduces the tidal flows (Vennell, 2012a). Previous studies have proposed 10% occupancy of the channel's cross-section (Bryden et al., 2004).

Figure 2.11 Schematic diagram of tidal farm (Myers & Bahaj, 2012).

2.5 Device and Project Development Issues

Researchers in academia and industry are working on the fundamental and applied research for making it feasible to generate electricity from tidal flows. Installing single or multiple conversion devices requires comprehensive and proper planning. Bahaj (2011) in his work listed down the areas of concern related to the conversion technology (devices) or a project development. Table 2.2 shows area of concern and major challenges in generating power from tidal currents in sea.

Researchers consider assessment of power potential and addressing the environmental impact as the initial blocks into investigating tidal stream energy. Deploying tidal current turbines in the sea requires huge funding. Resource assessments help in convincing the funding agencies on the profitability of a project. It helps to identify the site of tidal energy extraction and quantifies power available at that site. Energy production from a selected site depends on the understanding of a site. Therefore, a comprehensive investigation addresses multiple areas of concern such as site selection, available power, annual extractable power, seabed conditions, and environmental effects.

Table 2.2 Challenges and their relationship to conversion devices or project development.

Area of concern	Major challenges
Project specific	Site and resource assessment; Environmental Impact study; Array design and deployment.
Device specific	Electricity conversion, Device efficiency; Fixture and moorings; Connection to grid.

2.6 Resource Assessment of Tidal Stream Energy

Investigation of tidal stream resource takes into consideration, the sites power potential, bathymetry, flow speed, environmental affects and maritime planning (Bahaj & Myers, 2004; Garrett & Cummins, 2005). Researchers consider estimating power potential of site as major challenge (Connolly et al., 2011; Khan et al., 2009). Researchers use analytical, numerical and field measurement methods for estimating flow and power potential. In this regard investigators first measure the tidal flow speed. The measured tidal flow speeds is input-data for estimating the power potential.

Investigation of tidal stream energy cover studies related to characteristics of sea-depth, flow speed, power potential and environmental effects. Resource assessment indicates future success of a project in harness the tidal stream energy. It involves gathering and analysing data on the seabed and flow speed characteristics. Tidal flows are periodic and predictable resource unlike wind and wave energy. Predicting tidal flow speed and available energy requires few weeks of flow data. Numerical models use available data to accurately simulate the flow conditions of sea. Observations from the satellite and tidal stations provide data required for initializing and running a numerical model. In addition site specific measurements are made in order to gain further confidence. A survey which makes site measurement generally uses the Acoustic Doppler Current profilers (ADCP) at favourable points. Measuring instruments such as ADCP gather data on the sea-depth and flow speed for the scheduled time period. Therefore, comprehensive resource assessment requires considering multiple aspects for selected site. In coming sub section author review studies under following aspects:

1) Sea-depth (bathymetry).

2) Tidal flow speed.

3) Power potential.

4) Environmental aspects.

2.6.1 Sea-depth

Understanding the sea-depth characteristics is considered important for selected site. Sea-depth governs the dimensions of tidal current turbines. This in turn governs the capacity of device (Bahaj, 2011). Researchers use the satellite and survey data for gathering information on the sea-depth for any site. Open source satellite data are of coarse resolution (Figure 2.12). TPXO dataset is an example of satellite data (Figure 2.12). On the other hand a hydrographic survey gives accurate and high resolution sea-depth data. But hydrographic survey involves high capital cost. Researchers make efficient use of the satellite data to minimise area of interest for conducting the hydrographic survey. Ramos et al. (2014) used the nautical chart for studying bathymetry of tidal driven estuary the Ria Ribadeo, Spain. Nautical charts provide high-resolution data for the coastal regions that were surveyed in recent past. Government and selected private institutes generally conduct such survey and prepare the nautical charts.

Suitable sea-depth for installing tidal current turbine ranges from 25 to 50 m (Iyser et al., 2013). Depth in this range provides appropriate clearance for the conversion device from the water surface and seabed. A very interesting development shows that shallower depth less than 20 m can be used for installing micro-tidal current turbines. Hammar et al. (2012), in their work developed a site screening method for the micro tidal current turbines in shallower depths of Mozambique, Bazaruto Island. A review by Grabbe et al. (2009),supports this concept of extracting tidal stream energy in the shallower coastal waters. Their research investigation shows that 13% of the Norway's tidal current resources exist in the shallower sites.

Discussion from this section makes it clearer that sea-depth governs type of conversion device for a given site. Higher sea-depth favours installing first generation devices, which have larger turbine diameter. Shallower depth favours installing micro-tidal current turbines, which have smaller diameters.

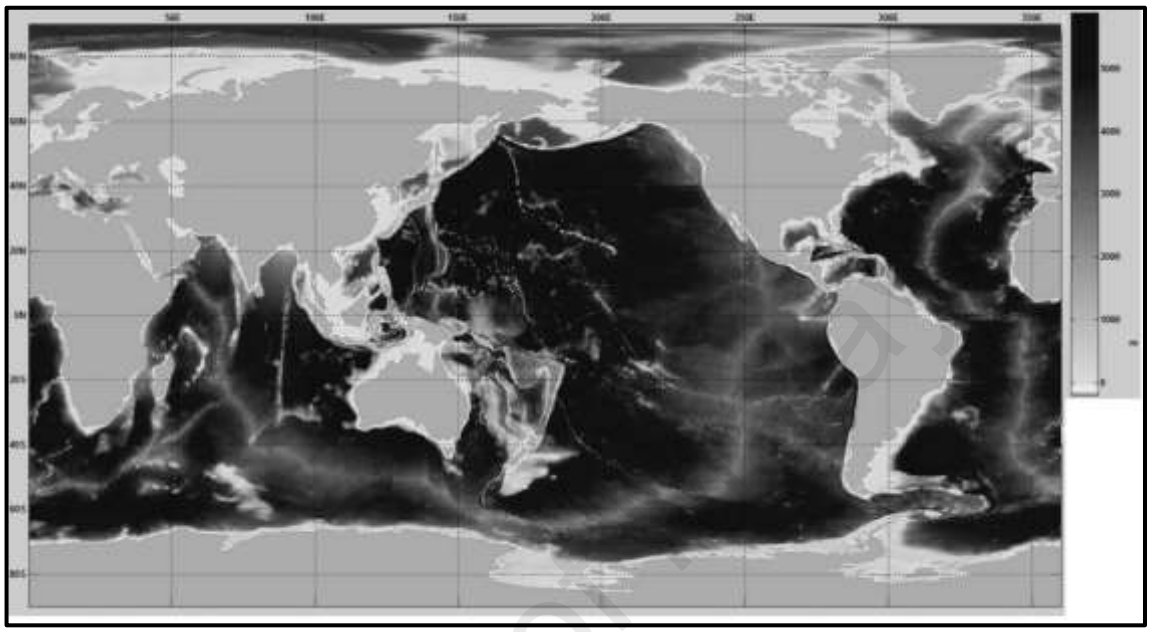

Figure 2.12 Visualization of sea-depth using satellite data.

2.6.2 Tidal Flow Speed

Tidal flow speed is primary parameter for assessing the energy potential of a given site. Researchers use experimental and numerical method for measuring tidal flow speed. Experimental method involves field measurement of tidal flow using measuring instrument such as the Acoustic Doppler Current profiler (ADCP). On site measurements involves high capital cost. In comparison with experimental exercise researchers consider the numerical methods to be cost effective.

2.6.2.1 Acoustic Doppler Current profiler

The Acoustic Doppler Current profiler uses the Doppler-effect for measuring flow velocity of the seawater (Figure 2.13). ADCP can be installed at seabed or on surface

attached with a boat. It listens to the echo of sent pulse and measure change in the pitch of echo. In turn the sound gets reflected from suspended particles in the seawater. These particles are generally suspended sediment. Small particles move at the same speed as the seawater, so the velocity it measures is velocity of seawater. Measurement is made at one point basis. Therefore, for measuring current velocity over a large area involves high capital cost. This is primary reason for researchers to prefer the ocean modelling over field measurements.

Figure 2.13 The Acoustic Doppler Current profiler from the NORTEK Ltd.

2.6.2.2 Ocean Modeling

Researcher's model flow dynamic of seawater using numerical ocean model. Numerical ocean model make use of satellite and survey data for initialising the prognostic variables. Primary variables such as bathymetry, sea surface elevation, sea surface wind velocity, salinity and temperature are available from satellite measurement for whole of

the earth's ocean. The advantage with numerical models being it can simulate flow for multiple points in a given domain. At the same time duration of measurement varies from an hour to months and years. In order to get tidal flow speed duration of 29 days is considered ideal.

2.6.3 Power Potential from Tidal Stream Resource

Estimating tidal energy is essential goal of any resource assessment. Researcher uses theoretical and numerical methods for estimating the tidal stream energy. Theoretical method involves creating one-dimensional model of a tidal channel. Bryden et al. (2004), Garrett and Cunnins (2005), and Vennell (2011a, 2011b, 2012b, 2013) in their research works successfully used simplified 1-D model to study energy extraction from a channel. In parallel researchers advocate use of two-dimensional and three dimensional numerical methods (Bryden et al., 2004; Garrett & Cunnins, 2005; Vennell, 2011a). One-dimensional model uses simplified representation of the real channel. However, actual tidal streams channel have complex topology and bathymetry. Therefore, two-dimensional and three-dimensional studies are becoming increasingly popular. In following sub section author reviews salient points from the theoretical and the numerical studies.

2.6.3.1 Theoretical Studies

Theoretical approach is simplifies real case in order to estimate power potential. Speed of the tidal flow stream is obtained by field measurements such as ADCP measurement. Modern equations have been proposed by researchers for estimation of the theoretical available tidal stream energy for tidal farm (Bryden et al., 2007). These equations include those proposed by Garrett and Cummins (Garrett & Cummins, 2005, 2007,

2008) and Vennell (Vennell, 2010, 2011a, 2011b, 2012b, 2013). Theoretical approach considers a simplified model for actual tidal channel (Figure 2.14).

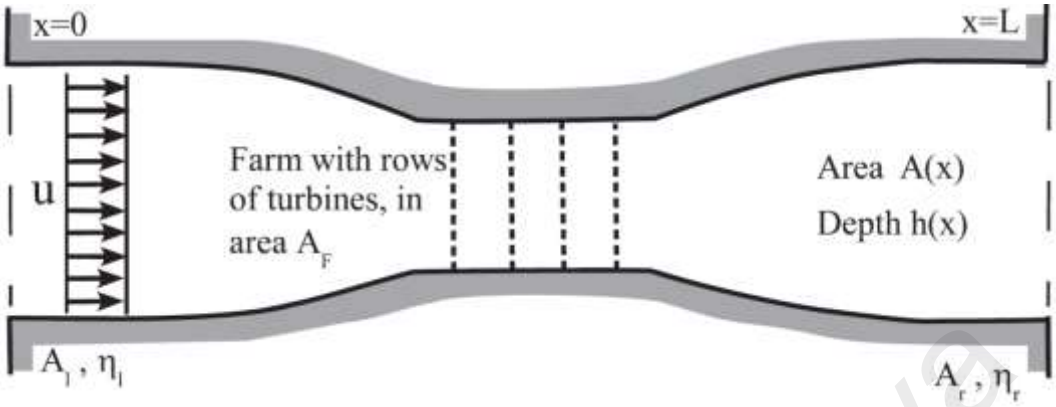

Figure 2.14 Schematic diagram of tidal channel with a rectangular cross-section are *A*, depth *h*, and peak tidal speed of *U*.

The peak power from tidal current at the selected site of a tidal channel is calculated using equation 2.4 (Vennell, 2011a).

$$P_{max} = \frac{4}{3\pi} \frac{\rho C_F^{peak}}{A^2} (U_o^{peak})^3 \qquad (W, Watt) \qquad (2.4)$$

where ρ is the density of sea water, C_F^{peak} is the optimal farm drag coefficient, A is the area of cross section, and U_o^{peak} is the transport amplitude at peak.

Tidal stream energy density in case of channel can be represented by considering a finite length and finite width channel linking two infinite oceans (Figure 2.15). Static head difference '*dh'* drive tidal flow between the two ends. Static flow model neglects effects resulting from time varying elevation between two ends.

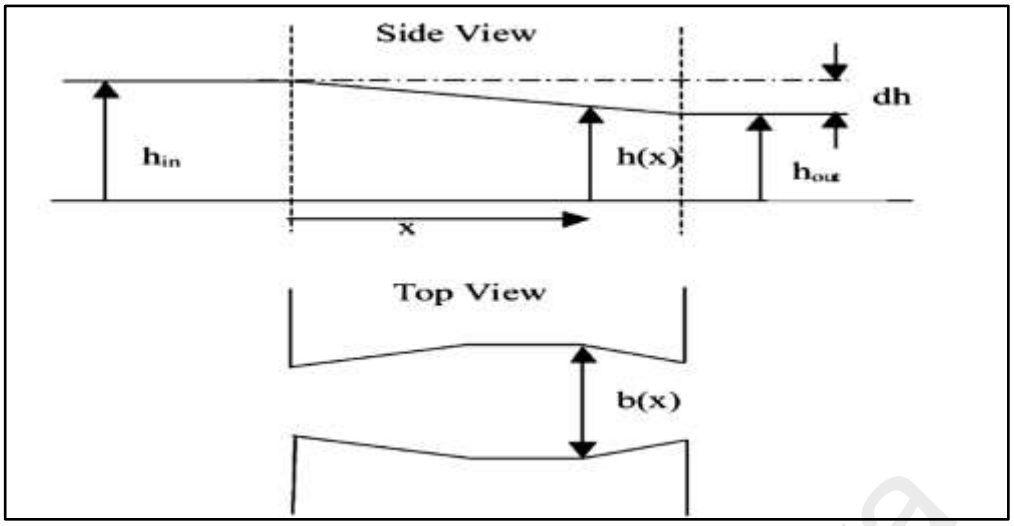

Figure 2.15 A simplified static model for a tidal channel linking two infinite oceans (Bryden et al., 2004).

Bryden et al. (2004), studied behaviour of tidal flow by considering changes in the momentum and conserving the mass of water passing through channel. Model assumes flow to be constant and one-dimensional across the cross section of channel. If channel width is *b* and depth is *h*, the mass passing in an infinitesimal time Δt can be represented as , $AU\rho\ \Delta t$, where A is the cross section (*h x b*) of channel. Rate of change of momentum:

$$\frac{D(Momentum)}{Dt} = \frac{\partial}{\partial t}\left(A\,U^2\rho\right)\Delta t + \ U\ \frac{\partial}{\partial x}\left(A\,U^2\rho\right)\Delta t \qquad (2.5)$$

Hydrostatic force per unit area due to head difference is given by:

$$F_h = -\rho g U\,\Delta t\frac{\partial h}{\partial x} \qquad (2.6)$$

In real channel the flow speed varies across width and depth. Simplified case assumes the drag force resulting from friction between flowing water, channel edges and seabed is equal to F_d.

$$F_d = -U\,\Delta t P_{er}\tau_o \qquad (2.7)$$

where τ_o is the shear stress and P_{er} is the wetted perimeter given by 2h+b.

If power is extracted at a rate of P_xW/m^3 then the retarding force due to power extraction is given by:

$$F_x = \frac{P_x A U \Delta t}{U} = P_x A \Delta t \tag{2.8}$$

The momentum equation for steady state condition can be written as:

$$U \frac{\partial}{\partial x} (AU^2 \rho) = -\rho g U A \frac{\partial h}{\partial x} - U P_{er} \tau_o - P_x A \tag{2.9}$$

Considering conservation of mass, and incompressible water volume discharge Q is given by:

$$\frac{\partial Q}{\partial x} = 0; Q = UA = Volume\ flux \tag{2.10}$$

Thus equation 2.9 can be rewritten as given below:

$$\left(1 - \frac{Q^2}{h^3 b^2 g}\right) \frac{\partial h}{\partial x} = \frac{\partial b}{\partial x} \frac{Q^2}{g h^2 b^3} - \frac{1}{\rho g b h} P_{er} \tau_o - \frac{P_x A}{\rho g Q} \tag{2.11}$$

Thus above equation can be solved to study impact of energy extraction on volume discharge and flow speed. In steady state conditions flow speed increases and depth decreases in the channel. But due to midway artificial energy extraction by tidal current turbine this balance is altered. Figure 2.16 shows how energy extraction influences flow speed of a channel.

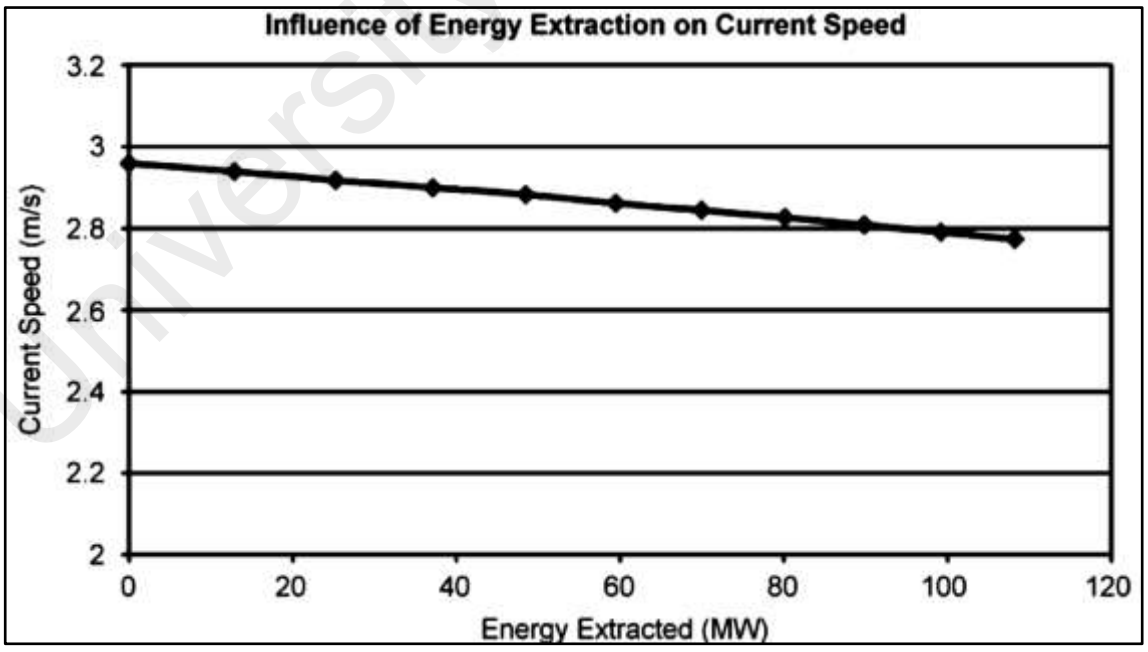

Figure 2.16 Energy extraction as function of reduction in tidal flow speed in a channel(Bryden et al., 2004).

Energy extraction causes decrease in flow speed of an undisturbed channel. Therefore, 100% occupancy of tidal channel is practically impossible. Extraction of 10% of energy from channel causes 3% reduction in free stream flow (Bryden & Couch, 2006). Energy extraction of 20% causes 6% reduction in flow speed of natural flow (Bryden & Couch, 2006). Therefore, research suggested that 10% energy extraction can be considered as limit to be environmentally acceptable (Bryden & Couch, 2006). For high energy extraction rates, any alteration in natural flow of channel should be considered. It was also found that effects of energy extraction can propagate upstream and downstream (Bryden et al., 2007). This one-dimensional model is simplified case of much complicated hydraulic domain. In practical cases two or three dimensional flow analysis is required.

Upper bound to maximum power generated by turbine in a tidal channel: Significant amount of electricity can be generated by using multiple turbines in a channel. But, use of too many turbines would block flow and interfere with other marine activities. Researchers try to suggest configuration of turbine for maximising the amount of power from a tidal channel. Garrett and Cummins (2007), in their work suggested ideal turbine model for energy extraction in a tidal channel. They found power loss is directly proportional to percentage occupancy of channel. This power loss is due to non-uniform flow between turbine wake and free stream flow. Energy losses take place with mixing of flow from turbine wake into free stream. Moving ahead Vennell (2010) combined 1D model of tidal channel with classical theory of tidal current turbines. The work showed maximising power available to a farm requires tuning of tidal current turbines for a given channel and turbine density. Optimal tunings depends on number of turbines in each row, channel geometry, bottom friction coefficient and tidal forcing (Vennell,

2010) (Figure 2.17). To maximise power output tidal current farms must occupy largest fraction of a channel cross section permitted by navigational and environmental constraints.

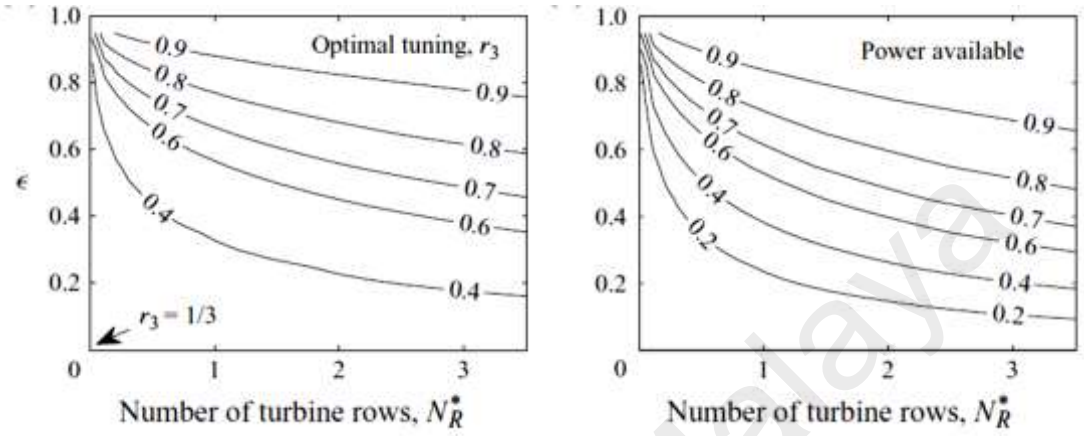

Figure 2.17 Tuning and power of tidal current farm in a channel.

2.6.3.2 Numerical Studies

Researchers use theoretical or numerical approach for estimating tidal power potential. Theoretical method reduces actual scenario to simple geometry with definite equation for maximum power. However, for actual field scale estimates require defining real field conditions. Numerical methods come closer to defining real boundary conditions for estimating tidal power potential. This section discusses on various research work that used numerical model for estimating tidal stream energy.

Walters et al. (2013), in his work used numerical model to obtain flow speed and estimate power for the Minas Pasage in the Bay of Fundy. The work used form drag factor to represent tidal turbines into a numerical flow model. The results show only a fraction of theoretical maximum power can be extracted because of reduction in flow induced due to presence of tidal turbine structures.

, incorporated the Princeton Ocean Model (POM) to model tidal flow of the Alas Strait, Indonesia. Figure 2.18 shows flow chart describing work flow of numerical model used in Blunden et al. (2013), work to assess tidal stream energy. The Alas Strait is suitable for extracting tidal stream energy as it provides shallow depth, high tidal currents and located far from shipping lanes. The study estimates annual energy yield of 330 GWh for depth limit of 40 m from the Alas Strait. This study shows array shapes can be simulated without the need to incorporate parameterization of turbines in the model.

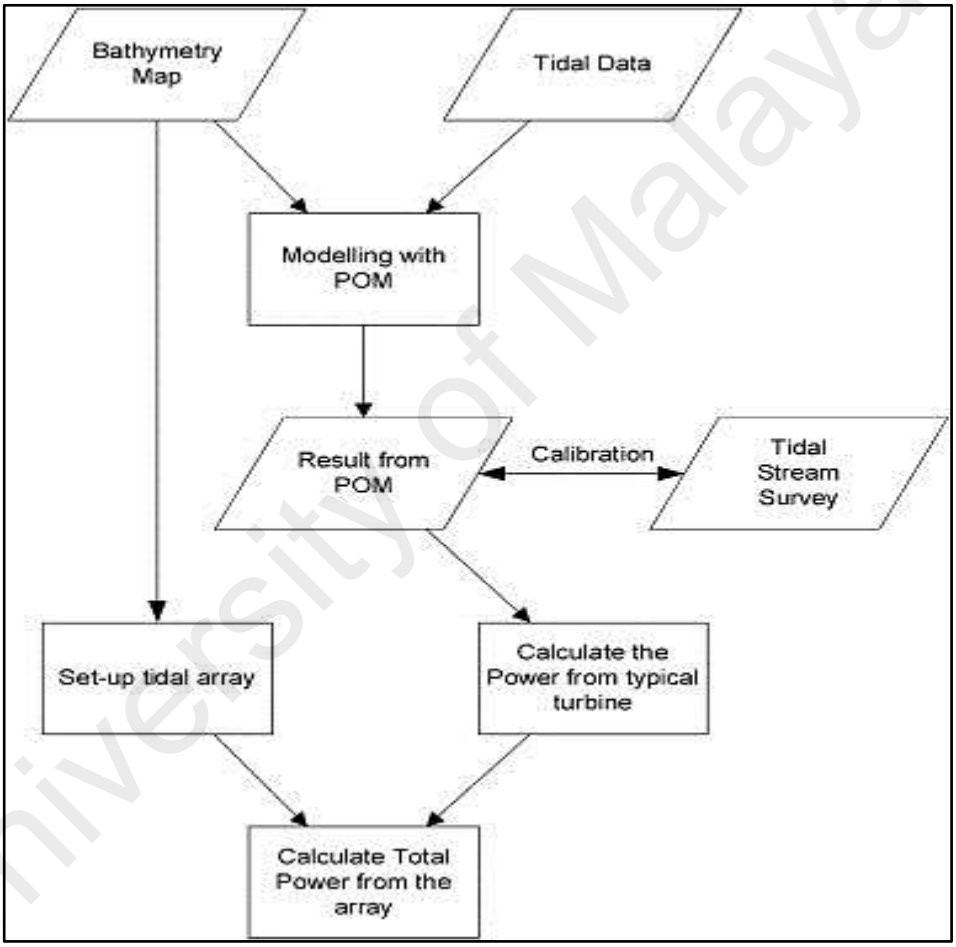

Figure 2.18 Flow chat for numerical model to assess tidal stream energy resource (Blunden et al., 2013).

Iyser et al. (2013), in a recent work analysed tidal power from first generation tidal current turbine for seven major sites located around United Kingdom (Figure 2.19). This work incorporated constraints relating to economy, tidal technology potential, and

environmental limit to energy extraction. The tidal flow data were obtained from Marine Atlas and analysed using Admiralty Total Tide software. The study estimates tidal energy at selected sites to be 17 TWh/year for an installed capacity of 7.8 GW.

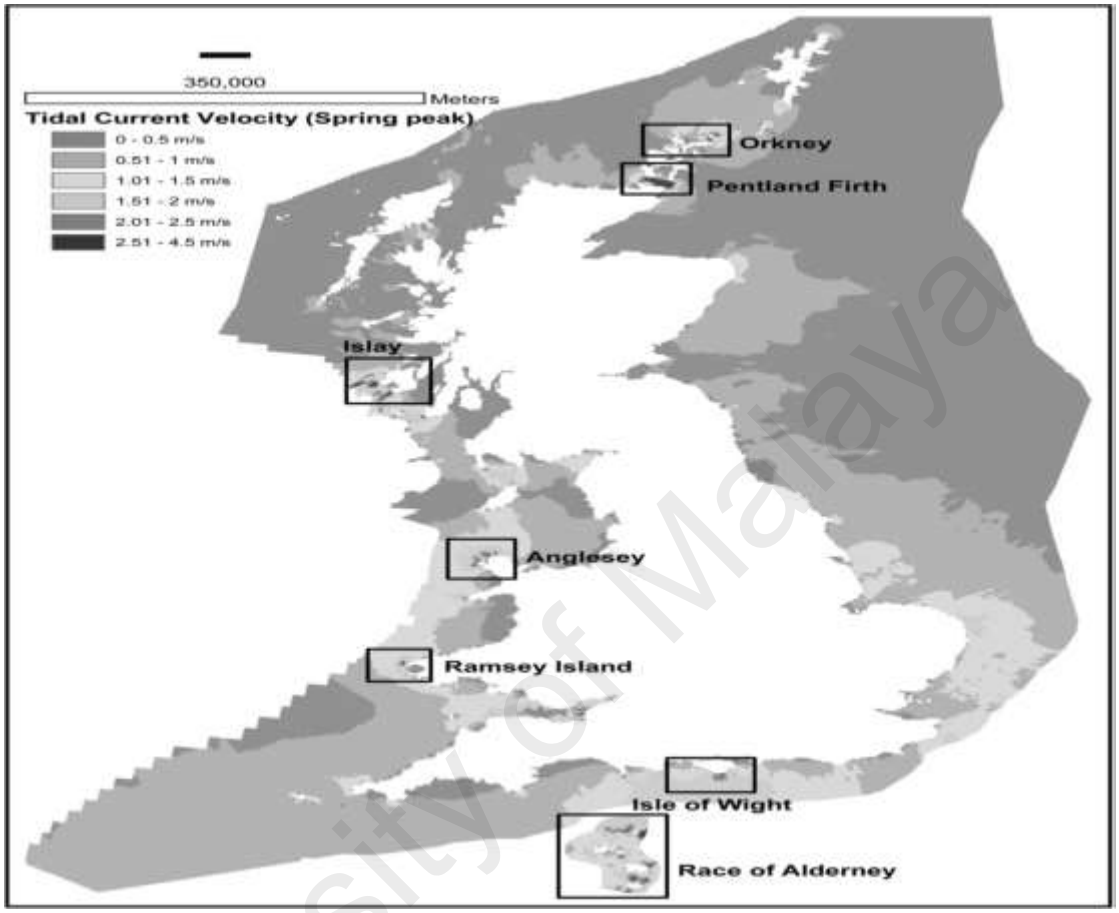

Figure 2.19 Mean spring peak current and specific regions of interest in the UK waters (Marine Atlas, UK) (Iyser et al., 2013).

The Pentland Firth is focal point for companies seeking to develop tidal stream power devices (Draper et al., 2014). The Pentland Firth is strait between Scotland and the Orkney Islands. Draper et al. (2014), used a depth averaged numerical model for estimating that 4.2 GW of power can be extracted from the site. Tidal flow simulation used DG-ADCIRS, a numerical solver for shallow water equations. The model bathymetry used survey and charted hydrographical data provided by Seazone Ltd. This model calculates extractable power from tidal stream using an equivalent depth-averaged bed roughness C_{te}. This roughness coefficient represents deployment of tidal

devices across cross-section A_b. The maximum average power is determined using equation

$$\bar{P} = \frac{1}{T}\int_0^T \left(\iint_{Ab} \rho C_{te} |u^3| \, dA\right) dt \tag{10}$$

where T is the tidal cycle, (12.41 hours for M2 tide) and ρ is the density of seawater. This study considered several locations (A to E) for placing tidal current device for calculating extractable power. Figure 2.20 shows region with significant tidal flow in the Pentland Firth.

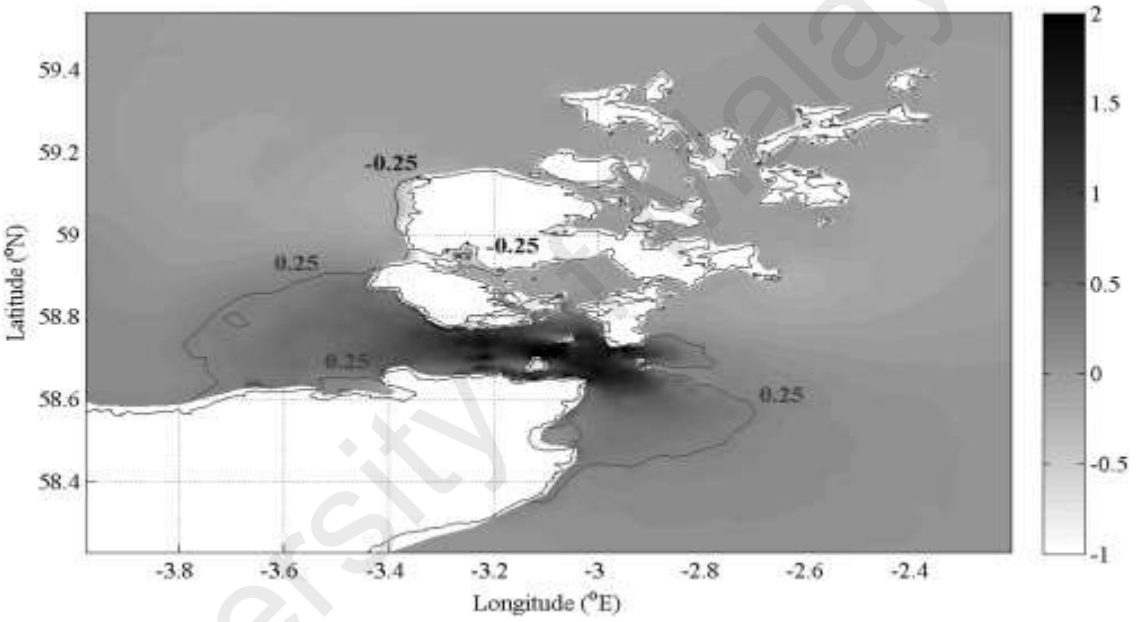

Figure 2.20 Tidal flow speeds in the Pentland Firth from the numerical model(Draper et al., 2014).

Chen et al. (2013a), in their work examined tidal energy resource in the Kinmen Island of Taiwan. This work used a refined three dimensional, semi implicit Euler Lagrange finite element model (SELFE). Kinmen County located on the southeast cost of mainland China comprises of small islands (Chen et al., 2013a). Three point A, B and C were selected for resource assessment, as shown in Figure 2.21. The study estimated annual energy outputs using a twin turbine rotor of 5 m diameter at three locations A,B, and C would be 51, 59, and 68 MWh, respectively. Figure 2.22 shows the distribution

of tidal stream energy flux from the numerical model.

Figure 2.21 Location of Kinmen Island, Taiwan and selected points (A,B,and C) for energy extraction(Chen et al., 2013a).

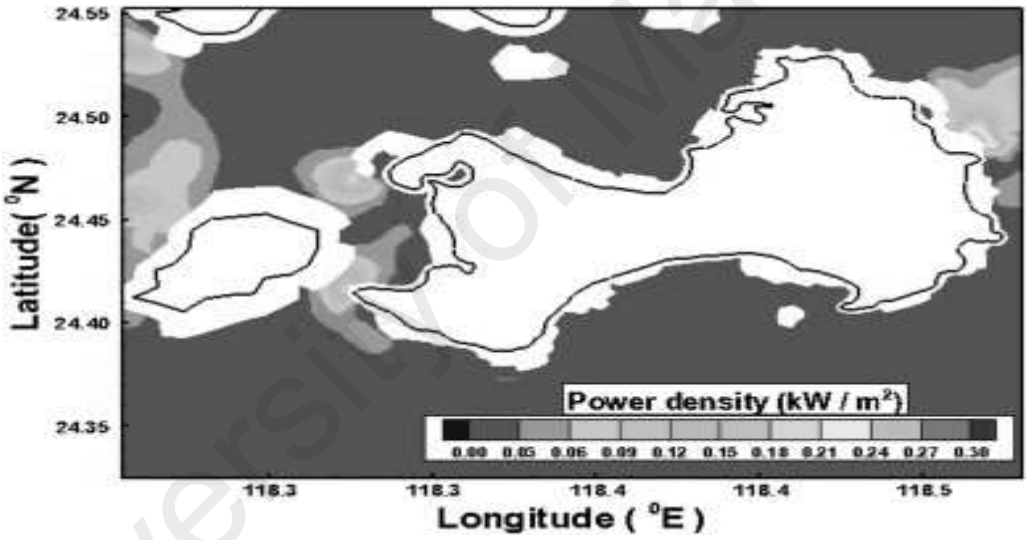

Figure 2.22 Power density distributions around the Kinmen Island at the (a) mid-flood and (b) mid-ebb of the mean spring tide(Chen et al., 2013a).

Numerical model prove to be reliable and cost effective tool on hands of researcher to estimate economic feasibility of tidal stream energy. Ramos et al. (2014), used 3-D numerical model to investigate viability of tidal farm to fulfil the electricity demands of the Port of Ribadeo located in a tidal driven estuary in the North-West Spain (Figure 2.23). The study estimates the Ria de Ribadeo has annual energy density of 72.56 $MWhm^{-2}$. The results also show a tidal farm of 25 turbines with rated power of 400kW is sufficient for electricity demand of the port. This study used Delft3D-FLOW a finite

difference code that solves the baroclinic Navier-Stokes and transport equations.

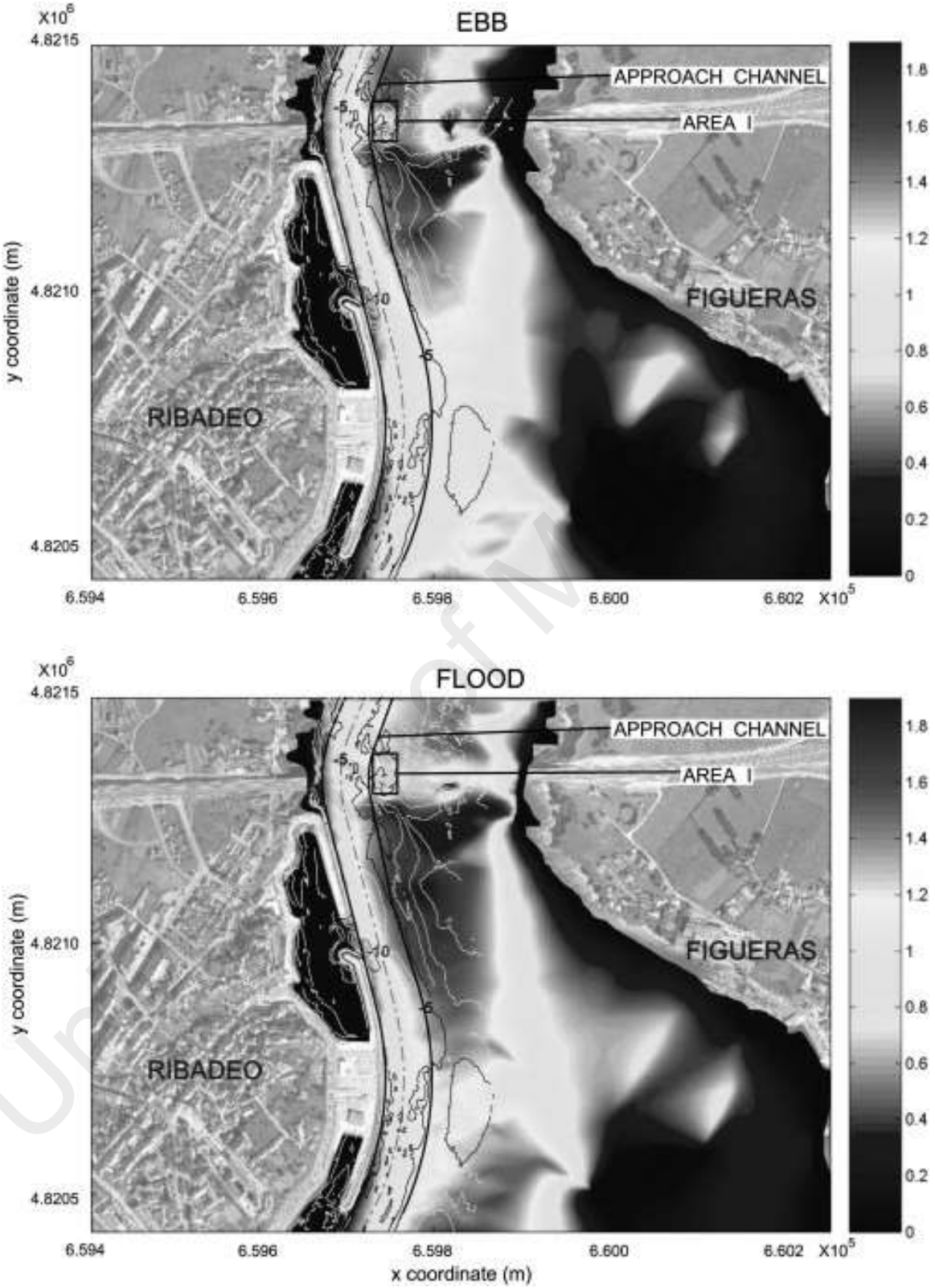

Figure 2.23 Mid-flood and ebb tidal flow speed at the Port of Ribadeo, from numerical model(Ramos et al., 2014).

Work et al. (2013), developed a three dimensional numerical model for assessment of the Beaufort River in the coastal South Carolina, USA. In another work, Draper et al. (2014), implemented a depth-averaged numerical model for the Pentland Firth. The work estimated maximum extractable power in the Pentland Firth using tidal stream converters (Adcock et al., 2013). Chen et al. (2013a), using a three dimensional finite-element model investigated tidal flows and power potential in the Taiwan Strait.

Analytical prediction results in the Alderney race shows selected site can realise energy yields in excess of 7.4TWh/year by use of tidal stream turbines. This estimated energy is equivalent to 2% of the UK requirement for the year 2000 (Bahaj & Myers, 2004). Another work on the same site by same authors indicated that with multiple array configurations, effect of size, and spacing (between rows and turbines), an energy output of 1.34TWh/year can be achieved (Myers & Bahaj, 2005). In year 2005, Electric Power Research Institute (EPRI) reported results from its resource assessment for the North America's tidal energy potential. The estimated total tidal and river in stream potential was estimated to be 140 TWh/year, which is 3.5% of 2004 national electricity supply for USA (Matheson & Thomson, 1973).

Georgia Tech Research Corporation conducted another exhaustive assessment of energy potential from tidal streams in USA ("Assessment of Energy Production Potential from Tidal Streams in the United States" 2011). This project created a database for tidal stream energy potential in the USA. Use of geographical information system (GIS) tools accelerated market for tidal energy conversion technology in USA (Defne et al., 2011a). The tidal currents were numerically modelled using calibrated Regional Ocean Modelling System (ROMS) (Defne et al., 2011b). Thus resource assessments give energy potential for a selected site, which can be extracted with use of tidal current turbines.

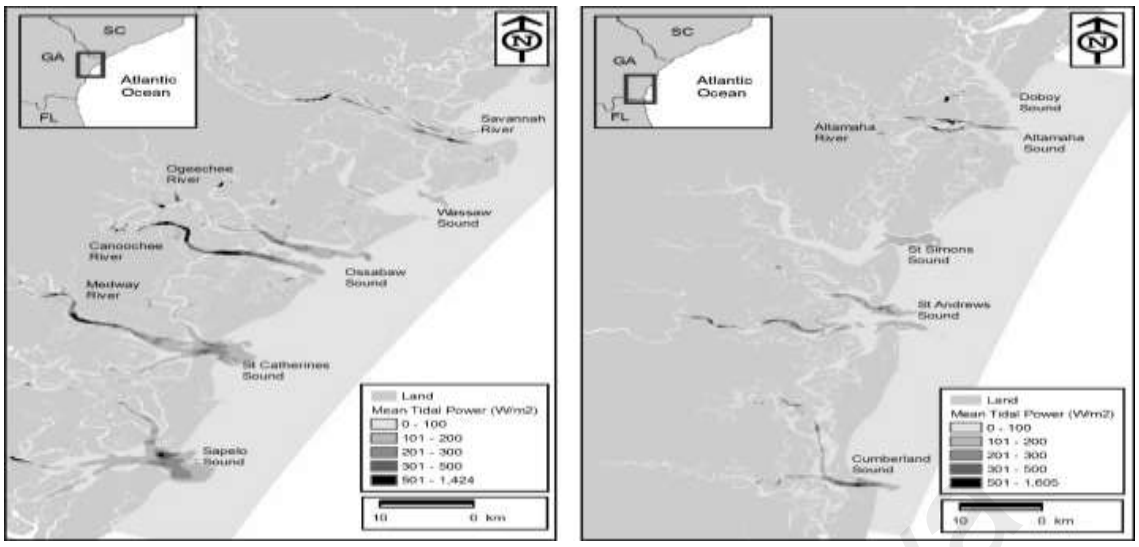

Figure 2.24 Mean power density maps along (a) the northern and (b) the southern coasts of Georgia from the GIS system (Defne et al., 2011a).

All the tidal stream energy present in a tidal channel cannot be extracted due to its effect on natural flow and ecology of tidal channel. Garrett and Cunnins (2005) and Vennell (2012b) developed one-dimensional (1-D) and two-dimensional (2-D) analytical model to investigate the maximum extractable tidal energy in a tidal channel assuming full and partial occupancy. Results suggested only a part of tidal energy is extractable due to possible environmental impact of tidal turbine system.

Yang et al. (2013), conducted 3-D numerical analysis using finite volume coastal ocean model (FVCOM). The study investigates effects on the vertical velocity profile, maximum extractable energy, and volume flux reduction across a channel due to presence of tidal current turbine systems. Results suggest maximum extractable power depends on turbine hub height in water column. It maximizes when hub-height is located in mid water depth.

Tidal energy extraction has effects on the flushing time, volume flux reduction and negatively affects the biogeochemical processes in estuaries. Results show the maximum extractable power from 3-D model fall in the range of analytical results. Therefore, numerical model can be used to assess extractable tidal energy potential in

tidal regions and effects of energy extraction on physical and biogeochemical transport processes.

Researchers widely start to use numerical model to study impacts on the marine environment due to operation of tidal farm. (Ramos et al., 2014), used a validated 3D numerical model to study impacts of tidal farm on transient and residual flows. The transient and residual flow velocities drive environmental processes such as sediment and pollutant transport, and nutrient dispersion. In this case study author's investigated tidal stream farm in the Ria de Ribadeo, an estuary in North west Spain. A momentum sink term in the model equation accounted for the energy extracted by tidal farm. The results showed transient flow patterns are concentrated near the farm, which weakens flow upstream and downstream by 0.25 m/s. However, residual flow circulation of the ria was not disturbed.

Malaysia has long coastline giving it conditions for harnessing tidal current energy. However, limited studies have investigated potential of tidal stream energy in the region. In one study Koh and Lim (2008) investigated potential of tidal stream energy in Malaysian waters. They proposed Pangkor Island and Sandakan coastline as potential site. However, the study provide a rough estimate of the resource contained in the Straits of Malacca, based on existing and rather coarse resolution altimetry products. The study used TPXO altimetry data for tidal flow speed calculation. It should be noted that TPXO satellite data are available over coarse resolution (Dushaw et al., 1997). As discussed earlier in this section that most studies use high resolution numerical model to accurately predict and estimate tidal stream energy. Therefore, in order to accurately investigate tidal stream energy a high resolution numerical model needs to be established. This study focuses on numerically modelling tidal flow in the Straits of Malacca. The Straits of Malacca is on west coast of Peninsular Malaysia which is highly

populated. In addition the Straits of Malacca provides narrow passage to sea water. Thus, investigating tidal stream energy in the Straits of Malacca can benefit large population on the west coast.

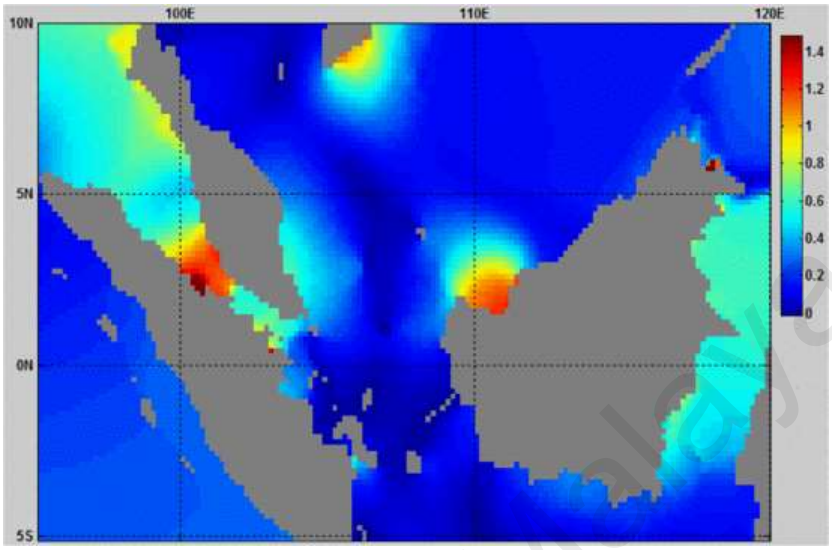

Figure 2.25 TPXO altimetry data for tidal flow in the Straits of Malacca and South China Sea (Koh & Lim, 2008).

2.7 Environmental effects of Marine Renewable Energy

Energy extraction from ocean alters the natural sea environments. Therefore, researchers study effects of energy extraction, device presence, and other ecological impact in short and long term basis. This study primarily concentrates on investigating flow speed, site selection and energy estimation for tidal stream energy. However, a literature review was conducted using previous studies in order to understand environmental impacts.

2.7.1 Marine Life

Currently, various marine species face extinction due to human activities. It is vital for research to ensure that the deployment of tidal current turbines does not intervene in or disrupt the natural habitats of marine life. The possible effects of sound, vibration, heat, oil spill and other effects need to be considered before the commercial operation of tidal farms. The effects of tidal current turbines can be static, dynamic, chemical, acoustic,

electromagnetic, energy removal and cumulative (Polagye, 2010a). This section highlights major findings from studies which try to address the environmental aspects of tidal current turbine installation.

The Fundy Energy Research Network (FERN) in the Acadia Centre for Estuarine Research Canada is an organisation which is investigating the biological and ecological effects alongside the development of tidal current turbines. It is involved in constant observation of marine life and environment. It monitors and tracks fishes and mammals to study the impacts of tidal turbines. Noise pollution is studied by the measurement and characterisation of both ambient and device noises. VEMCOTM acoustic transmitters are implanted in marine animals to monitor changes in their behaviour and movements (Redden, 2010). Marine Current Turbines Ltd (MCT) conducted a comprehensive study on the environmental impact of its marine energy devices (SeaGen) (Keenan et al., 2011) in Strangford Lough. The main conclusion of the report claimed that no major impact on the marine life occurred in Strangford Lough. However, a small scale change on seals' behaviour and distribution was observed. Seals attempted to avoid the marine current structure. The seabed life was also monitored and no evidence of significant changes was found.

Extraction of marine energy near to shore may change the flow patterns and water mixing. It can alter food delivery patterns, marine organism reproduction patterns, and modify temperature variation (Myers & Bahaj, 2010). These findings were reported in an environmental study of the Northwest National Marine Renewable Energy Center in the University of Washington. Nevertheless, the report stated that not all effects might lead to negative impacts on marine life. Most of the environmental effects from tidal current turbines will be the same as in the offshore wind and oil industry. Therefore, the information from the offshore wind and oil industry can provide critical inputs (Polagye, 2010b).

2.7.2 Bio-Fouling

Oceans provide habitats for living organisms and micro-organisms. Tropical waters provide better nutrients for faster growth of these habitats compared to other parts on the Earth(Chua, 1979) . Thus, deployment of tidal current turbines would interact with habitats. As previous section discussed study need to be carried out to analyse the effects of such deployments on marine life. At the same time, sea water can hamper the functioning of turbines through fouling. Fouling occurs in sea water, but more so in tropical waters (Chua, 1979; Leijon et al., 2006). The main fouling organisms found in the Straits of Malacca are compound tunicates (Botryllus,), green mussels (Perna Viridis), oysters (Pinctada), algae, barnacles, amphipods, nereids, serpulids, and gastropods (Chua, 1979; Koo et al., 2012; Saharuddin et al., 2012). Green mussels and algae can impact on rotor blades, while Botryllus can impacts on the support structures of the tidal turbines(Shi et al., 2013). Therefore, turbine blades and structures need to be coated with antifouling materials in order to protect them from the repository stresses (Saharuddin et al., 2012; Shi et al., 2013).

2.7.3 Ocean Health Index

Marine renewable energy generates electricity using technologies such as tidal barrage, tidal current turbines, wave converters, salinity gradient converters and ocean thermal converters. Offshore tidal and wave farms are the new industries currently occupying the marine spaces. Table 2.3 list the effect of marine technologies on environment . In a comprehensive literature review we found marine renewable energy have both positive and negative effects. Halpern et al. (2012) work on the ocean health index (OHI) recently published in *Nature* measures the healthiness of the ocean within 171 Exclusive Economic Zones (EEZs). This review proposed, to relate the marine renewable energy industry to ocean healthiness quantitatively using OHI. The study

identified data gaps and suggests improvements in treatment of MRE forOHI calculations. It is suggested to include MRE effects under pressure *(p_i)* or resilience *(r_i)* variables based on the MRE technology type, stage of operation and its effects on OHI goals.

Table 2.3 Environmental impact due marine renewable energy on human and sea life.

	Tidal Energy	**Wave Energy**	**OTEC**	**Salinity Gradient**
Physical Presence of Device	Physical barriers to migratory species.(Masden et al., 2009)	Artificial habitat for different organisms, attracts pelagic organisms, providing fish aggregation (Addis et al., 2006; Langhamer et al., 2009).	Large pipes extend to deep sea, new habitat for species (creating reef effect)	
Dynamics Effects of Devices and Energy Removal Effects	Turbine blade strike due to high tip velocity (danger to diving birds and fishes) Blockage to turbulent and natural flow cause changes to benthic sediment scouring and alteration of sediment transportation (Besio & Losada, 2008).	Restricts vertical movement of organisms, prey and predator aggregation. Restriction of shipping lanes (transportation)	Effects not known	
Chemical	Potential spill of hydraulic fluid and leaching of anti-fouling plants	Potential spill of hydraulic fluid and leaching of anti-fouling plants.	Potential spill of ammonia highly dangerous to fishes and leaching of anti-fouling paints.	
Acoustic	Noise has effects on sea animal communication, reproduction, orientation, and prey and predator	Noise has effects on sea animal communication, reproduction, orientation, and prey and		

	sensing.	predator sensing.		
Electro-Magnetic Fields (EMF)	Localised EMFs created around cables transiting electricity have effect on migrating sea species (Wilhelmsson & Malm, 2008)	Localised EMFs created around cables transiting electricity have effect on migrating sea species (Kirschwink, 1997; Wilhelmsson & Malm, 2008)		Same as other technologies
Physical Presence of Device	Physical barriers to migratory species.	Artificial habitat for different organisms, attracts pelagic organisms providing fish aggregation.	Large pipes extend to deep sea, new habitat for species (creating reef effect)	

2.8 Summary

This section reviewed various aspects of tidal stream energy related to present study. Clearly various nations start to look at tidal stream energy as viable renewable source for generating electricity. Seagen a 1.2 Mw converter is the world's first commercial tidal current turbine in operation at the Strangford Lough, Northern Ireland. Many projects are in development and commissioning stages. This chapter looked into multiple aspects of tidal stream energy development, such as design aspect of commercial TCT, studies related to environmental impact; methods for assessing power potential; criteria for selecting site; parameters governing availability of tidal stream energy; also discussed the theoretical, experimental and numerical research works. Studies investigating tidal stream energy resources need to look into bathymetry of area; magnitude of flow speed during tidal cycle; power potential; environmental impacts; and commercial feasibility.

Various commercial converts exist for harnessing tidal stream energy for generating electricity. However, this review also indicates that TCT design is still in early stages of

developments. Research works primarily focus on improving TCT design, performance, structural stability and other related technological issues. At same time various research works, focus to identify site in ocean with higher concentration of tidal stream energy. This work falls into this category of research. Investigating tidal stream energy resource primarily requires through understanding of sea bed and flow conditions in area of interest. Further, investigators estimate power potential of selected site using flow data. This review also looked into project development issues such as environmental impact studies, array design and development; fixture and moorings.

Researchers use theoretical, numerical and experiment methods for assessing tidal stream energy resources. Based on this review it is clear that field measurements require huge capital. Therefore, this study uses numerical method for investigating tidal flow speed and bathymetry. In this regard, the author reviewed works which used numerical tools for investigating tidal stream energy resources from across the world. Findings suggest researchers prefer using two-dimensional and three-dimensional numerical model for obtaining flow speed, as they closely depict real scenario. However, some research works also use theoretical model. This work uses three dimensional numerical model and satellite data for estimating tidal flow, and investigating sea depth respectively. Further this study uses theoretical method for estimating power potential. Literature review found no research work thoroughly investigated tidal stream energy resources in the Straits of Malacca using accurate method. Therefore, this work tried using robust reliable methods for investigating tidal stream energy resources of the Straits of Malacca.

CHAPTER 3

METHODOLOGY

3.1 Introduction

Presents study investigated the characteristics of sea depth (bathymetry), speed of tidal stream, and power potential in the Straits of Malacca. In this regard a numerical model was developed to obtain dynamics of the tidal flow using Princeton Ocean Model (POM).

Figure 3.1 shows the work flow and various methods used in the present investigation for achieving the objectives. Black rectangle represents the three objectives of this study i.e. (*i*) determining speed of tidal flow; (*ii*) Select sites with high tidal energy flux; and (*iii*) computing power potential.

- First, the flow chart presents the process for creating the numerical model of the Straits. Major steps involved in preparing the numerical model includes creating the initial and boundary condition, validation, calibration and running the model.
- Second step of process involves setting up the criteria for selecting suitable sites with high concentration of tidal energy flux. Two parameters are vital to determine suitability of a site i.e. suitable sea depth and tidal flow speed.
- Last step describes method for estimating the power potential of selected site. It involves defining the design specifications and power rating of tidal current turbines. This study first computed power potential of selected site using single tidal current turbine. Further, a set of multiple turbines were considered to determine aggregate power potential.

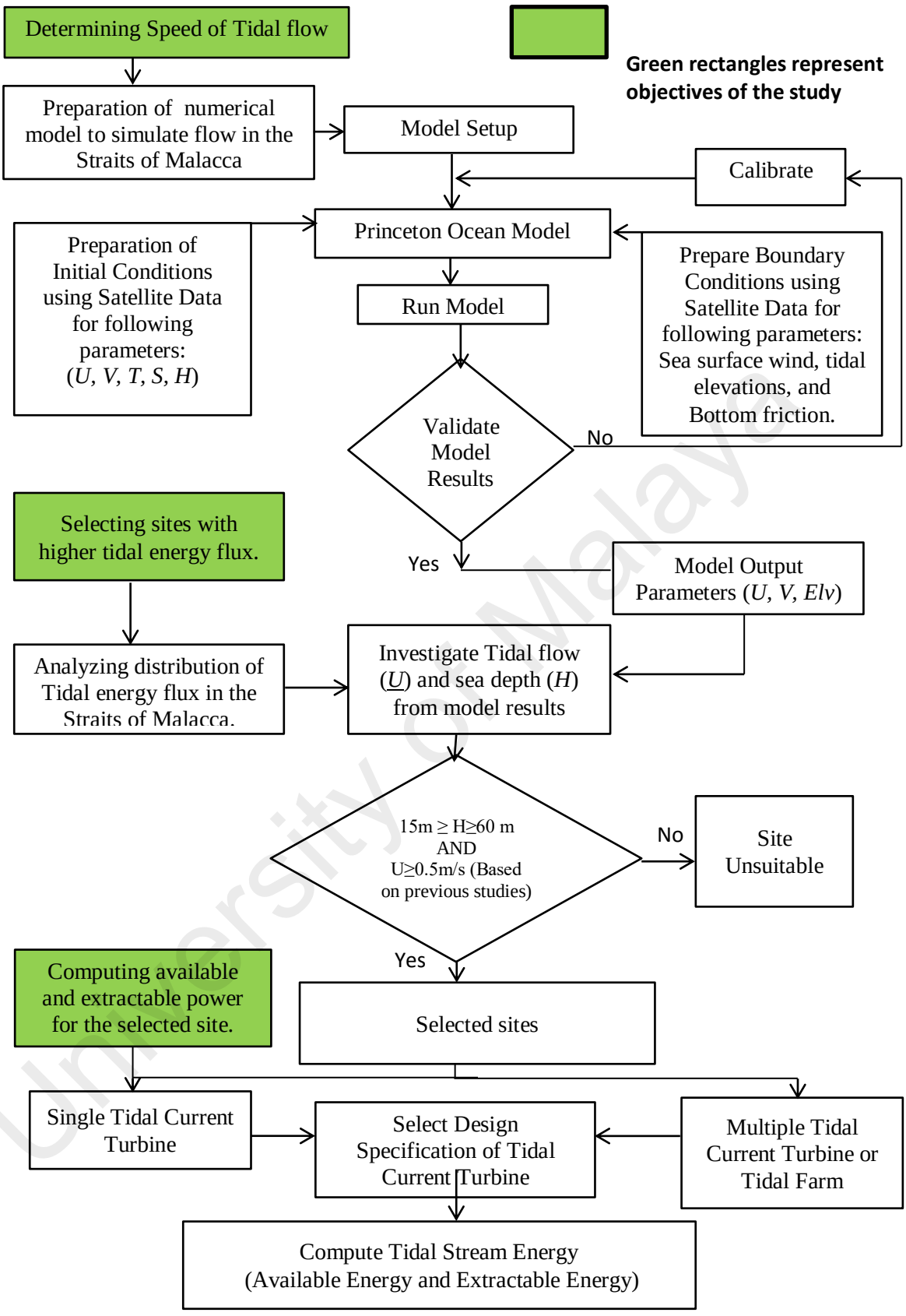

Figure 3.1 Flow of research work.

Section 3.2 to 3.6 discusses working principle of POM. Section 3.7 shows the model setup for the Straits of Malacca. This study investigated speed and sea depth throughout the Straits of Malacca in order to select site with high concentration of tidal stream energy. Section 3.9 sets the criteria for selecting site using obtained results. Section 3.10 discusses analytical method for determining power potential at the selected site using model results. As discussed in the chapter 2, tidal current turbines convert the kinetic energy of tidal flows into useful electricity. This investigation computed the available and extractable tidal stream power for the selected sites by considering design of commercial tidal current turbines. Section 3.10.3 presents the design specification of the selected commercial tidal current turbine.

3.2 Background Theory of Princeton Ocean Model

The Straits of Malacca is tidally driven narrow passage between the Peninsular Malaysia and Sumatra Island. Investigation shows that the Straits have shallow depth along most parts and continental shelf at north. This study first simulates flow speed of tidal stream in the Straits of Malacca. Therefore the study selected a numerical model which could accurately simulate the flow in the shallow coastal waters. Researchers suggest that a numerical model should use the sigma coordinate system for dealing with shallow topographic variability of coastal waters or over continental shelf and slopes. Princeton Ocean Model (POM) uses the sigma coordinate system and produces realistic flow for the coastal waters driven by tides (Mellor et al., 1998). POM was developed to solve oceanographic problems. POM is widely accepted and validated model. It is a three-dimensional finite difference, time dependent, sigma (σ) coordinate and coastal ocean circulation numerical model (Mellor, 2004). Researchers use it for modeling oceanographic phenomenon such as waves, tides, oceanic circulation, convection, eddies, global ocean heat budget, sea water temperature and salinity distribution (Mellor, 2004). This study uses POM for modeling the tidal flow in the Straits of Malacca. This section presents theory and numerical modules of POM.

POM code is available from POM home page at http://www.aos.princeton.edu/WWWPUBLIC/htdocs.pom (APPENDIX-A). Alan Blumberg and George L. Mellor initially created this code. In recent years major contributors in developing and maintaining POM comes from following researchers i.e. Tal Ezer, Leo Oey, Jim Herring, Lakshmi kantha and Boris Galperin and others (Mellor, 2004). There are various versions of POM. This study uses POM code called 'pom2k.f'. Users need to write their own code for setting up their own problem. In this way POM code adapts to problem specific local initial conditions, lateral and surface boundary conditions.

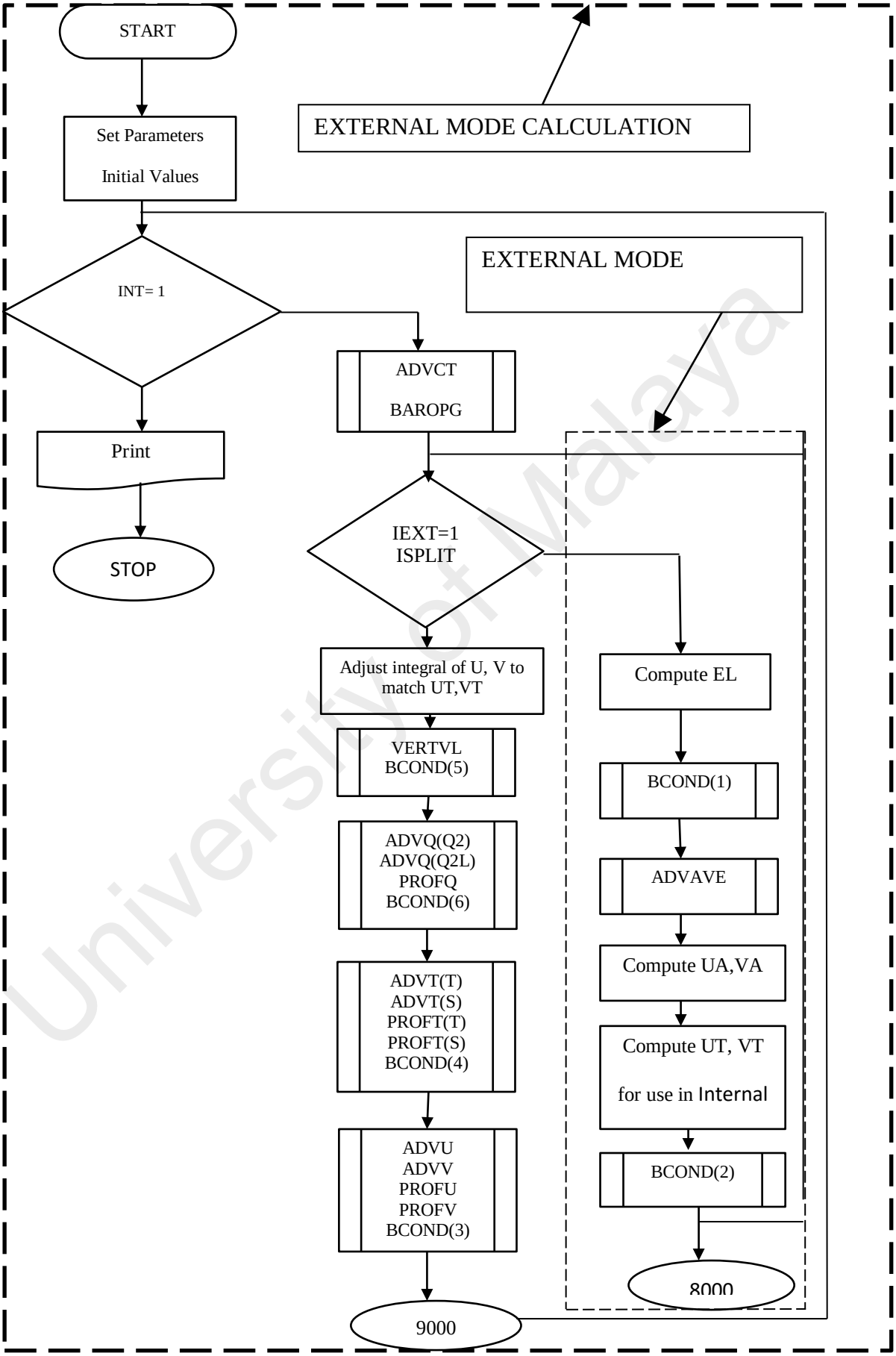

Figure 3.2 Flow diagram of the POM code (Mellor, 2004).

The code uses FORTRAN 77. Figure 3.2 shows flow diagram of code and its subroutines. The principal features of model are as follows:

1. *The vertical coordinate has same number of grid points for various depths. Grid points are scaled on the water column depth, which is also known as sigma coordinate system.*
2. *The horizontal grids use curvilinear orthogonal coordinates and an Arakawa C differencing scheme.*
3. *The vertical time differencing is implicit whereas the horizontal scheme is explicit. This allows fine vertical grid resolution near surface and bottom boundary layers.*
4. *The* vertical *mixing coefficients use second moment turbulence closure sub-model.*
5. *The model has free surface and split time step. The external mode portion of the model is two dimensional and uses a short time step based on the CFL condition and external wave speed. The internal mode is three dimensional and uses a long time step based on CFL condition and internal wave speed(Mellor, 2004) .*

The model uses Arakawa C-grid in horizontal finite difference scheme. The subroutines ADVT, ADVQ, ADVCT, ADVU, ADVV and ADVAVE respectively contains scheme for advection, horizontal diffusion, pressure gradient and Coriolis terms. The subroutine BCOND specifies open boundary conditions. In order to model the Straits of Malacca in POM, local variables were used and are defined in this chapter.

3.3 Governing Equations of Numerical Model

The developed model implements sigma (σ) coordinate along depth and an orthogonal coordinate along the horizontal direction. The sigma coordinate system spans from 0 to

-1. The free surface is located at σ = 0 and the bottom at σ = -1. The transformation is given in eq.3.1 to 3.4:

$$x^* = x, \tag{3.1}$$

$$y^* = y, \tag{3.2}$$

$$\sigma = \frac{z-\eta}{H+\eta}, \tag{3.3}$$

$$t^* = t \tag{3.4}$$

where x, y, z are the Cartesian coordinates; $D = H + \eta$ where H(x,y)is the bottom topography and $\eta(x, y, t)$ is the surface elevation. The σ ranges from σ = 0 at z = η to σ = -1 at z =-H. In the model, slow moving internal gravity waves and fast moving external mode define the dynamics of coastal cycle.

3.3.1 Internal Mode

In the internal mode, the basic equations were embedded in three-dimensional sigma coordinate system.

Continuity equation:

$$\frac{\partial UD}{\partial x} + \frac{\partial VD}{\partial y} + \frac{\partial \omega}{\partial \sigma} + \frac{\partial \eta}{\partial t} = 0 \tag{3.5}$$

where *U*, *V*, are the mean velocity in the horizontal direction and ω is the mean velocity in the vertical σ directions; η is the sea surface elevation above undisturbed level. And '*H*' is the depth of sea; '*D*' is the summation of η and H.

The momentum equation:

$$\frac{\partial UD}{\partial t} + \frac{\partial U^2 D}{\partial x} + \frac{\partial UVD}{\partial y} + \frac{\partial U\omega}{\partial \sigma} - fVD$$

$$+ \; gD\frac{\partial \eta}{\partial x} + \frac{gD^2}{\rho_o}\int_\sigma^0 \left[\frac{\partial \rho}{\partial x} - \frac{\sigma}{D}\frac{\partial D}{\partial x}\frac{\partial \rho}{\partial \sigma}\right] d\sigma = \frac{\partial}{\partial \sigma}\left[\frac{K_M}{D}\frac{\partial U}{\partial \sigma}\right] + F_x \tag{3.6}$$

$$\frac{\partial VD}{\partial t} + \frac{\partial VUD}{\partial x} + \frac{\partial V^2 D}{\partial y} + \frac{\partial V\omega}{\partial \sigma} - fUD$$

$$+ \; gD\frac{\partial \eta}{\partial y} + \frac{gD^2}{\rho_o}\int_\sigma^0 \left[\frac{\partial \rho}{\partial y} - \frac{\sigma}{D}\frac{\partial D}{\partial y}\frac{\partial \rho}{\partial \sigma}\right] d\sigma = \frac{\partial}{\partial \sigma}\left[\frac{K_M}{D}\frac{\partial V}{\partial \sigma}\right] + F_y \tag{3.7}$$

where g is the acceleration due to gravity; ρ_o is the density of sea water; ρ is the fluid density minus the horizontal averaged density;

Transport equations of temperature and salinity:

$$\frac{\partial TD}{\partial t} + \frac{\partial TUD}{\partial x} + \frac{\partial TVD}{\partial y} + \frac{\partial T\omega}{\partial \sigma} = \frac{\partial}{\partial \sigma}\left[\frac{K_H}{D}\frac{\partial T}{\partial \sigma}\right] + F_T - \frac{\partial R}{\partial z}$$

$$\frac{\partial SD}{\partial t} + \frac{\partial SUD}{\partial x} + \frac{\partial SVD}{\partial y} + \frac{\partial S\omega}{\partial \sigma} = \frac{\partial}{\partial \sigma}\left[\frac{K_H}{D}\frac{\partial S}{\partial \sigma}\right] + F_S \tag{3.8}$$

where T is the temperature and S the is salinity; R is the short wave radiation flux and K_H is the vertical turbulent flux coefficients;

Turbulence energy equations are as follows:

$$\frac{\partial q^2 D}{\partial t} + \frac{\partial Uq^2 D}{\partial x} + \frac{\partial Vq^2 D}{\partial y} + \frac{\partial \omega q^2}{\partial \sigma}$$

$$= \frac{\partial}{\partial \sigma}\left[\frac{K_q}{D}\frac{\partial q^2}{\partial \sigma}\right] + \frac{2K_M}{D}\left[\left(\frac{\partial U}{\partial \sigma}\right)^2 + \left(\frac{\partial V}{\partial \sigma}\right)^2\right] + \frac{2g}{\rho_0}K_H\frac{\partial \tilde{\rho}}{\partial \sigma} - \frac{2Dq^3}{B_1 l} + F_q \tag{3.9}$$

$$\frac{\partial q^2 lD}{\partial t} + \frac{\partial Uq^2 lD}{\partial x} + \frac{\partial Vq^2 lD}{\partial y} + \frac{\partial \omega q^2 l}{\partial \sigma}$$

$$= \frac{\partial}{\partial s}\left[\frac{K_q}{D}\frac{\partial q^2 l}{\partial \sigma}\right] + E_1\left(\frac{lK_M}{D}\left[\left(\frac{\partial U}{\partial \sigma}\right)^2 + \left(\frac{\partial V}{\partial \sigma}\right)^2\right] + \frac{E_3 g}{\rho_0}K_H\frac{\partial \tilde{\rho}}{\partial \sigma}\right) - \widetilde{W}\frac{Dq^3}{B_1} + F_l \tag{3.10}$$

where l is the turbulence length scale; K_M, K_q are the vertical turbulent flux coefficients; and $\widetilde{W}$ is the wall proximity function.

The model uses horizontal viscosity and diffusion part as given below:

$$F_x = \frac{\partial}{\partial x}(H\tau_{xx}) + \frac{\partial}{\partial y}(H\tau_{xy}) \tag{3.11}$$

$$F_y = \frac{\partial}{\partial x}(H\tau_{xy}) + \frac{\partial}{\partial y}(H\tau_{yy}) \tag{3.12}$$

$$F_T = \frac{\partial}{\partial x}\left(HA_H\frac{\partial T}{\partial x}\right) + \frac{\partial}{\partial y}\left(HA_H\frac{\partial T}{\partial y}\right) \tag{3.13}$$

$$F_S = \frac{\partial}{\partial x}\left(HA_H\frac{\partial S}{\partial x}\right) + \frac{\partial}{\partial y}\left(HA_H\frac{\partial S}{\partial y}\right) \tag{3.14}$$

$$F_{q^2} = \frac{\partial}{\partial x}\left(HA_H\frac{\partial q^2}{\partial x}\right) + \frac{\partial}{\partial y}\left(HA_H\frac{\partial q^2}{\partial y}\right) \tag{3.15}$$

$$F_{q^2 l} = \frac{\partial}{\partial x}\left(HA_H\frac{\partial q^2 l}{\partial x}\right) + \frac{\partial}{\partial y}\left(HA_H\frac{\partial q^2 l}{\partial y}\right) \tag{3.16}$$

where q^2 is the turbulence energy; $\tau_{xx} = 2A_M\frac{\partial U}{\partial x}$; $\tau_{yy} = 2A_M\frac{\partial V}{\partial y}$; and $\tau_{xy} = \tau_{yx} = A_M\left[\frac{\partial U}{\partial y} + \frac{\partial V}{\partial x}\right]$. Here A_M are horizontal turbulence coefficients.

3.3.2 Vertical Boundary Condition

The vertical boundary conditions for continuity equation are as follows:

$$\omega(0) = \omega(-1) = 0 \tag{3.17}$$

The boundary condition for the momentum equations are as follows:

$$\frac{K_M}{D}\left(\frac{\partial U}{\partial \sigma}, \frac{\partial V}{\partial \sigma}\right) = -(< wu(0) >, < wv(0) >), \sigma \to 0 \tag{3.18}$$

$$\frac{K_M}{D}\left(\frac{\partial U}{\partial \sigma}, \frac{\partial V}{\partial \sigma}\right) = C_z[U^2 + V^2]^{0.5}(U, V),\ \sigma \to -1 \tag{3.19}$$

$$C_z = MAX\left[\frac{k^2}{[ln\{(1+\sigma_{kb-1})H/z_0\}]^2}, 0.0025\right] \quad (3.20)$$

where k = 0.4 is the von Karman constant and z_0 is the roughness parameter. The equation 3.18 - 3.20 are derived by matching solution to the law of the wall.

The boundary conditions on transport equation for salinity and temperature are as follows:

$$\frac{K_H}{D}\left(\frac{\partial T}{\partial \sigma}, \frac{\partial S}{\partial \sigma}\right) = -(< w\theta(0) >), \sigma \to 0 \quad (3.21)$$

$$\frac{K_H}{D}\left(\frac{\partial T}{\partial \sigma}, \frac{\partial S}{\partial \sigma}\right) = 0, \ \ \sigma \to -1 \quad (3.22)$$

The boundary condition for the turbulence energy equations are as follows:

$$\left(q^2(0), q^2 l(0)\right) = \left(B_1^{2/3} u_\tau^2(0), 0\right) \quad (3.23)$$

$$\left(q^2(-1), q^2 l(-1)\right) = \left(B_1^{2/3} u_\tau^2(-1), 0\right) \quad (3.24)$$

where B_1 is the turbulence closure constant; and u_τ is the friction velocity at the top or bottom.

3.3.3 External mode

The external mode equations are obtained upon integrating the internal mode equations over the depth; from $\sigma = -1 \ to \ \sigma = 0$ on boundary conditions mentioned in the section 3.3.2.

The surface elevation equation:

$$\frac{\partial \bar{U} D}{\partial x} + \frac{\partial \bar{V} D}{\partial y} + \frac{\partial \eta}{\partial t} = 0 \quad (3.25)$$

The momentum equations for the external mode are:

$$\frac{\partial \bar{U}D}{\partial t} + \frac{\partial \bar{U}^2 D}{\partial x} + \frac{\partial \overline{UV}D}{\partial y} - f\bar{V}D \quad +$$

$$gD\frac{\partial \eta}{\partial x} - \frac{gD}{\rho_o}\int_{-1}^{0}\int_{\sigma}^{0}\left[D\frac{\partial \rho'}{\partial x} - \frac{\sigma'}{D}\frac{\partial D}{\partial x}\frac{\partial \rho'}{\partial \sigma}\right]d\sigma' d\sigma = -\big(wu(0)\big) + \big(wu(-1)\big) + \tilde{F}_x \quad (3.26)$$

$$\frac{\partial \bar{V}D}{\partial t} + \frac{\partial \bar{U}\bar{V}D}{\partial x} + \frac{\partial \bar{V}^2 D}{\partial y} - f\bar{U}D \quad +$$

$$gD\frac{\partial \eta}{\partial y} \int_{-1}^{0}\int_{\sigma}^{0}\left[D\frac{\partial \rho'}{\partial y} - \frac{\sigma'}{D}\frac{\partial D}{\partial y}\frac{\partial \rho'}{\partial \sigma}\right]d\sigma' d\sigma = -\big(wu(0)\big) + \big(wu(-1)\big) + \tilde{F}_y \quad (3.27)$$

The equations discussed are split into two modes. The vertically integrated equations are in external mode, while the vertical structure equations are in internal mode. This is desirable to save computing time.

3.4 External-Internal mode interaction

Numerical scheme calculates the given variables in the external and internal modes (Figure 3.2-3.3). External mode calculates sea surface elevation (el) and vertically averaged velocities (*ua*, *va*). Internal mode calculates *u*, *v*, *t*, *s* and turbulence quantities.

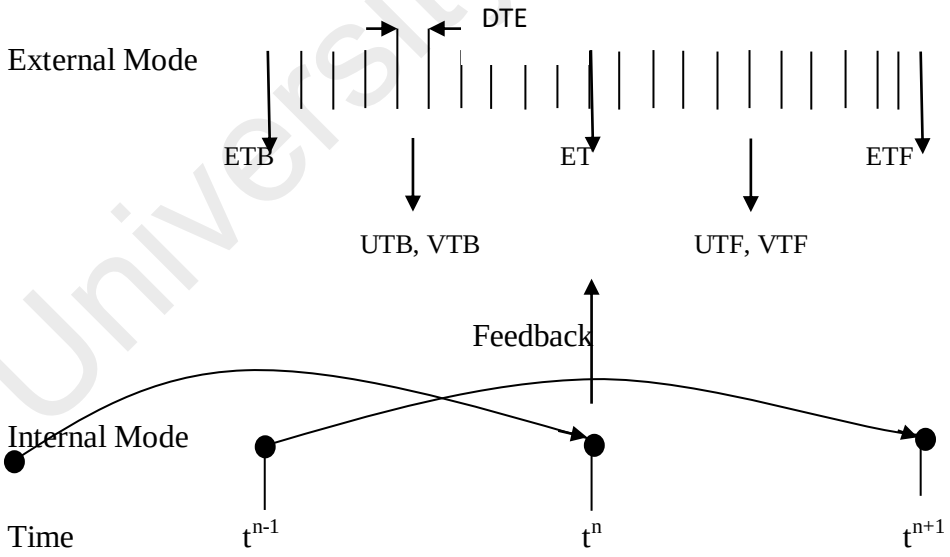

Figure 3.3 Illustration of interaction between external and internal mode.

External mode uses short time step DTE, whereas internal mode uses long time DTI. Given all variables are known at time step t^{n-1} and t^{n} . The external mode leap frongs many time with time step DTE until $t = t^{n+1}$. The external mode provides sea surface tidal elevation to internal mode. The internal mode provides integrals of momentum advection, density integrals and bottom stress to external mode, as shown by feedback line in Figure 3.3.

3.5 Grid Arrangement

POM uses staggered grid arrangement as shown in Figure 3.4 and 3.5 for external and internal mode respectively. The figures also show location of variables on finite difference grid. Figures uses nomenclature of variables similar to that used in the FORTRAN code pom2k.

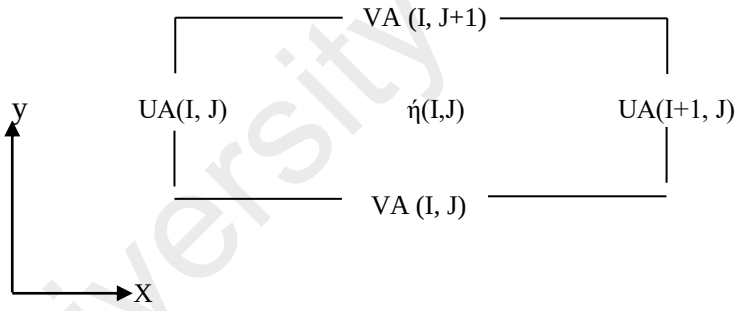

Figure 3.4 Two dimensional grid arrangement for external mode.

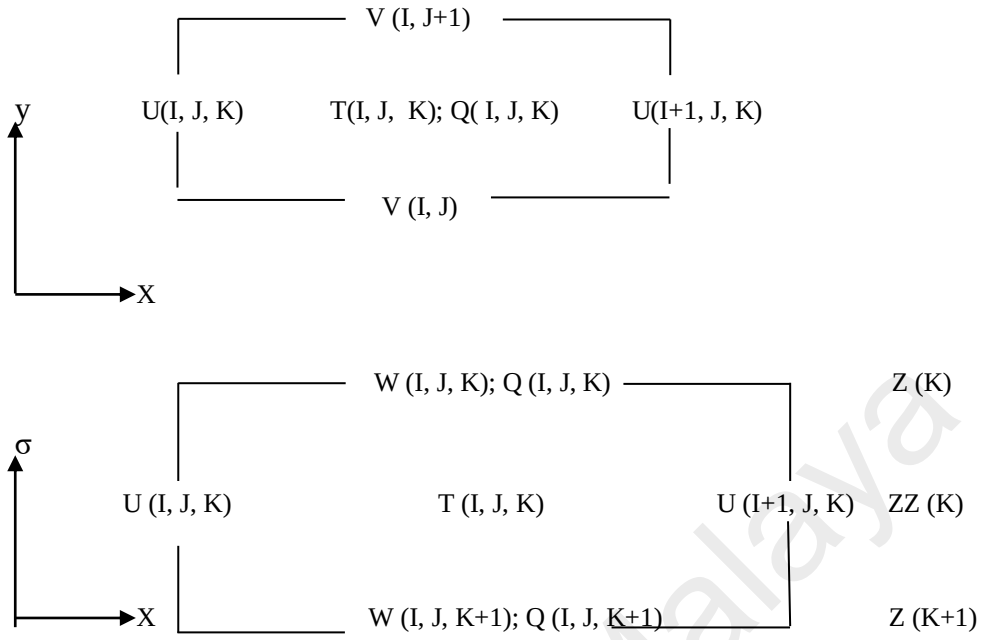

Figure 3.5 Three dimensional grid arrangement for internal mode.

In Figure 3.5 T represents t (seawater temperature), s (seawater salinity) and rho (density). Q represents Km (vertical kinematic viscosity), Kh (vertical diffusivity), q2 (twice the turbulence K.E.), or q2l (turbulence length scale).

3.6 Time Step Constraints

Numerical scheme applies the Courant Friedrichs Levy (CFL) computational stability condition on the vertical integrated external mode, transport equations according

$$\Delta t_E \leq \frac{1}{C_t}\left|\frac{1}{\delta x^2}+\frac{1}{\delta y^2}\right|^{-\frac{1}{2}} \tag{3.28}$$

where $C_t = 2(g\,H)^{1/2} + U_{max}$; U_{max} maximum velocity.

The internal mode time step criterion is similar to external mode as shown in equation 3.29.

$$\Delta t_I \leq \frac{1}{C_T}\left|\frac{1}{\delta x^2}+\frac{1}{\delta y^2}\right|^{-\frac{1}{2}} \tag{3.29}$$

where $C_T = 2C + U_{max}$; C_T is the maximum internal gravity wave speed (m/s).

Figure 3.4 and 3.5 shows the grid arrangement for external and internal mode respectively. In setup for a coastal ocean condition ration of time steps $\Delta t_I / \Delta t_E$ is 30-80 or larger (Ezer et al., 2002).

3.7 Model Setup for the Straits of Malacca

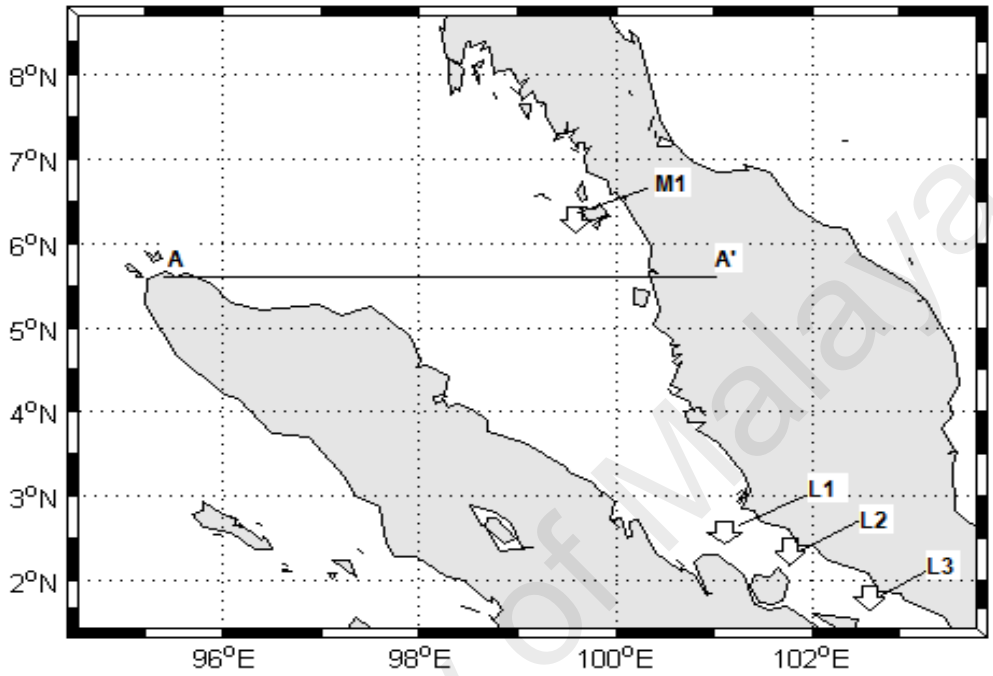

Figure 3.6 Map showing numerical domain and observation points L_1, L2, L3, and M_1 in the Straits of Malacca. Along line AA' a vertical profile of sea water salinity and temperature was investigated. .

The Strait of Malacca model has free surface, bottom following vertical sigma coordinate. The computational mesh is an orthogonal curvilinear coordinate based on work of Blumberg and Mellor (1983) . The model domain lay between 1°50' N to 8° N latitude and 95° 50' E to 102°50' E longitude (Figure.3.6). Bathymetry uses ETOPO1 satellite data of one minute interval from the National Geophysical Data Centre (NGDC). See APPENDIX B for source of bathymetry data. Model has four open boundaries. It uses a grid of 110 x 94 in the east (x) and north (y) directions, with horizontal resolution of 800 m (Δx and Δy). Model has 11 layers of sigma coordinate in vertical direction, σ= (0, -0.055556, -0.11111, -0.22222, -0.33333, -0.44444, -0.55556, -0.66667, -0.77778, -0.88889, -1). Model uses a time step of 240 second and output was

saved at hourly interval. Model was run for the month of January-2012 to February-2012. Simulation covered two spring and neap tidal period. A through error analysis was conducted to calibrate and validate the model. Chapter 4 presents the results from error analysis. In addition results were also compared with field measurements and previous studies.

3.7.1 Initial and Boundary Conditions of the Model

Primary variable used for defining the initial conditions includes the sea water density, sea surface salinity, temperature, elevation and flow speed. Primary boundary conditions defined in model includes the sea surface wind velocity, solar heat, and tidal elevations.

The climatological data for seawater salinity (S) and temperature (T) uses satellite data from Levitus94 dataset (Figure 3.7 and Figure 3.8); APPENDIX B. Initial sea water density was defined for each grid in the model (Figure 3.9). Atmospheric boundary forcing for sea surface wind (Figure 3.10) and heat fluxes (Figure 3.11) uses daily reanalysis dataset. It uses satellite data from the European Centre for Medium-Range Weather Forecasts (ECMWF) with 0.5 x 0.5 resolutions; APPENDIX B. Tidal flow speeds of model were compared with measurements from two observation points at T1 and T2. Further validation of monthly surface current was made with previous works of (Wyrtki, 1961) and Rizal et al. (2012) on the Straits of Malacca.

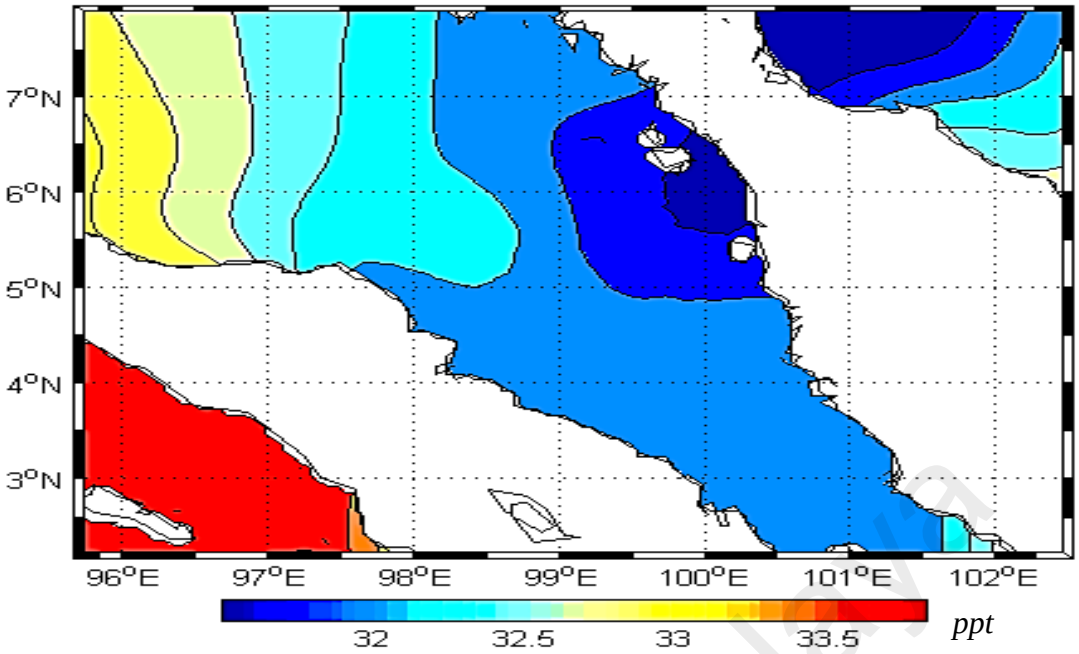

Figure 3.7 Initial conditions of sea surface salinity (unit ppt) used in the numerical model of the Straits of Malacca (1st January-2012).

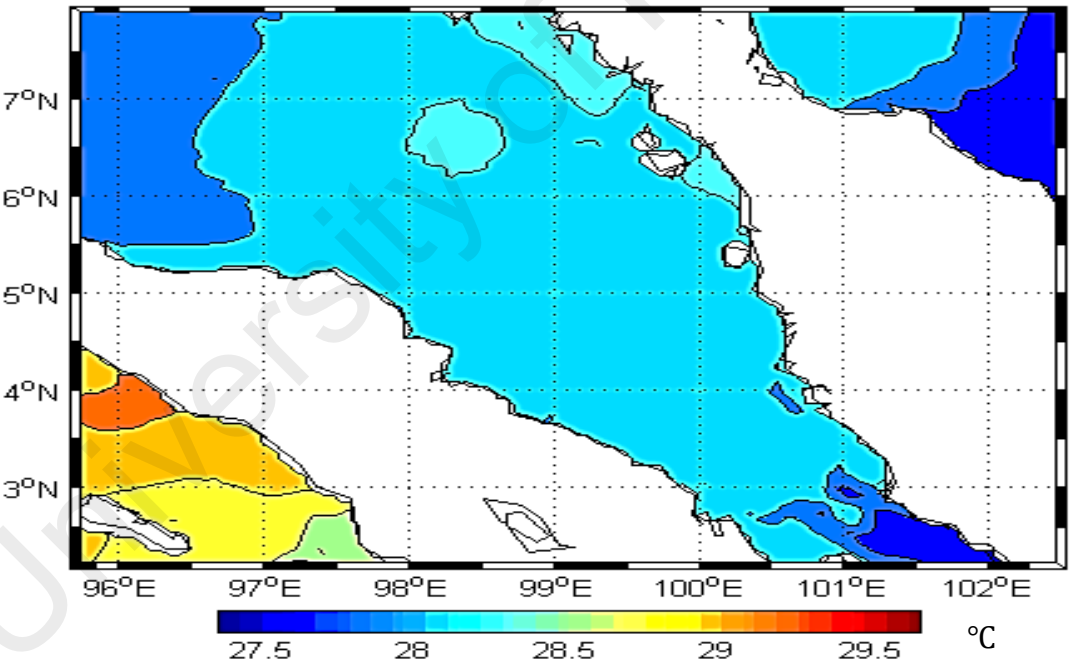

Figure 3.8 Initial condition of sea surface temperature (°C)used in the numerical mode of the Straits of Malacca (1st January-2012).

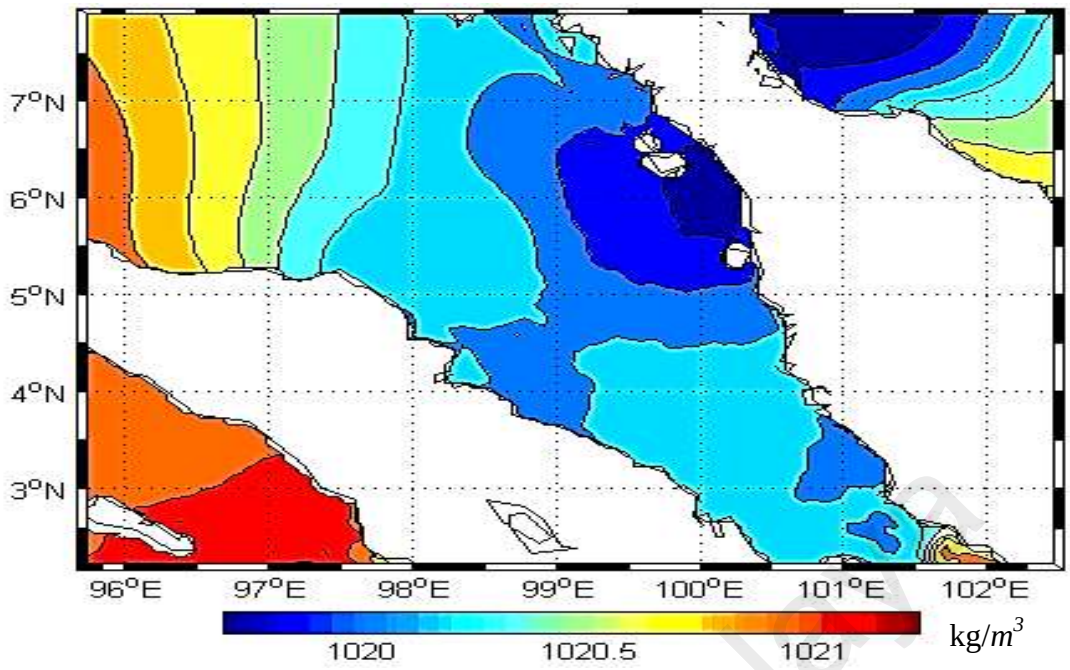

Figure 3.9 Initial condition of sea water density (ρ, kg/m^3) used in the numerical model of the Straits of Malacca (1st January-2012).

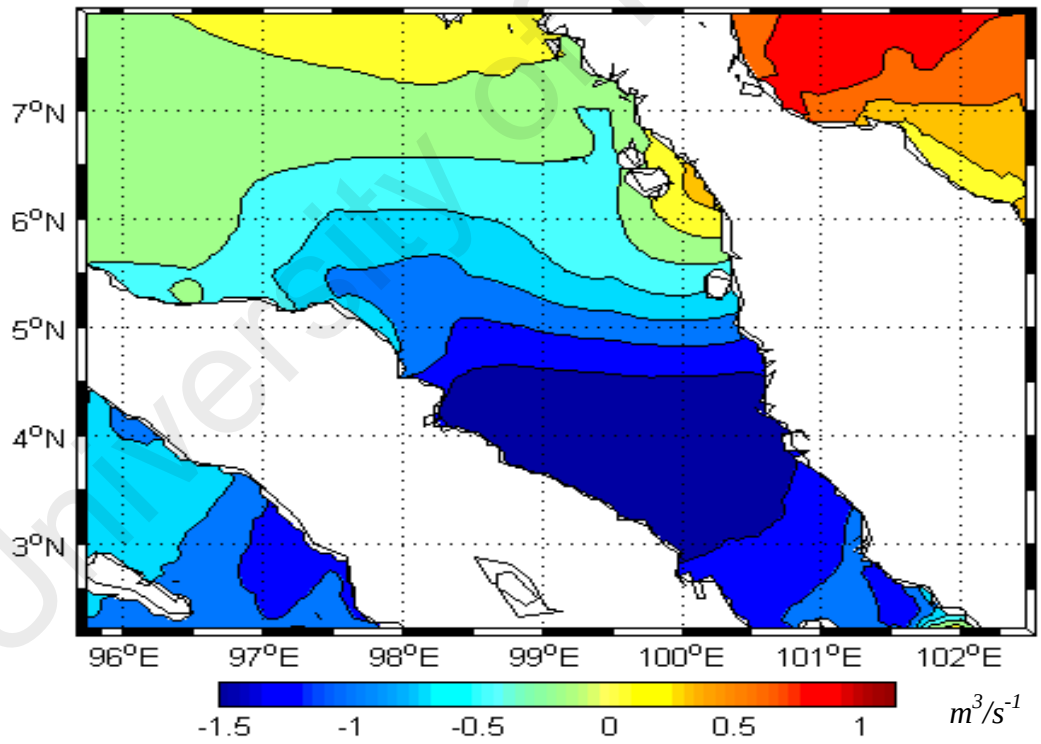

Figure 3.10 Sea surface wind flux (m^3/s^{-1}) in the Straits of Malacca used as surface boundary condition in the model (1st January-2012).

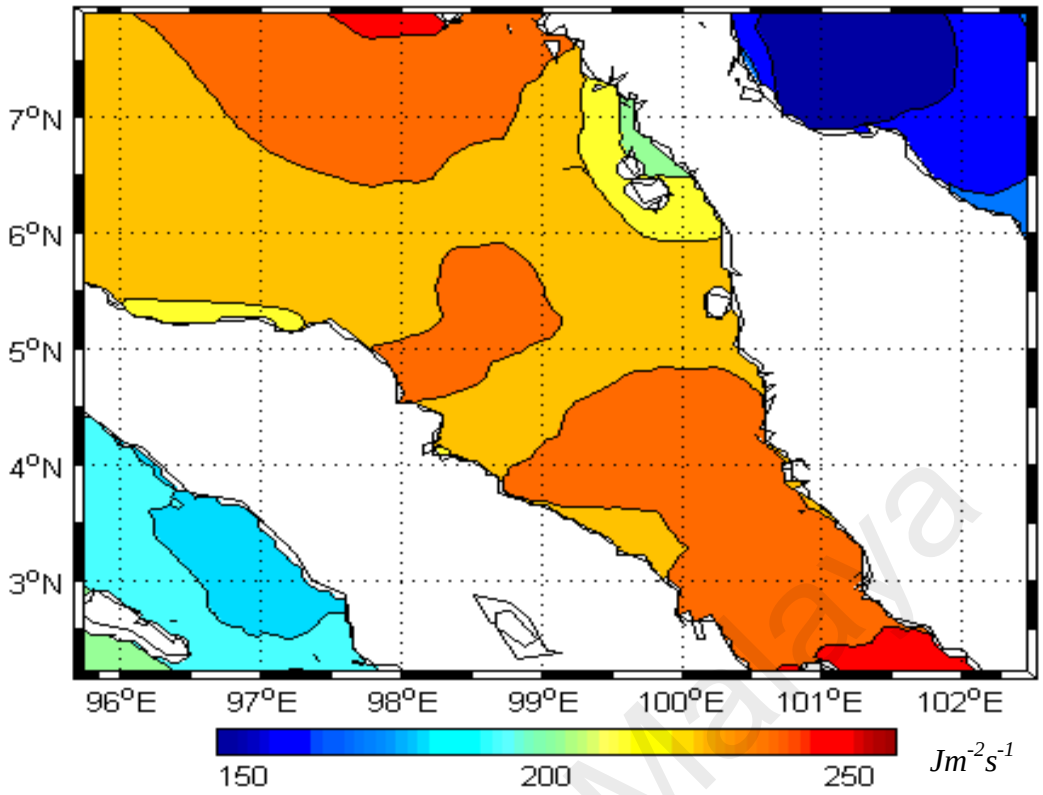

Figure 3.11 Sea surface heat flux ($Jm^{-2}s^{-1}$) in the Straits of Malacca used in the numerical model as surface boundary conditions (1st January-2012).

3.7.2 Tidal Boundary Conditions in the Model

The water in the Straits of Malacca experiences semidiurnal tide. Model uses tidal elevations (η) as initial condition at the open boundaries (Figure 3.12).

$$\eta = \sum f_k h_k \cos(\sigma_k - g_k + V_k + u_k) \tag{3.30}$$

where f and u are the nodal corrections for amplitude and phase, h and g are the tidal constituents, σ is the constituent of angular speed, t is the time in GMT, and V is the equilibrium constituent.

The model open boundaries were forced with eight major tidal constituents ((M2 S2 N2 K2 K1 O1 P1 Q1). Tidal constituents were obtained from the OSU tidal prediction software that uses TPXO global tidal solution dataset ("The OSU TOPEX/Poseidon Global Inverse Solution TPXO,"); APPENDIX B.

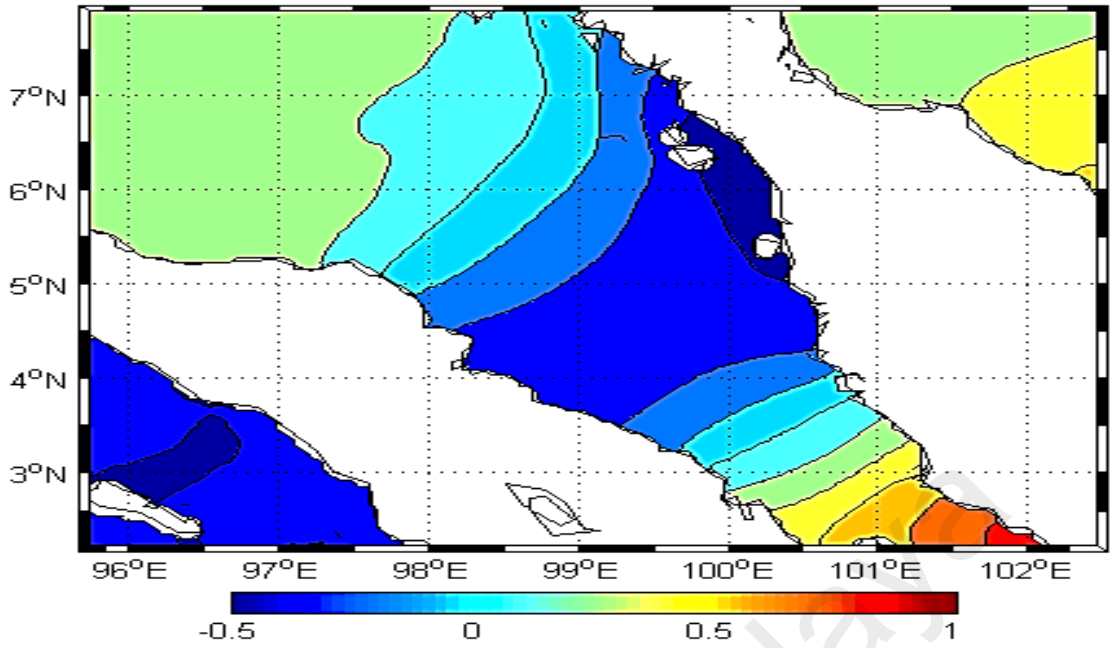

Figure 3.12 Initial conditions of tidal elevation (m) in the Straits of Malacca.

3.8 Validation of Numerical Model Results

Present POM model used the high resolution satellite data for initializing and defining the primitive parameters such as sea depth, tidal elevation, salinity and temperature. This made sure that model gave realistic results. Further the model results were validated with the field observations at tidal stations. In addition satellite data and previous research works also helped to further validate the model results. Chapter 4 presents through model validation and error analysis results for following parameters:

- *Sea water elevation*: Tidal elevation was compared for two tidal stations L1 and M1 (Figure 3.6).
- *Tidal flow speed:* Three observation points L1, L2, and L3 (Figure 3.6) were used to validate the tidal flow speed of model.
- *Sea water salinity and temperature*: In addition Figure 3.6 shows line AA' along which vertical profile of sea water salinity and temperature were compared with previous works.

To assess the success of the POM model the model results and field measurements were subjected to statistical indicators such as the coefficient of determination (R2) as given in eq.3.31.

$$R^2 = \frac{\left[\sum_{i=1}^{n}\left(O_i - \overline{O_i}\right)\cdot\left(P_i - \overline{P_i}\right)\right]^2}{\sum_{i=1}^{n}\left(O_i - \overline{O_i}\right)\cdot\sum_{i=1}^{n}\left(P_i - \overline{P_i}\right)} \tag{3.31}$$

where the observed and estimated values are P_i and O_i respectively, and the total number of result data is given by n.

3.9 Resource Assessment of Tidal Stream Resource

Resource assessment of tidal stream energy is first step towards successful device deployment (Blunden & Bahaj, 2006). Resource assessment primarily investigates suitable sites for installing conversion device and power potential of site. In addition, resource assessment studies environmental concerns and effects of tidal current devices on marine eco-system. A brief review of environmental effects was provided in literature review. Further this study focus to assess tidal stream energy resource in the Straits of Malacca. Following sections illustrates methodology for assessing the tidal stream energy resources using result of the numerical model. Methodology address following objectives:

1. Criteria for selecting site with high concentration of tidal stream energy.
2. Assessment of power potential of selected sites.
    2.1 Available and extractable power for single tidal current turbine.
    2.2 Available and extractable power for multiple or farm configuration.

3.10 Criteria of Selecting Site for Tidal Stream Turbines

Based on previous studies this study considered following site specific parameters for selecting suitable site(Blunden & Bahaj, 2007; Blunden et al., 2013).

1) Flow speed of tidal stream (m/s) at a given site.

2) Sea-depth (m) at the chosen site.

Table 3.1 shows criteria for selecting site for energy extraction in a channel or Straits. Sea depth, tidal flow speeds are major consideration for selecting of a site. A mean tidal flow speed of 1 m/s is considered desirable for extraction of tidal stream energy because most of TCTs have starting speed of 0.5 m/s; therefore, a mean tidal flow speed of 1 m/s would provide enough flow to start generating power (Blunden et al., 2013; Chen et al., 2013b; Work et al., 2013). Sea depth at site needs to consider diameter of turbine, clearance from seabed and clearance from sea surface. Various resource assessment works consider a depth from 15 to 60 m suitable for installing tidal conversion device at selected site (Blunden et al., 2013).

Table 3.1 Characteristics of suitable site for tidal stream energy extraction.

Characteristics	Criteria
1. Sea depth (H)	15 m $\geq$ H $\geq$ 60 m
2. Flow speed (U)	U$\geq$ 1 m/s

3.10.1 Parameters Determining Flow Speed

Average tidal flow speed varies in the range of 0.2 to 3.5 m/s. Tidal stream moving with higher speed hold higher kinetic energy. Site with significant speed are considered suitable for installation of tidal current turbines. In addition, engineers consider specifications of tidal current turbine for deciding suitable flow speed. Tidal current turbines extract only a part of available energy due to their design limitations. Tidal

stream converters are still in early development phase. Among various design concepts only few devices reached at commercial stage (Bahaj, 2011). Converting devices start to produce electricity above a given minimum flow speed. This minimum threshold flow speed above which devices start to produce electricity is called cut-in speed or start-up speed. In addition an upper cut off speed is set above that converting devices stop electricity generation. Cut off speed prevents structural failure when operating at higher tidal flow speed.

3.10.2 Parameters Determining Sea-Depth

A site must offer a minimum sea-depth for the deployment of tidal current turbine (Legrand, 2009). This minimum characteristic depth includes:

1) Maximum rotor diameter.

2) Top clearance from the sea water surface.

3) Bottom clearance from the seabed.

Maximum rotor diameter depends on the design specification of tidal current turbine. Generally rotor diameter of various commercial devices falls in the range of 1 to 16 meter. European Marine Energy Centre Ltd (EMEC) suggests top clearance of 5 m for allowing recreational activities(Scruggs & Jacob, 2009). It also minimizes turbulence and wave loading effects on the tidal current turbine. In addition top-clearance prevents damage from floating materials to tidal current turbines. Previous studies suggest a bottom clearance of 25% from the available sea depth. This minimizes turbulence and shear loading from bottom boundary layer (Scruggs & Jacob, 2009).

3.11 Assessment of Tidal Stream Energy

In this work, two scenarios were considered for computing tidal stream power at selected sites.

1. Annual power output from single tidal current turbine.
2. Annual power output from multiple tidal current turbines or tidal farm configuration.

Further this study calculated the capacity factor of device that indicated extracted electricity from the available energy over time.

3.11.1 Available Power from Flowing Water

Tidal stream energy is the kinetic energy of flowing seawater. The available energy density *(P_{avl})* is given by:

$$P_{avl} = \frac{1}{2}\rho V^3 \tag{3.32}$$

where ρ the water density (kg/m^3) and V is the flow speed (m/s). Figure 3.13 shows available tidal energy density at various flow speeds based on eq.3.32.

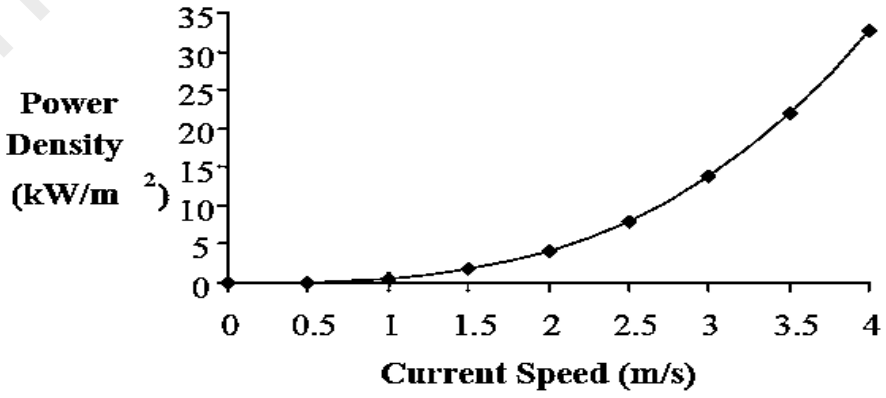

Figure 3.13 Relation between flow speed (m/s) and tidal stream energy density (kW/m^2).

3.11.2 Available and Extractable Energy from Single Device

(i) Available Power

Tidal current turbines generate electric power by intercepting the flowing fluid. The power available to a single tidal current turbine is given as:

$$P(t) = \frac{1}{2}\rho A_T [V(t)]^3 \qquad (3.33)$$

where *V(t)* is the instantaneous flow speed (*m/s*), A_T is the swept area (m^2) or cross sectional area of the turbine rotor, *P(t)* is the available power (Watt) .

Therefore, available power is directly related to fluid density and cube of flow speed. Water is 832 times denser than air, and generates significant power at slower speed. For example a wind turbine operates at rated speed of 13 m/s, while a tidal current turbine operates at rated speed of 2 m/s (Fraenkel, 2002). Literature review shows that there are two types of turbine rotors. First being horizontal axis turbine and second being vertical axis turbines. The physical principles of extracting energy are similar to wind turbines(Fraenkel, 2002).

(ii) Extractable Power

Tidal stream energy received at the rotor blades from the tidal flow is called available energy. However, only a part of available energy from tidal streams is extractable. Extractable energy depends on overall efficiency of turbine and theoretical upper limit for extracting energy from the free stream. Theoretical upper limit for extracting energy from a free stream is 59.2 per cent, which is referred as the Bentz limit (Fraenkel, 2002; Garrett & Cummins, 2005, 2008).

Turbine overall efficiency consists of following components (Matheson & Thomson, 1973):

1) Efficiency of turbine ($\eta_{Turbine;}$ theoretical upper limit 59.2%).

2) Drive train efficiency ($\eta_{Drive\ Train;}$ 96%).

3) Generator efficiency ($\eta_{Generator}$; 95%).

4) Power conditioning efficiency ($\eta_{PowerConditioning}$; 98%).

Therefore, overall efficiency of tidal current turbines also called power coefficient (C_p) given as:

$$C_p = \eta_{Turbine} . \eta_{Drive\ Train} . \eta_{Generator} . \eta_{PowerConditioning.} \quad (3.34)$$

A common value for turbines overall efficiency is 40%. Thus, only a part of available tidal stream energy at turbine rotor is extractable.

Extractable power from single turbine rotor is given as:

$$P_{ext}(t) = \frac{1}{2} C_p . \rho A_T [V(t)]^3 \quad (3.35)$$

where C_p is the capacity factor of turbine rotor; $V(t)$ is the instantaneous flow speed (m/s), A_T is the swept area (m) or cross sectional area of the turbine rotor, $P_{ext}(t)$ is the extractable power (Watt) .

The power extracted by tidal stream turbine varies with time and depends on design specification. Tidal current turbines start to produce electricity at a specified minimum speed known as cut-in speed (V_{in}). It achieves maximum performance at rated speed (V_r). Each turbine stops above cut-off speed (C_{cs}) for safety considerations (Figure 3.14). Therefore, power from tidal current turbine with time is given as:

$$P_e = \begin{cases} 0; \ V(t) < V_{in} \\ \frac{1}{2} C_p \rho A V^3; \ V_{in} \leq V \leq V_r \\ 0; \ V \geq V_{cs} \end{cases} \quad (3.36)$$

where P_e is the electric power output; C_p is the power coefficient.

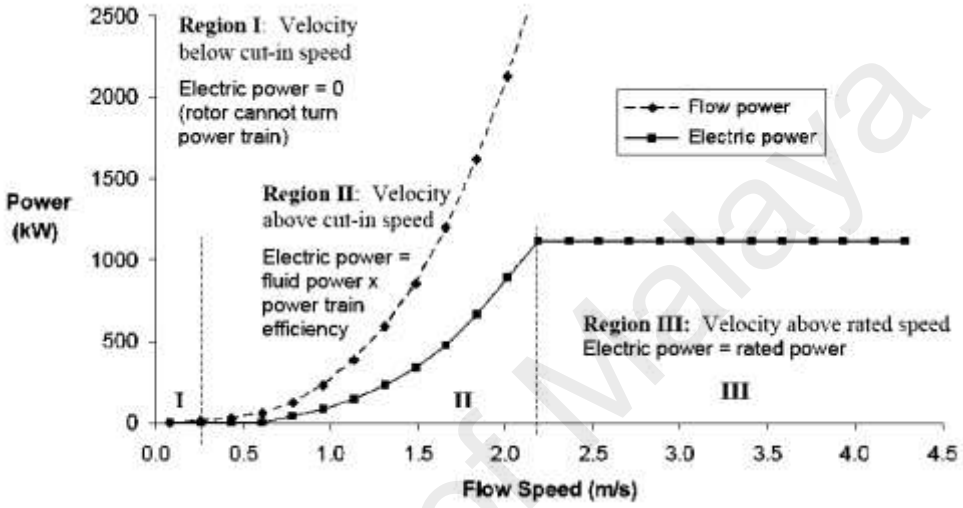

Figure 3.14 Curve showing a turbine's power output against flow speed (Matheson & Thomson, 1973).

(iii) Available Energy

Integrating equation-3.33 overtime gives total available energy for that duration, given by:

$$E(t) = \int_0^T P(t)dt \quad (3.37)$$

(iv) Extractable Energy

Integrating electric power output over time gives electric energy (E_e) given by:

$$E_e = \int_0^T P_e(V,t)dt \quad (3.38)$$

(v) Capacity Factor

Capacity factor is industry accepted index for acceptability of energy extraction. Higher value of capacity factor indicates that device efficiently convert higher amount of available energy. Capacity factor (C_f) is defined as ratio of extractable electric energy for a given duration to ideal energy output (E_{rated}) if tidal current turbine would operate at rated speed throughout the same period.

$$Cf = \frac{E_e}{E_{rated}} \tag{3.39}$$

3.11.3 Available and Extractable Energy for Tidal Farm Configuration

Available and extractable power for tidal current farm with N turbine system can be computed by adding power from individual turbines as in equation 3.32.

$$P_{avl} = \sum_{ai=1}^{N} P_{ai} \tag{3.40}$$

$$P_{ext} = \sum_{ei=1}^{N} P_{ei} \tag{3.41}$$

where P_{ai} ($Watt$) is the available power at single turbine rotor, P_{ei} (W) is the extractable power from single turbine rotor; P_{avl} (W) and P_{ext} (W) are the tidal current farm's total available and extractable power.

3.11.3.1 Specifications of Tidal current turbine

Table 3.2 specifies the design specification of two tidal current turbines. These specifications were used in computing available and extractable power from the Straits of Malacca. Figure 3.15 and 3.16 shows the selected tidal current turbines i.e. (i) the Open Hydro and (ii) the Gorlov tidal current turbine.

Figure 3.15 Open Hydro horizontal axis tidal current turbine.

Figure 3.16 Gorlov vertical axis tidal current turbine.

This study considered the Open Hydro turbine with 10 m diameter and 1 Mw rated power. On the other hand the Gorlov turbine has 2.5 m diameter, 1 m height and rated power of 1.5kW. These turbines were selected because each one represents two popular design concepts.

The Open Hydro is horizontal axis with larger rotor area, where as the Gorlov is vertical axis turbine with smaller rotor area. This selection of turbine allows to better understanding performance of turbine in the Straits of Malacca.

Table 3.2 Specification of two type of tidal current turbine selected for assessment of resource.

Name	Dimension(D,H)	Rated Power	Cut-in Speed (m/s)	Cut-off Speed (m/s)
Open Hydro	10 m (D)	1MW	0.6	2.5 m/s
Gorlov	2.5m (D) 1 m (H)	1.5kW	-	1.5 m/s

3.11.3.2 Layout of Tidal Current Farm

This work considered a hypothetical tidal farm with three rows for computing the available and extractable power for the selected sites in the Straits of Malacca (Figure 3.17). The lateral spacing and downstream spacing were determined based on the proposed diameter. This study considered tidal farms with 50, 100, and 500 units of tidal current turbines in order to simplify the process of computing power potential.

According to the "Assessment of Tidal Energy Resource: Marine Renewable Energy Guides", the suggested lateral spacing (the distance measured between axis of rotation of adjacent turbines) is 2.5D (Legrand, 2009). This lateral spacing is proved to be sufficient to prevent merging of wakes produced by adjacent turbines (Myers et al., 2011; Myers & Bahaj, 2010). On the other hand, the suggested downstream spacing is 10D. However, studies have shown that the wakes can extend beyond 10D downstream (Myers et al., 2011; Myers & Bahaj, 2010). In fact, it is reported that the effect of wake is still sensible at 20D downstream (Myers & Bahaj, 2010). For 20D downstream, the velocity generally recovers to more than 90% of the initial velocity. Hence, this research

work used a 20D downstream spacing. Figure 3.18 shows the layout of the marine current turbine farm (a schematic diagram).

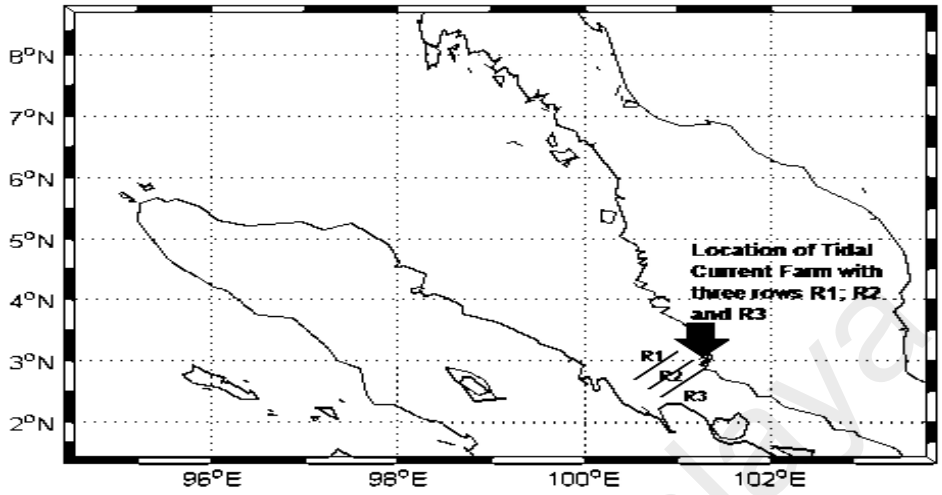

Figure 3.17 Schematic diagram showing a tidal current farm in the Straits of Malacca.

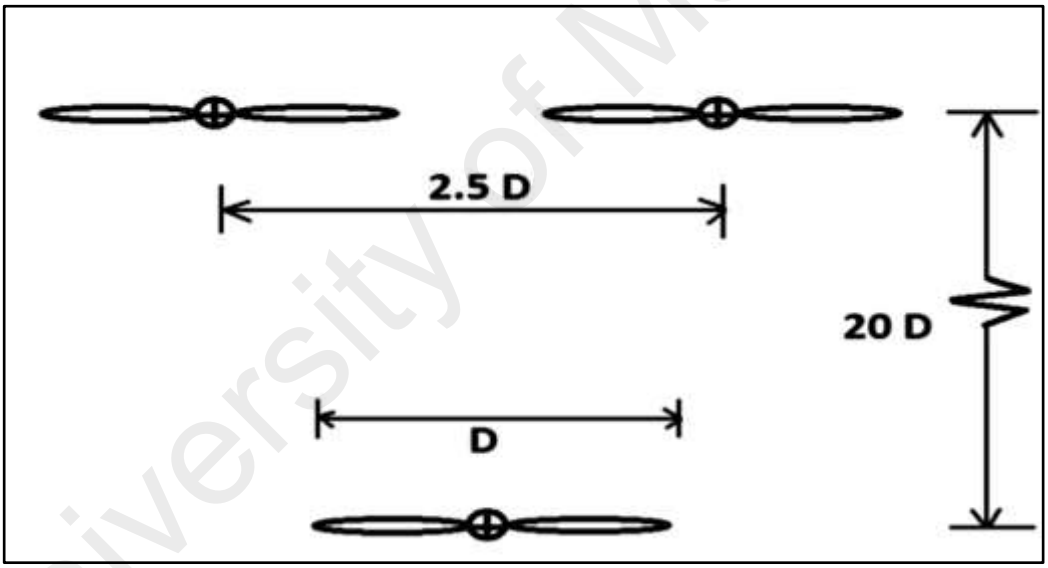

Figure 3.18 Layout of tidal current turbine farm, where D is diameter of turbine rotor.

3.12 Summary

This chapter presented the methodology for achieving primary objectives of this study. First this chapter explained the numerical model used for simulating the tidal flow in the Straits of Malacca. Then criteria was set for selecting site suitable for energy extraction. At the end this chapter presented various equations, methods and assumptions used for estimating the power potential of selected site.

Numerical model uses satellite data for preparing initial and boundary condition. Model are then validated and calibrated against measurement and satellite data. Then model was run for duration of two months which covered two spring-neap tidal cycle. Then, this study analysed the sea depth and flow speed using the results of the numerical model. This helped to identify site with suitable flow speed, sea-depth and tidal energy flux. Later theoretical methods were used for estimating available and extractable energy from tidal stream energy at selected sites.

CHAPTER 4

RESULT AND DISCUSSION

4.1 Introduction

This study investigated tidal flow in the Straits of Malacca to identify suitable sites for installing tidal current device. Further this study computed the power potential of these sites. The model results show that specific sites provide favourable sea-depth and tidal flow speed for installing tidal current turbines in the Straits of Malacca.

First, this study thoroughly investigated the sea depth in the Straits of Malacca using high resolution satellite data. Then this study investigated the tidal flow speed using the numerical model at various grid points. Further analysis on the distribution of tidal stream energy flux was conducted and presented in this chapter. At last this study estimates annual available and extractable tidal stream power. In depth result and discussion is provided for following parameters:

- Model validation results by comparing model estimations of various parameters with observation at the tidal stations and with previous studies.

- Bathymetry of Straits of Malacca with particular focus on the region with suitable sea depth in the range of 15 to 60 m for installing tidal current turbines.

- Select site for extracting tidal stream energy by analysing the tidal flow speed and tidal energy flux distribution in the Straits of Malacca.

- Estimation of annual available and extractable tidal stream energy at the selected sites in the Straits of Malacca using analytical methods.

4.2 Tidal Elevations

The tidal elevations results of the numerical model were verified with the observations at two tidal stations namely the Permatang Sedepa (L_1); and the Kuah (M_1; as shown in Figure 3.6) for month of January, 2012. The National Hydrographic Center, Malaysia provided the elevation data for the two stations (National-Hydrographic-Centre, 2012). Figure 4.1 and 4.2 shows good fit between the numerical and observation tidal elevation for the station L_1 and M_1 respectively. Results show that 89.85 % of the estimated tidal-elevation data points match with actual observation at station L_1. Similarly for station M_1; 88% match was found between the numerical and observed data. Thus, we conclude that model satisfactorily estimated the tidal elevation for the Straits of Malacca.

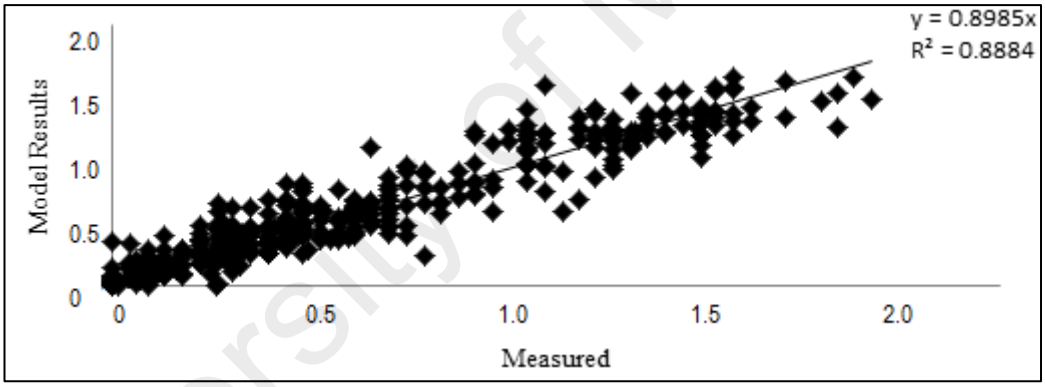

Figure 4.1 Correlation between model and measured tidal elevation from 15-30 January, 2012 at station L_1.

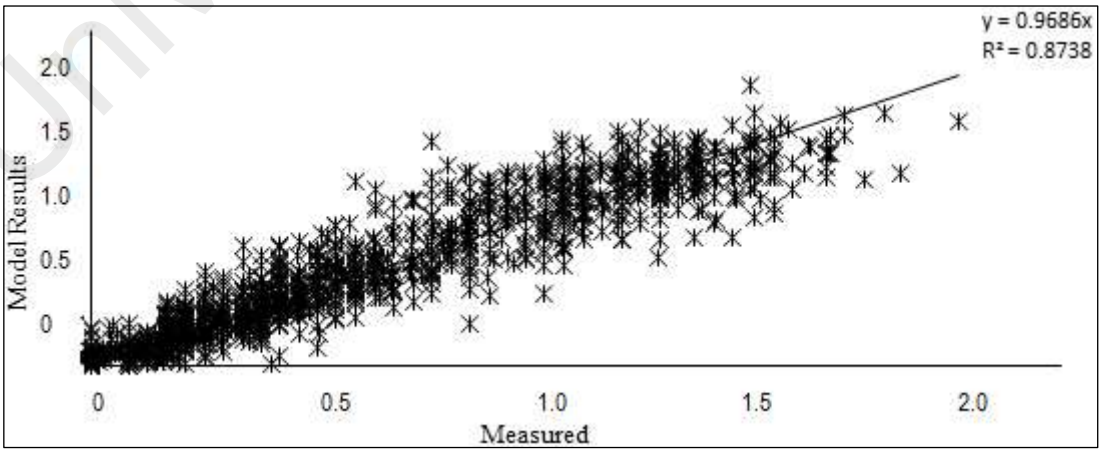

Figure 4.2 Correlation between model and measured tidal elevation from 15-30 January 2012 at M_1.

4.3 Validation of tidal flow speed

4.3.1 Comparison of Peak Tidal flow velocity

The peak tidal flow velocities were compared with the field measurements at three tidal stream stations. The National Hydrographic Centre, Royal Malaysian Navy provided the observation data (National-Hydrographic-Centre, 2012). Three points are off Permatang Sedepa (L_1), off Raleigh Shoal (L_2) and off Tanjung Segenting (L_3 as shown in Figure 3.6). Table 4.1 shows the peak flow velocity from the observation and model results. Phase of peak flow shows excellent match. In addition satisfactory match were found for the peak tidal flow speed. Slight deviations were found between the model and field measurement. This may be due to use the fact that we used depth averaged tidal flow speeds from the model for comparison with observation data.

Table 4.1 Comparison of flow speed obtained from computation model and observation at station L_1, L_2, and L_3.

Location			Observed		Computation model	
	Latitude	Longitude	Current(m/s)	Phase(,GMT)	Current(m/s)	Phase(,GMT)
L_1	2.40N	101.00E	1.14	295	1.30	287.23
L_2	2.07N	101.57E	1.08	310	1.00	303.32
L_3	1.38N	102.44E	0.97	46	0.89	39.46

4.3.2 Comparison of Time Series Tidal Flow Velocity

Results for the time varying tidal flow were verified with observations at station L_1 and L_2 (Figure 3.6). The tidal flow speed data for the two points were available from the National Hydrographic Centre, Malaysia for year 2012. Figure 4.3 and 4.4 shows comparison of the tidal flow speed between observation and numerical model at station

L_1 and L_2. At Permatang Sedepa the observation and numerical model results showed a match of 96.05% for the tidal flow speed. Similar high correlation was found at the Off Raleigh Shoal (L_2), where 93.05% of the data point from the numerical model match with the observed of tidal flow speed. A high-resolution model was used with best available data points for initial condition and boundary forcing to minimise errors. Clearly, the numerical model achieves high accuracy in predicting the tidal flow speed compared to tidal elevation. Further, this study uses these time varying tidal flow speed to estimate power of selected sites. Therefore, it was important to have a model that gave high accuracy for the tidal flow speed.

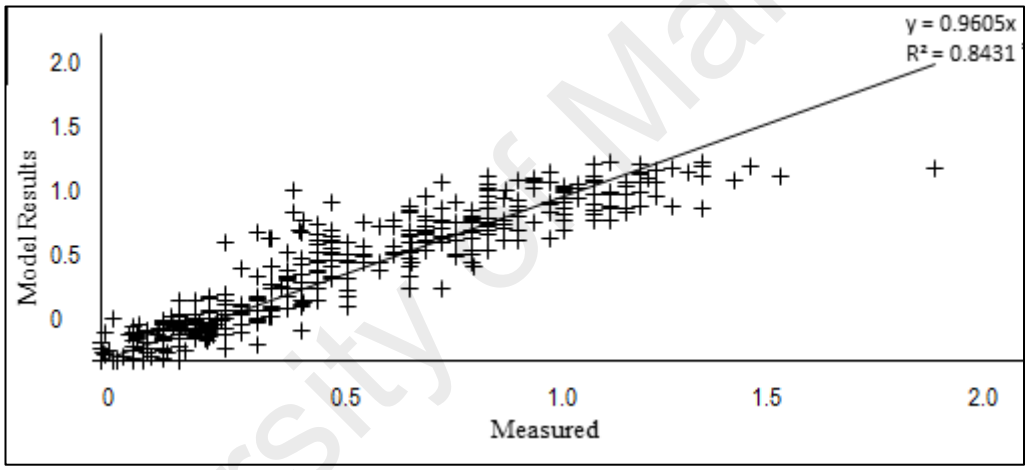

Figure 4.3 Correlation for the tidal flow speed between model and observation data for January,2012 at L_1.

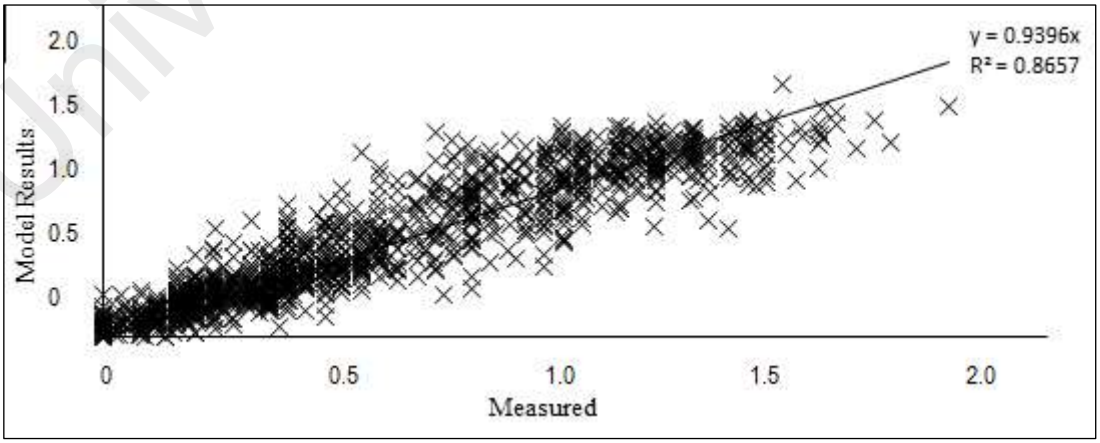

Figure 4.4 Correlation for the tidal flow speed between model and observation data for January,2012 at L_2.

4.4 Validating temperature and salinity

This section compares the model results with previous studies for two parameters i.e. the sea water salinity and sea water temperature. Unit parts per thousand (ppt) is used for measuring sea water salinity. While, sea water temperature is measured in degree Celsius (°C) scale.

Sea surface temperature (SST) and sea surface salinity (SSS) were found to be uniform in the Straits of Malacca which is in agreement with the field observations of Wyrtki (1961). Model results show stratification along continental shelf along the sea depth greater than 80 m (Figure 4.5 a, and b). Stratification is an oceanic phenomenon which occurs along higher depths. Stratification is characterised by a sudden decrease in the sea water temperature and increase in the sea water salinity. Keller and Richards (1967) in their work reported that stratification occurs in the Straits of Malacca along the continental self. Therefore, model results is in agreement with observation of Keller and Richards (1967). Figure 4.5 shows in-situ salinity and temperature for a vertical section along line AA' (Figure 3.6).

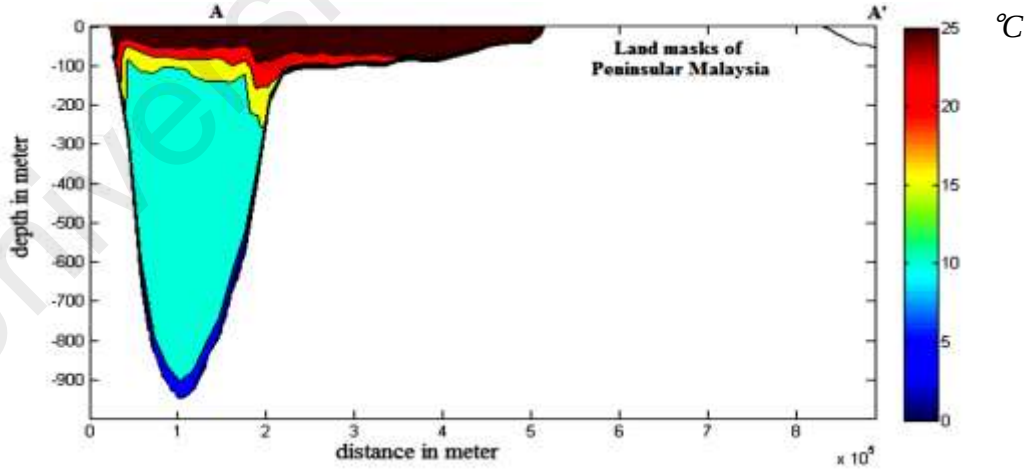

(a)

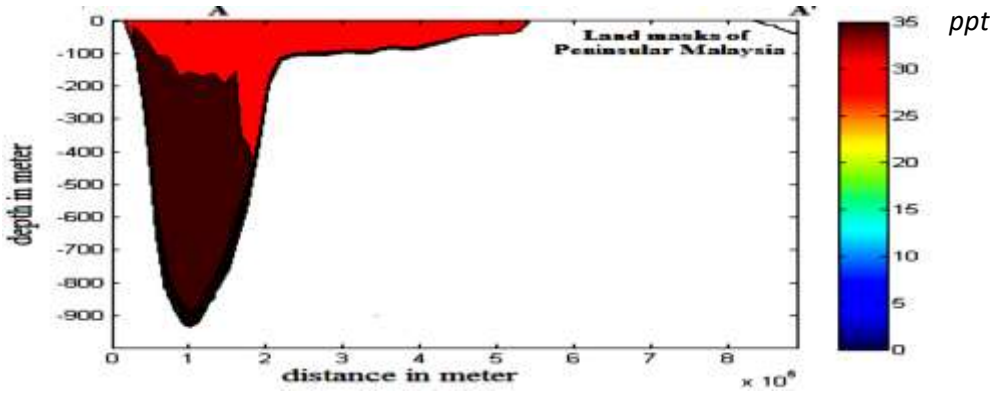

(b)

Figure 4.5 Stratification along section AA' (a) in situ sea temperature (°C) and; (b) in-situ salinity (ppt) in the Straits of Malacca along section AA' (Figure 3.6).

4.5 Sea surface current

Surface current from the present model was compared with the works of previous researchers, shown in Figure 4.6. Results of the surface current in the Straits of Malacca for the month of February agrees with field expedition conducted by Wyrtki (1961) and numerical results from (Rizal et al., 2012) (Figure 4.6). It further gave confidence into the results of model for the Straits of Malacca.

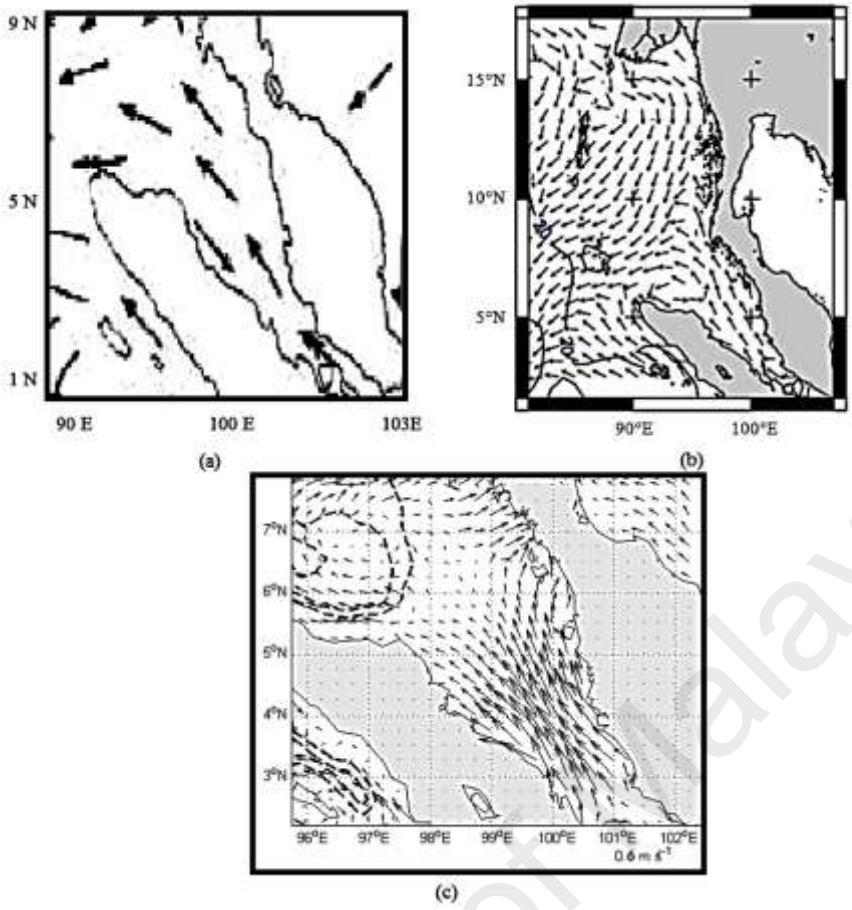

Figure 4.6 Straits of Malacca surface current for month of February from (a) Wyrtki (1961) observations (b) Rizal et al. (2012) HAMSON model and (c) present POM model.

4.6 Analysis of Bathymetry

Bathymetry is the study of sea depth equivalent to land topography. This section presents through analysis for the bathymetry of the Straits of Malacca. It is important to collect information for prevailing sea depth at various parts of the Straits. Tidal current turbine installation requires certain minimum depth. In addition installing tidal current turbine is considered impractical beyond certain depth due to the high cost involved in building monopole. Figure 4.7 shows bathymetry of the Straits of Malacca using satellite data ETOPO1 (Amante & Eakins; Amante & Eakins, 2009). ETOPO 1 is a one minute global relief model of the Earth's surface which integrates the ocean bathymetry and land topography. It uses satellite and altimetry dataset to give accurate profile of bathymetry.

The Straits of Malacca is located between the Peninsular Malaysia and Sumatra Island. Sea depth between 400 to 1500 m is prevalent in the Andaman Sea. Andaman Sea and the Straits of Malacca are joined by a continental shelf (Figure 4.8). Sea depth of 100m prevails towards the Straits of Malacca along the continental shelf. Therefore, deep and steep bathymetry features can be found at the northern regions of the Straits. However, shallow sea depth prevails along the central and southern parts of the Straits. Sea depth ranging from 10 to 60 m characterizes central and southern parts of the Straits.

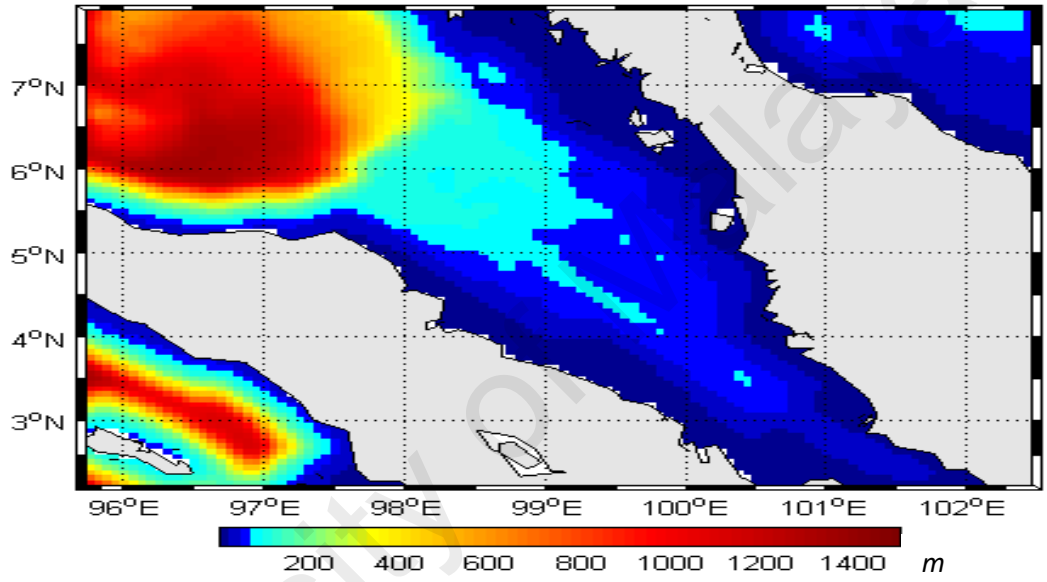

Figure 4.7 Variation of sea depth (*m*) in the Straits of Malacca.

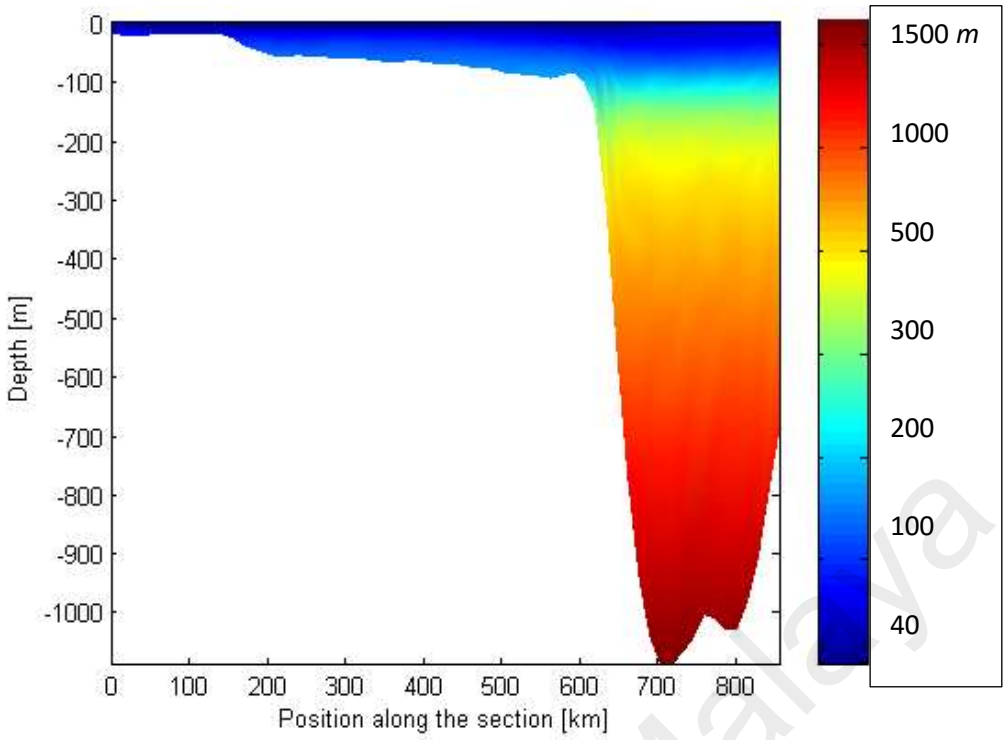

Figure 4.8 Sea depth (*m*) variations along continental shelf from the Straits of Malacca to Andaman Sea.

4.6.1 Suitable Sea depth for extracting Tidal Stream Energy

Based on criteria set in the chapter 3, a sea depth between 15 to 60 m is considered suitable for installing tidal current turbines. Therefore, this work identified regions in the Straits of Malacca with sea depth in the acceptable range. Figure 4.9-4.10 shows region in the Straits of Malacca with suitable sea depth. Suitable sea depth prevails near the coastline of Peninsular Malaysia especially along the southern coastline (Figure 9). Thus, study needs to concentrate at these regions in order to select site for extracting energy from tidal currents in the Straits of Malacca. Suitable sea depth does not guarantee these regions to have significant tidal stream energy.

However, site with significant tidal stream energy must fall somewhere in region within the identified suitable sea depth. Next section presents results and analysis of the tidal flow speed in the Straits of Malacca. Tidal energy extraction sites need to have suitable sea depth as well as significant tidal flow speed.

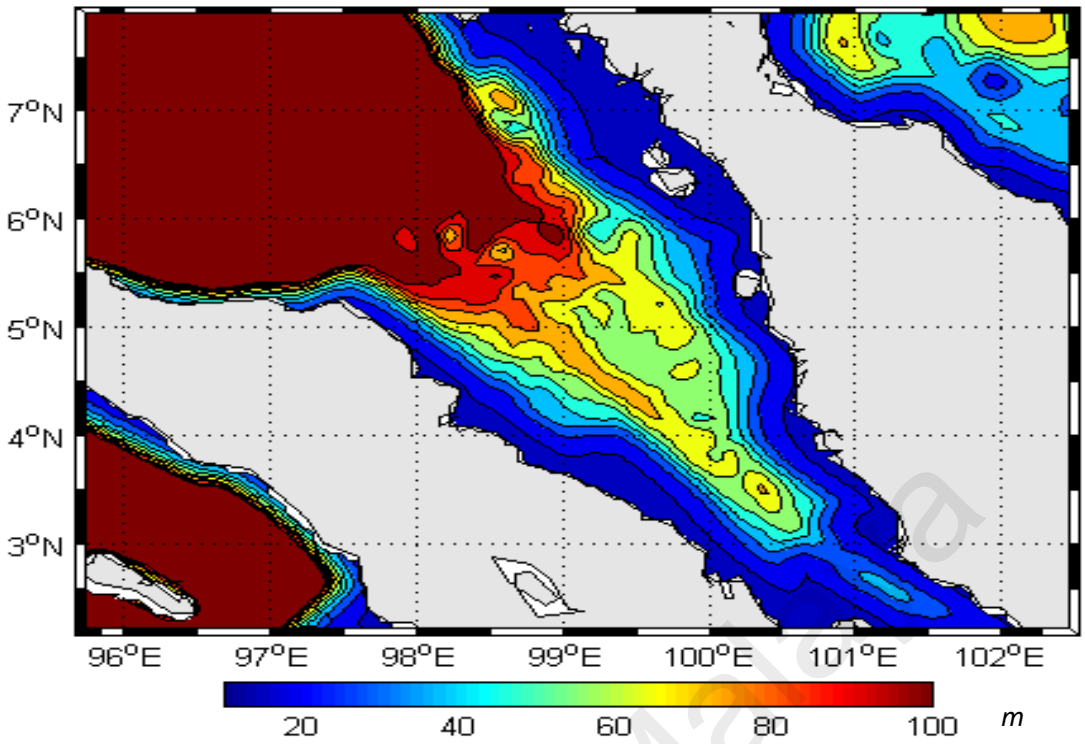

Figure 4.9 Regions in the Straits of Malacca providing sea depth below 100 m.

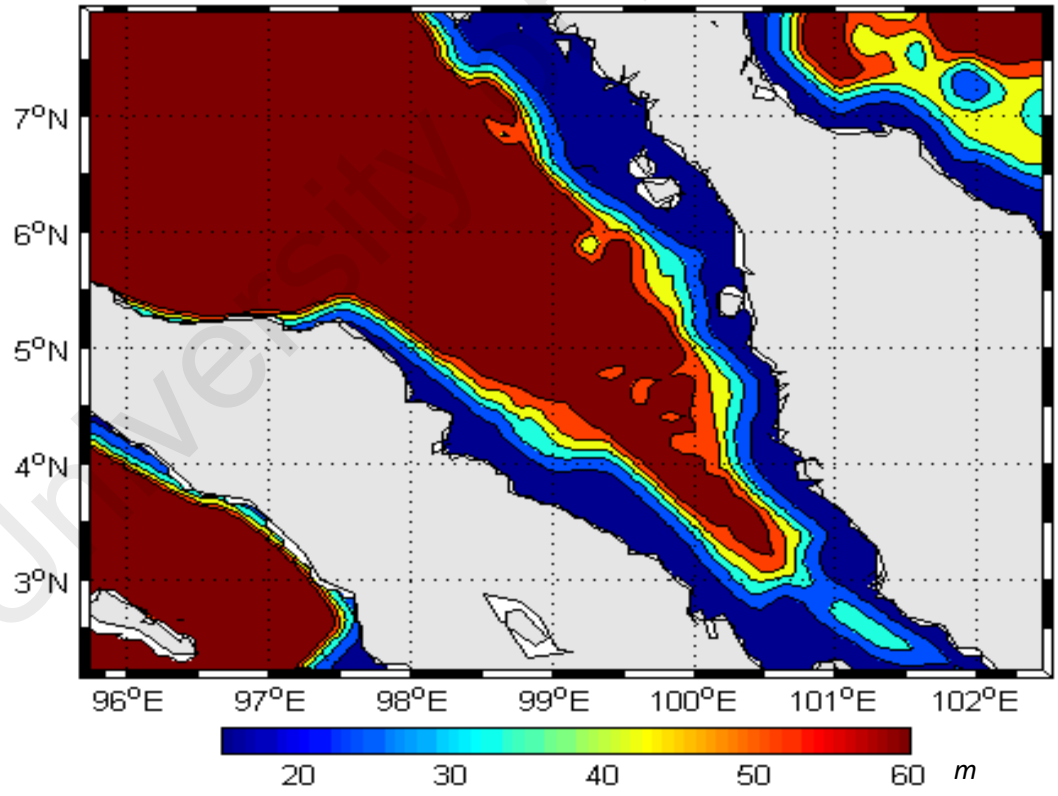

Figure 4.10 Region in the Straits of Malacca providing sea depths from 15 to 60 m.

4.7 Tidal Flow Velocity

The Straits of Malacca receives semi-diurnal tide with two high and low tides on a given day. Thus, semi-diurnal tides shows rise and fall of sea waters two times around the mean sea level. As discussed in the literature review, tide creates potential difference in water level between two regions in sea. This potential difference gives rise to the tidal currents. Therefore, analysis of tidal flow velocity needs to consider time of flood (high tide) and ebb tide (low tide). In addition considering time of spring and neap tide is equally important. During spring tide higher magnitude of tidal currents are generated. However, during the neap tide lower magnitude of tidal currents are generated. Therefore, various phases of tide were considered for investigating the tidal flows in the Straits of Malacca.

Results present tidal flow speed, direction and elevation during the spring and neap tide. Figure 4.11 and 4.12 shows the tidal flow and elevation during the spring and neap tide in the Straits of Malacca. Tidal flow speed varies from 0.1 to 1.7 m/s from the spring to neap tide. Peak flow of 1.7 m/s prevails in the central and southern parts of the Straits (Figure 4.11-4.12). Results also show lower range flow speed at the northern part of the Straits. In regions with higher depth a typical flow speed ranges from 0.1 to 0.7 m/s. Thus, less significant flow speed prevails in the northern part near the continental shelf. Nevertheless, narrow regions of the Strait receive significant tidal flow suitable for extracting tidal stream energy.

4.7.1 Tidal Flow during Spring Tide

Results show significant tidal flow occurs in the central and southern part of the Straits (Figure 4.11-4.12). Average tidal flow speed of 1 m/s is considered economical for extracting power (section 3.10). Sea level rises approximately 2 m above the mean sea level during the high tide in the spring phase, (Figure 4.11 (a)). This generates tidal flows of 1.5 ms^{-1} moving in the southeast direction (Figure 4.11 (b)). During the low tide, sea level fall 1.4 m below mean sea level (Figure 4.11 (c)). This generates tidal flow of 1.25 ms^{-1} moving in the north-west direction (Figure 4.11 (d)).

4.7.2 Analysis of Tidal Flow during Neap Tide

Lower water level rise and flow prevails during the neap tide. However, even during the neap tide a peak flow can reach around 1 m/s in the Straits of Malacca. It should be noted that southern and central parts only receive significant flow during neap tide. Figure 4.12 shows the tidal flow and elevation for flood and ebb tide during neap period. High tide causes sea level to rise up to 0.4 m above the mean sea level (Figure 4.12 (a)). This generates low magnitude flow moving at 0.5 ms^{-1} towards the southeast direction (Figure 4.12 (b)). In the same period during the low tide water level falls 0.6 m below the mean sea level (Figure 4.12 (c)). It causes tidal flow of 0.6 m/s moving towards the north-west direction (Figure 4.12 (d)).

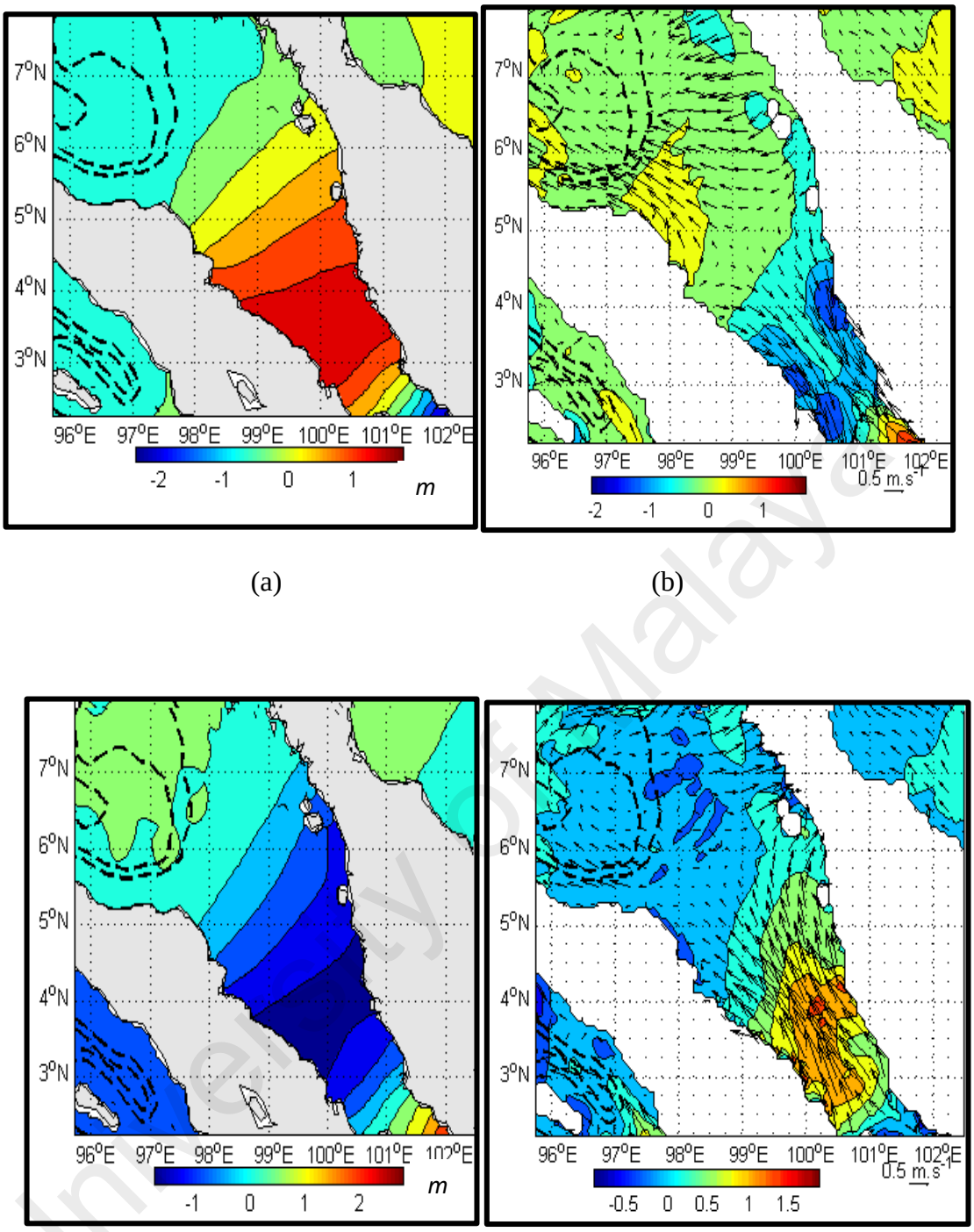

Figure 4.11 Distribution of tidal flow and elevation in the Straits of Malacca on day in the spring tidal period (a) Tidal elevation (η,) during flood tide. (b) Tidal flow (m/s) during flood tide; (c) Tidal elevation (η,) during ebb tide; (d) Tidal flow (m/s) during ebb tide.

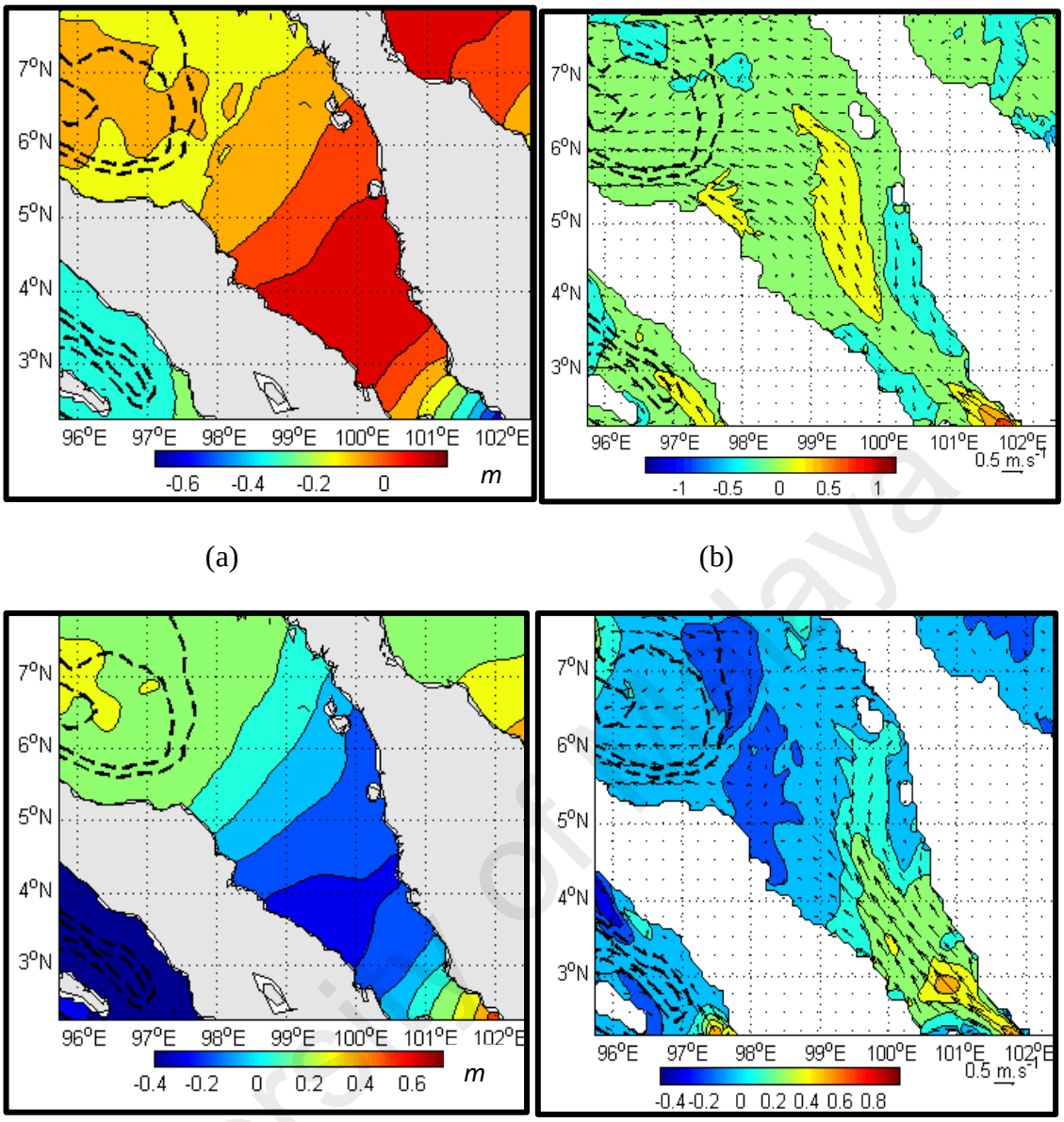

Figure 4.12 Distribution of tidal flow and elevation in the Straits of Malacca on a day in the neap tidal period (a) Tidal elevation (η,) during high tide. (b) Tidal flow (m/s) during high tide; (c) Tidal elevation (η,) during low tide; (d) Tidal flow (m/s) during low tide.

Results clearly show that the southern parts of Strait receive higher flow, while rest of the region have lower flows. This is due to the fact that central and southern parts of the Straits of Malacca are shallower then north-west part. In addition southern and central parts provide narrowing effect due to constrained topography.

4.8 Sites suitable for harnessing tidal stream energy

This study identified three sites in the Straits of Malacca suitable for harnessing tidal stream energy. Selecting sites required taking into consideration two major parameters. First parameter is the magnitude of tidal flow speed and the second being sea depth.

The coastline of the Straits of Malacca runs along the eight major states. Following are seven major states (figure 4.13):

1) Perlis
2) Kedah
3) Penang
4) Perak
5) Selangor
6) Negeri Sembilan
7) Malacca, and
8) Johor

Figure 4.13 Political map of the Peninsula Malaysia, showing coastal states on the west coast.

This study investigated bathymetry, and flow speed along eight coastal states of Peninsular Malaysia. Bathymetry in the Straits of Malacca along most states was found suitable (Figure 4.10). However, suitable flow speed was only found along, Perak, Selangor, Malacca, and Johor (Figure 4.11 and 4.12). Further investigations found

bathymetry less than 15 m in the Straits along Johor coastline. In addition this region has high water traffic as it is a major shipping lane. Thus among coastal water of eight states only three states fulfil both the criteria of having suitable flow speed from tide and sufficient sea depth.

4.8.1 Analysis of Tidal Flow Velocity

As discussed in Chapter 2 most tidal current turbines have start up speed around 0.5 m/s. An average speed of 1 m/s from spring to neap tide is considered economical for harnessing tidal stream turbine (section). This acceptable velocity was chosen as site selection criteria in Chapter 3. Further tidal flow velocity from the numerical model was analysed to determine suitable sites in the Straits of Malacca for harnessing tidal stream energy.

For ease of study we divided the Straits of Malacca into four study zones from the south to north. Co-ordinates of division are shown in Table 4.2. In each zone five measuring grid points were selected to investigate variation of tidal flow speed from spring to neap. Results from numerical model gave the tidal flow speed at each of this grid points. Selected grid points are shown in Figure 4.14. Flow velocity from model results for each point covers 60 days. Figure 4.15 to 4.18 shows the time variation of tidal flow speed at the five grid point from zone-I to IV. The study duration covers four spring and four neap tidal periods.

Table 4.2 Division of the Straits of Malacca into four study zones.

Latitude (°)	Zone Name
1.5°N to 3°N	I
3.0°N to 4.5°N	II
4.5°N to 6.0°N	III
6.0°N to 8.0°N	IV

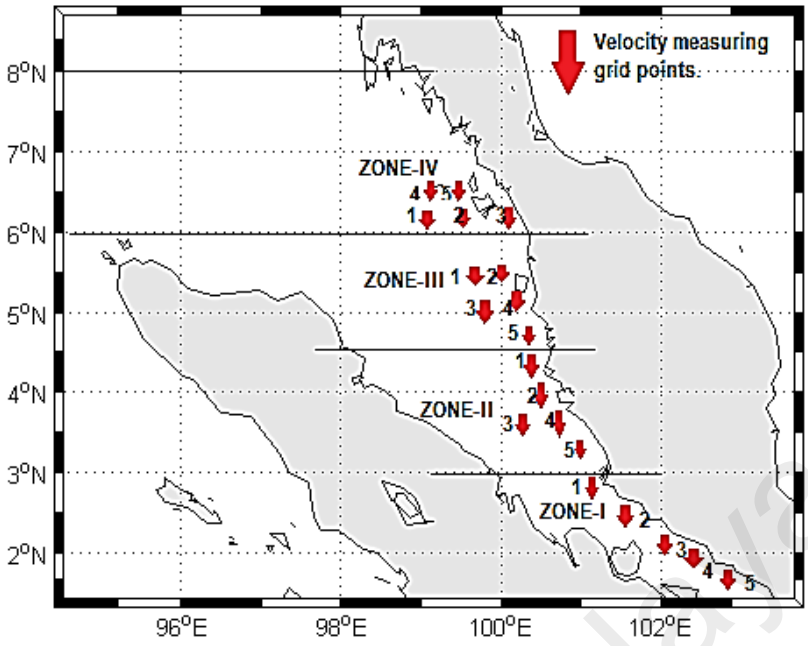

Figure 4.14 Map showing four study zones and five measuring points in each zone.

It is clear from Figure 4.15 that zone I is suitable for harnessing tidal stream energy. Tidal flow speed remains above acceptable limits (1 m/s) for most part of the tidal period for all five measuring points in zone I. Therefore, zone I is suitable for installing and assessing tidal stream energy. Figure 4.16 shows that zone II is also suitable for harnessing tidal stream energy. Tidal flow speed remains around the acceptable limits for all five measuring points in zone II from spring to neap tide. Therefore, zone II is also suitable for installing and assessing tidal stream energy.

Investigation of Figure 4.17 shows that zone III is not suitable for harnessing tidal stream energy. Tidal flow speed remains below the acceptable limits for all five measuring points from the spring to neap tide. Therefore, zone III is unsuitable for installing and assessing tidal stream energy. In addition, Figure 4.18 shows that zone IV is also not suitable for harnessing tidal stream energy. Tidal flow speed remains below acceptable limits for all five measuring points in zone IV from spring to neap tide.

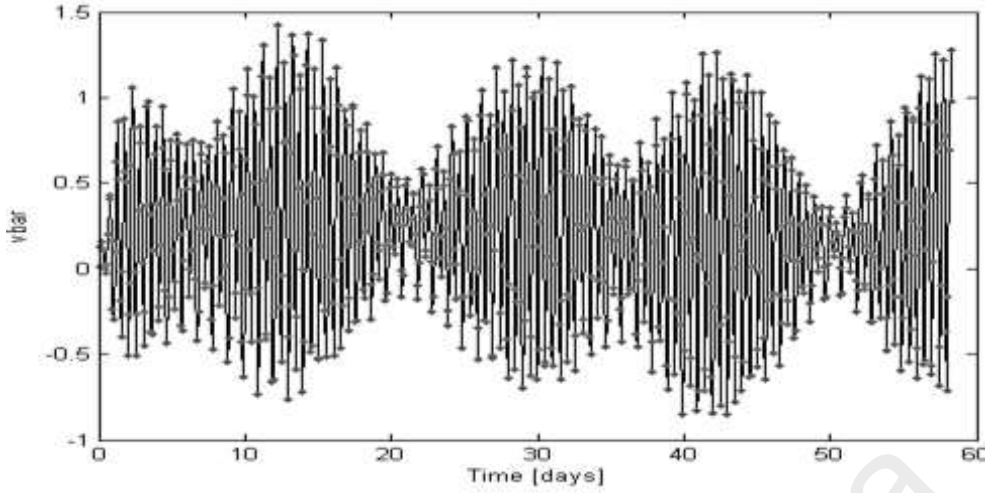

(a)

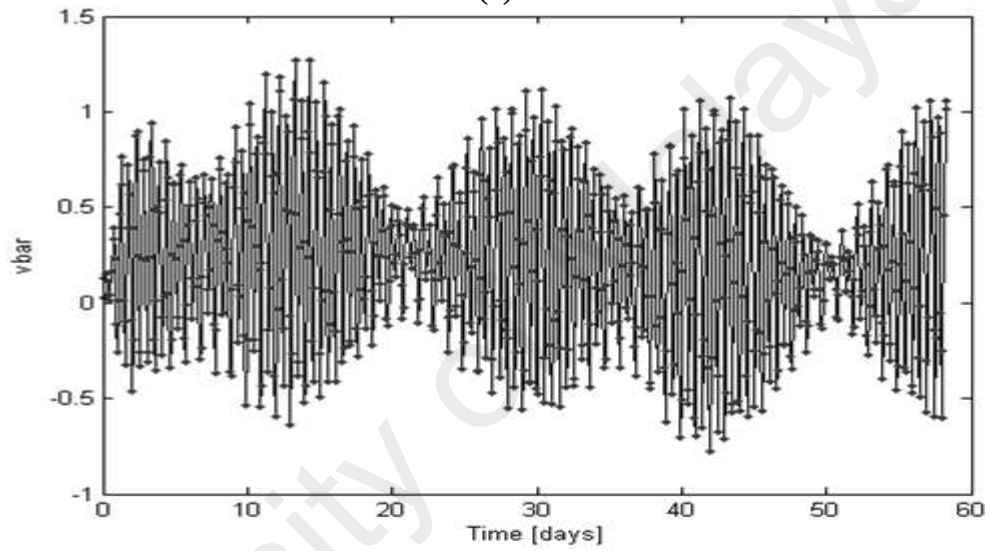

(b)

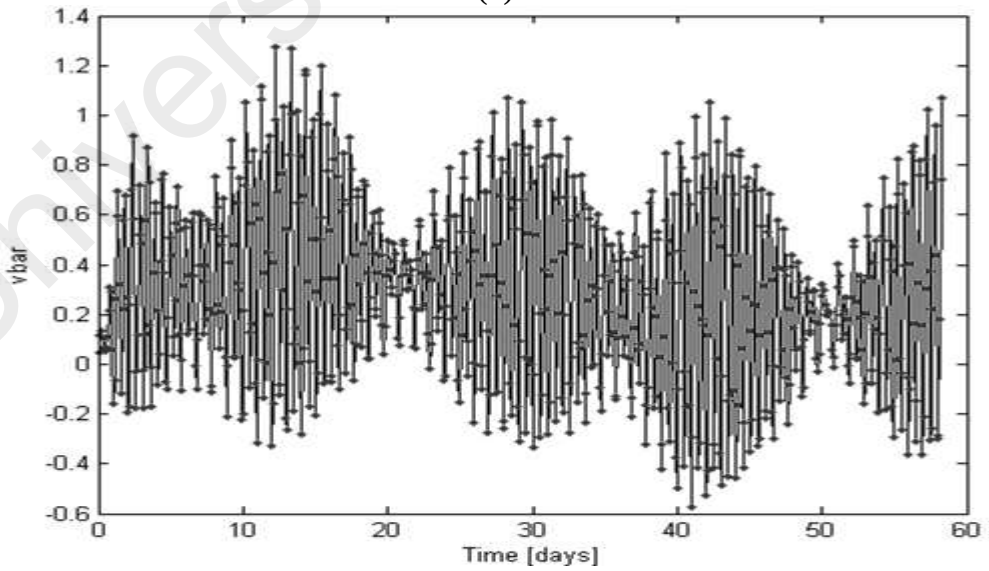

(c)

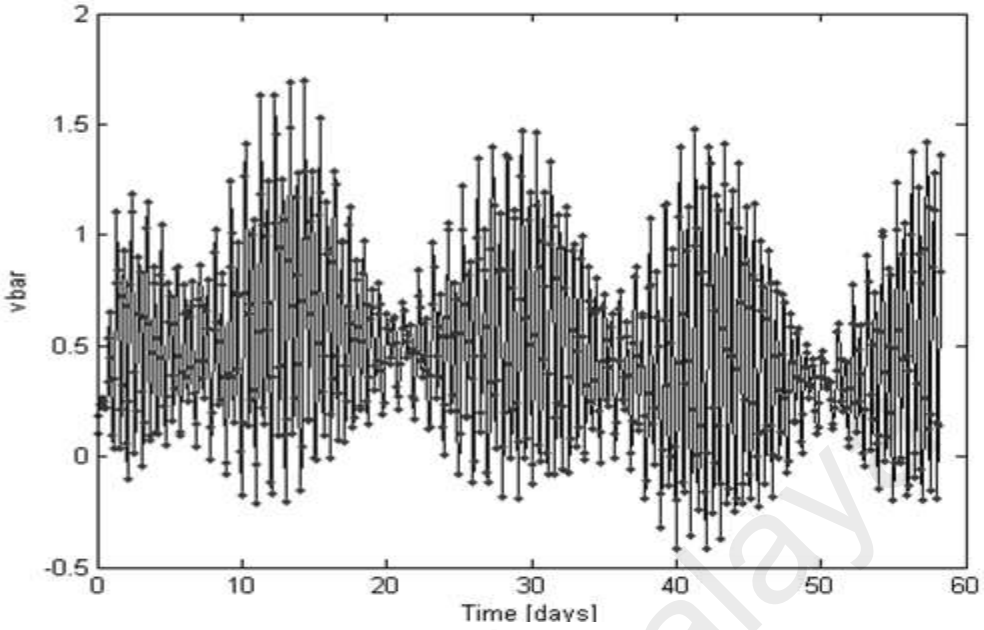

(d)

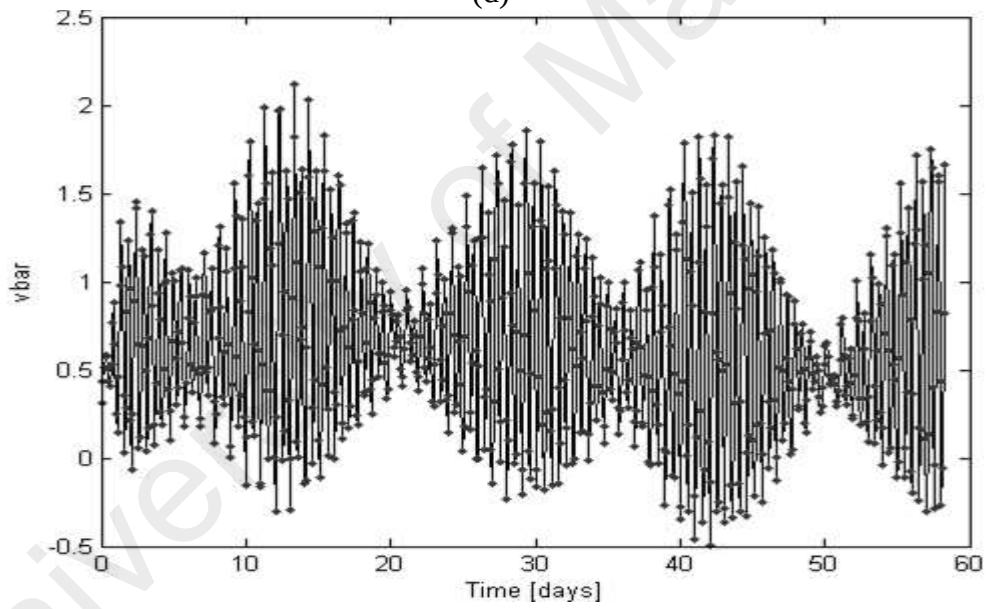

(e)

Figure 4.15 Variation of tidal flow speed at five grid points in zone-I shown in (a), (b), (c), (d) and (e) respectively (a, b, c, d, and e represents five measuring points in Zone-I).

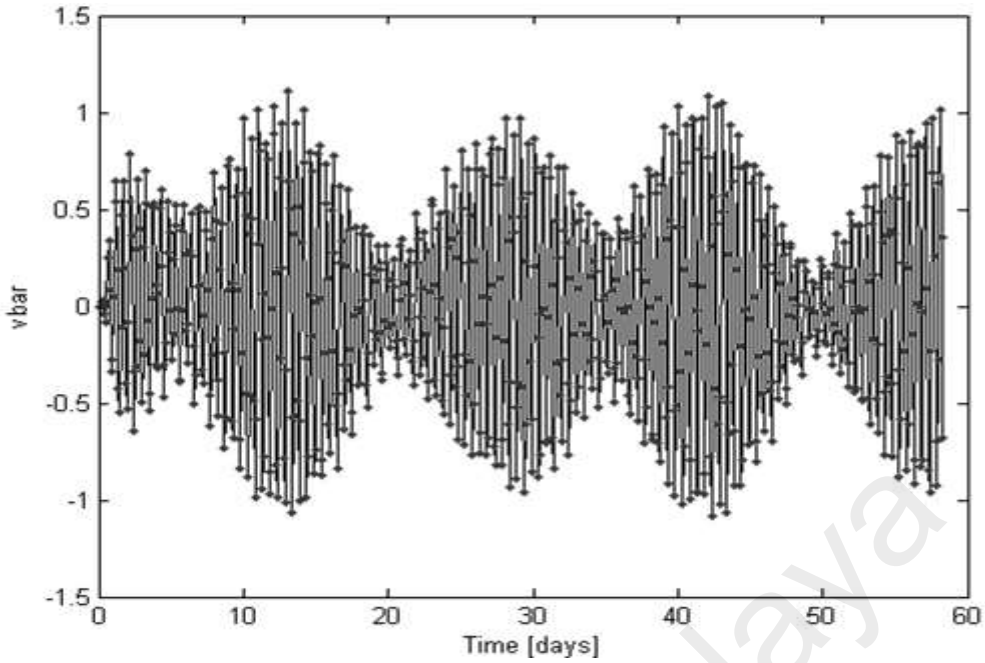

(a)

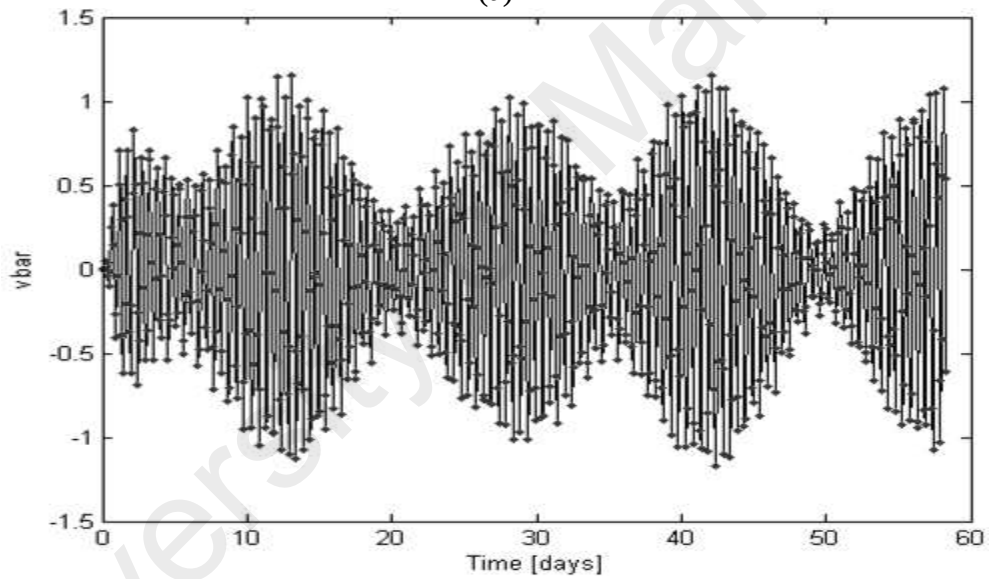

(b)

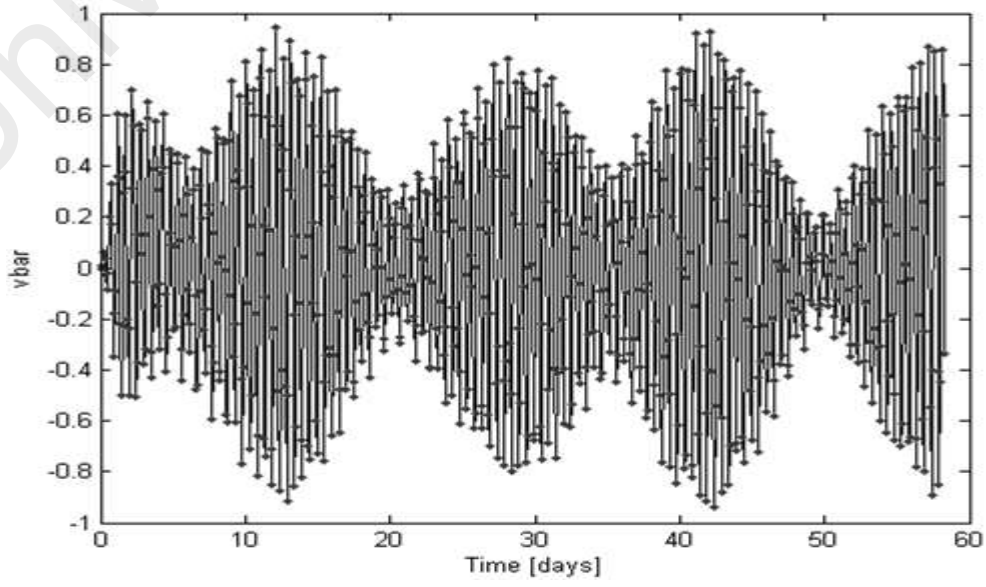

(c)

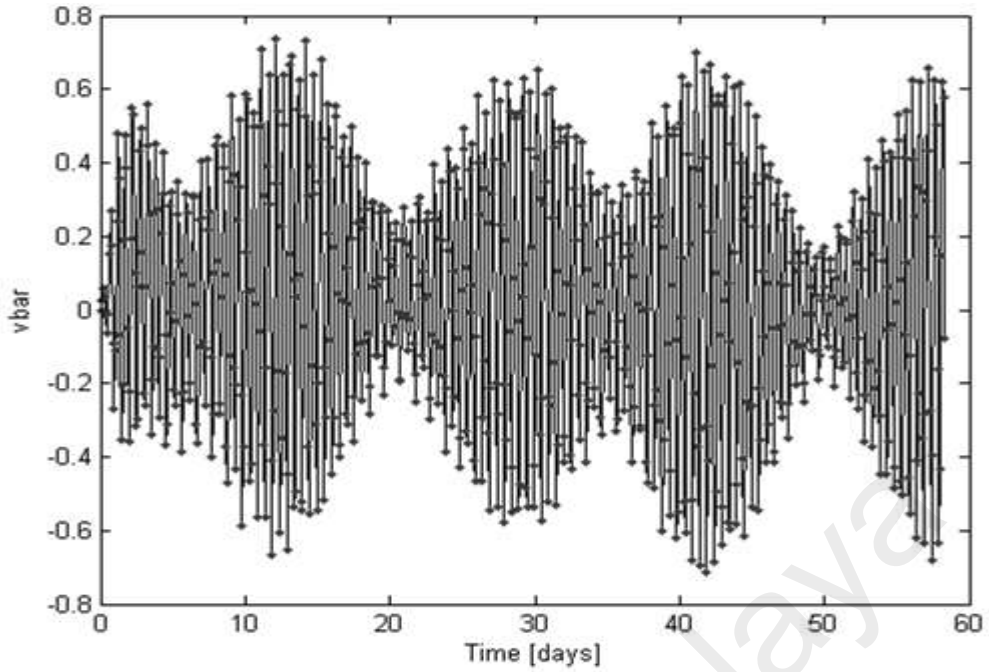

(d)

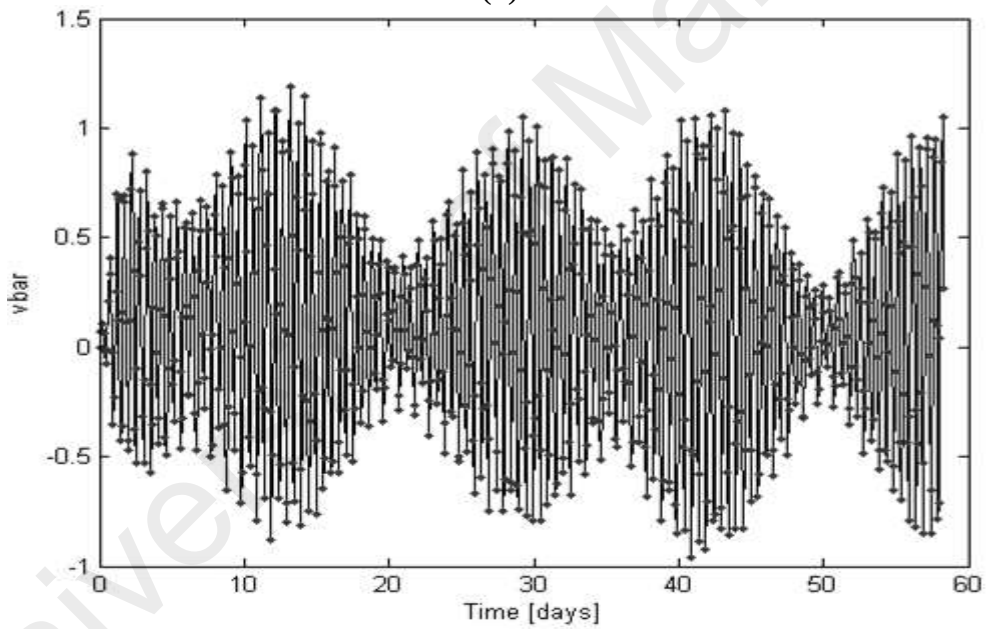

(e)

Figure 4.16 Variation of tidal flow speed at five grid points in zone-II shown in (a), (b), (c), (d) and (e) respectively (a, b, c, d, and e represents five measuring points in Zone-II).

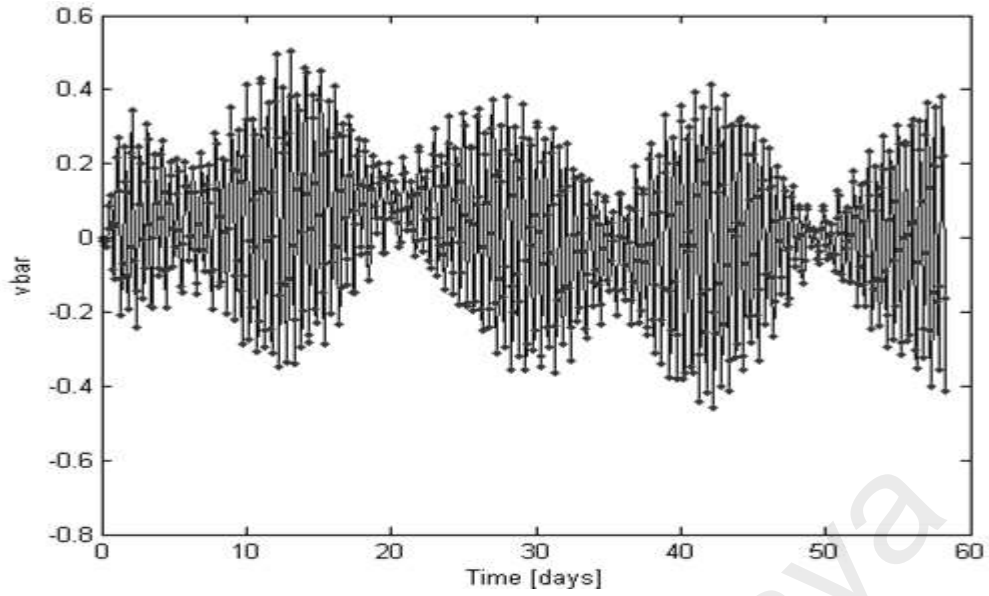

(a)

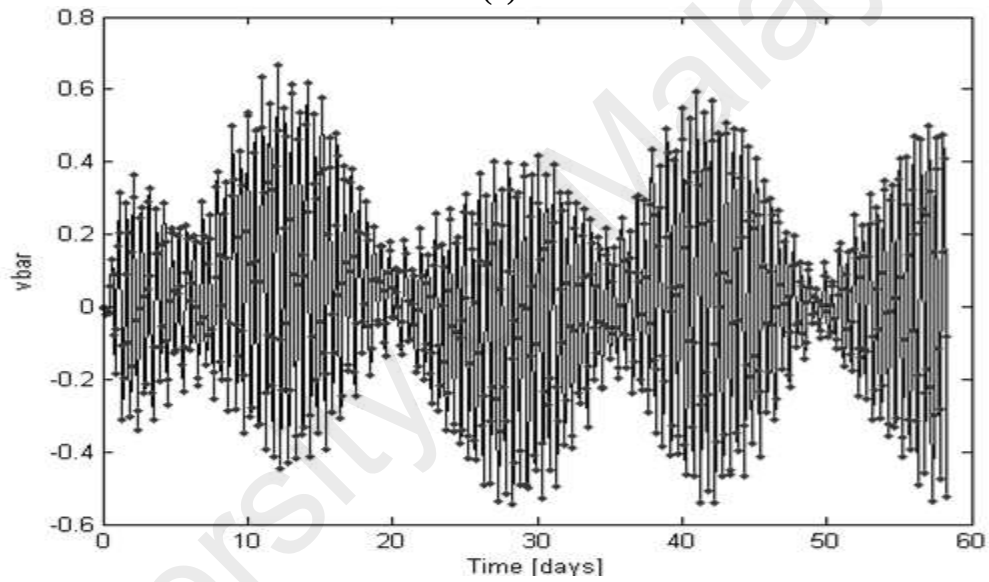

(b)

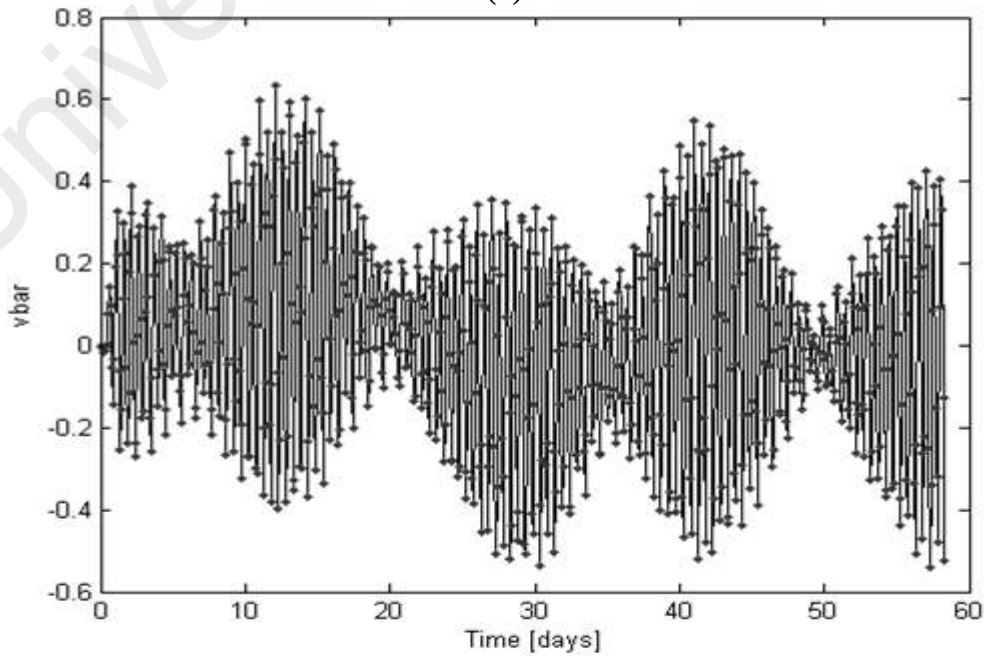

(c)

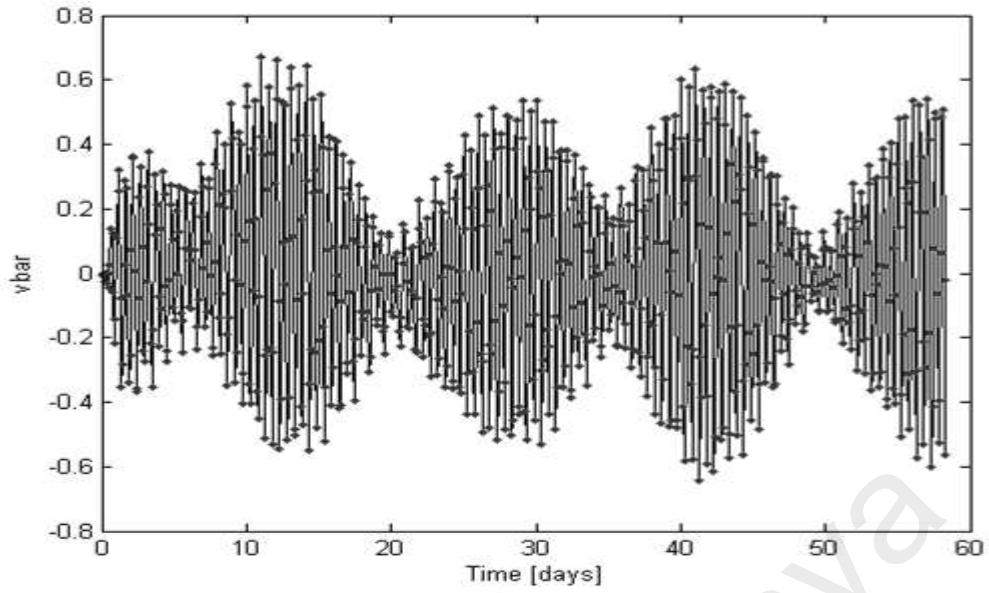

(d)

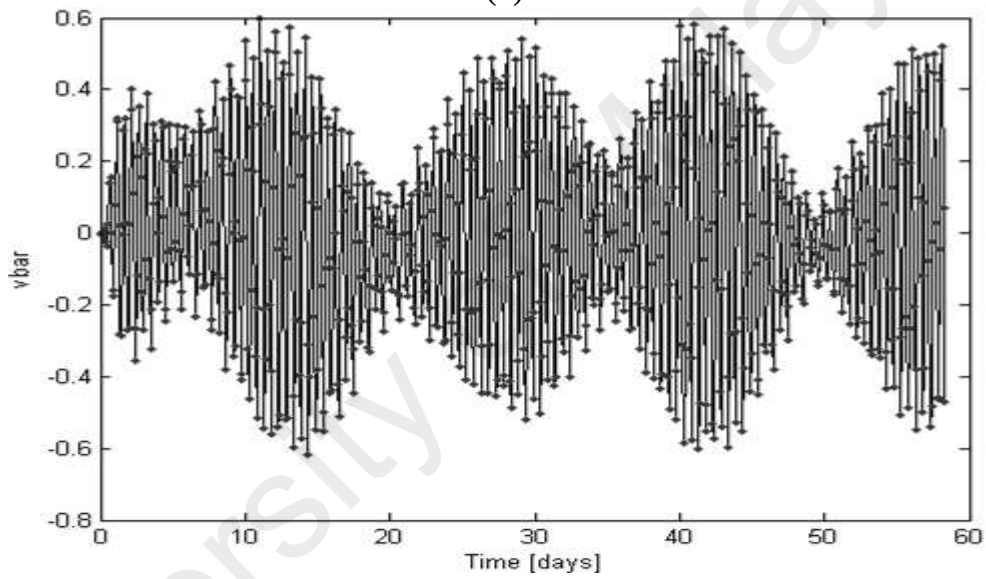

(e)

Figure 4.17 Variation of tidal flow speed at five grid points in zone-III shown in (a), (b), (c), (d) and (e) respectively (a, b, c, d, and e represents five measuring points in Zone-III).

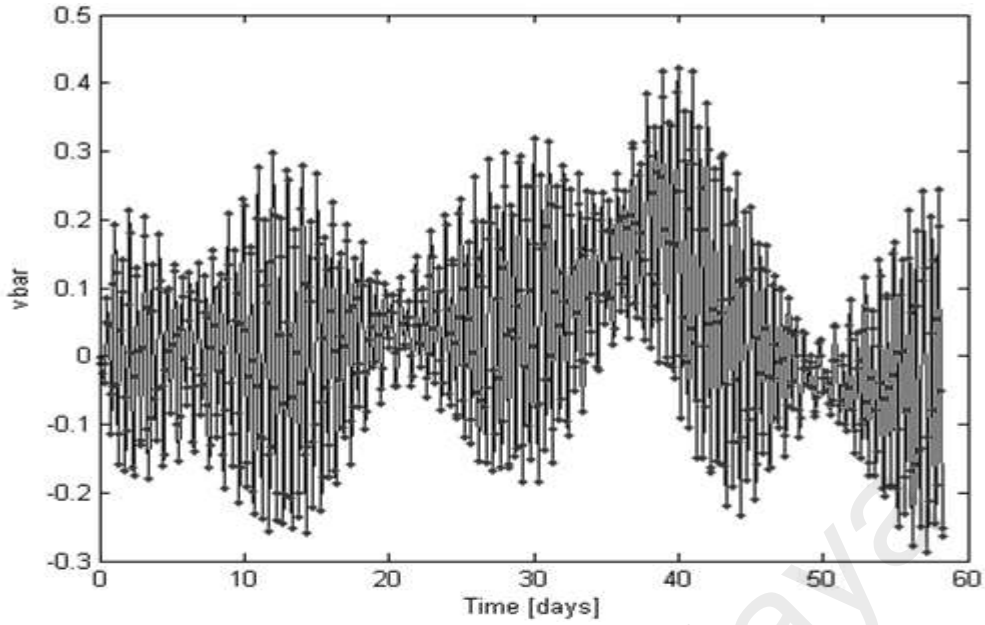

(a)

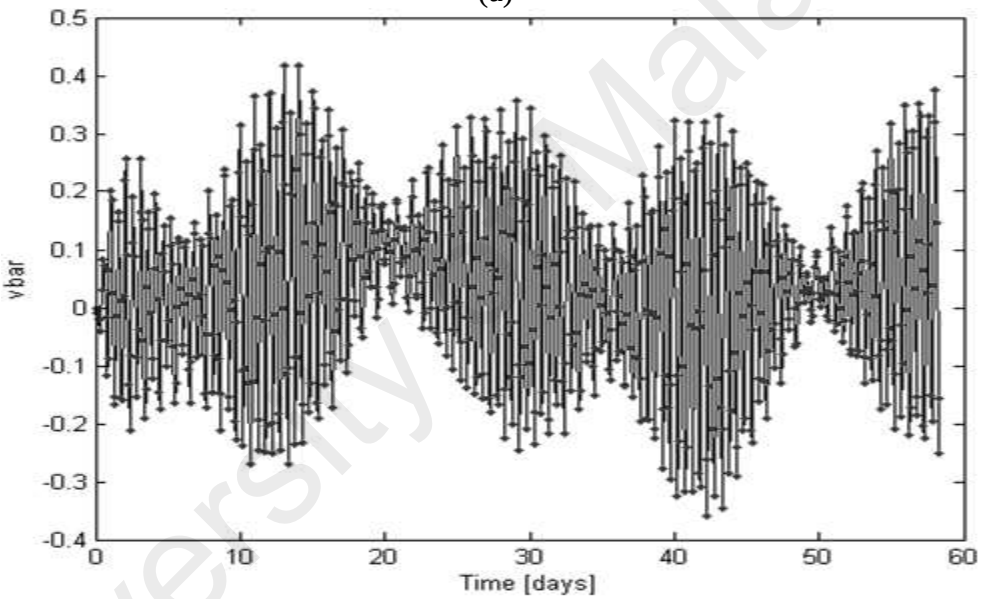

(b)

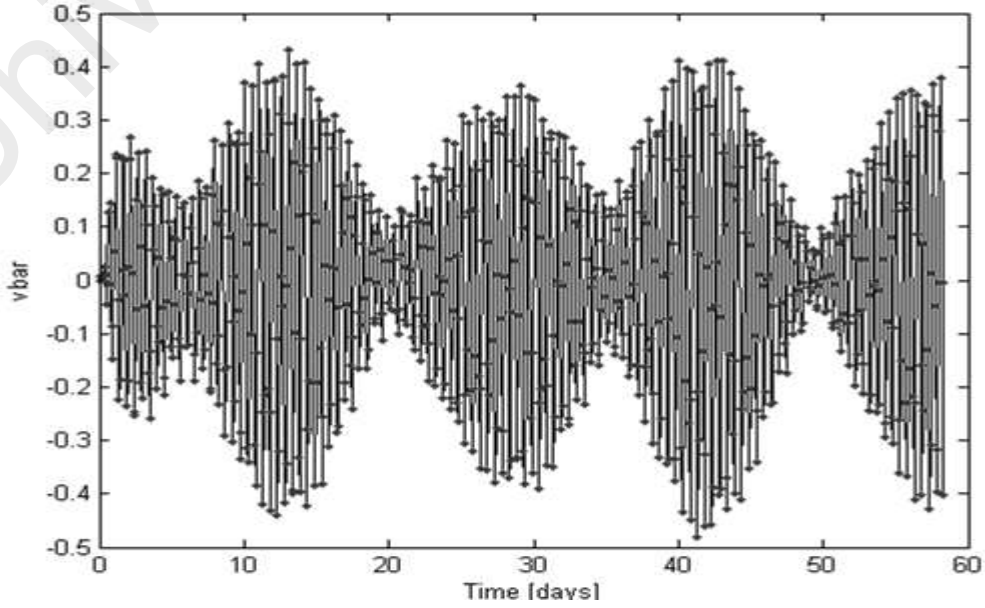

(c)

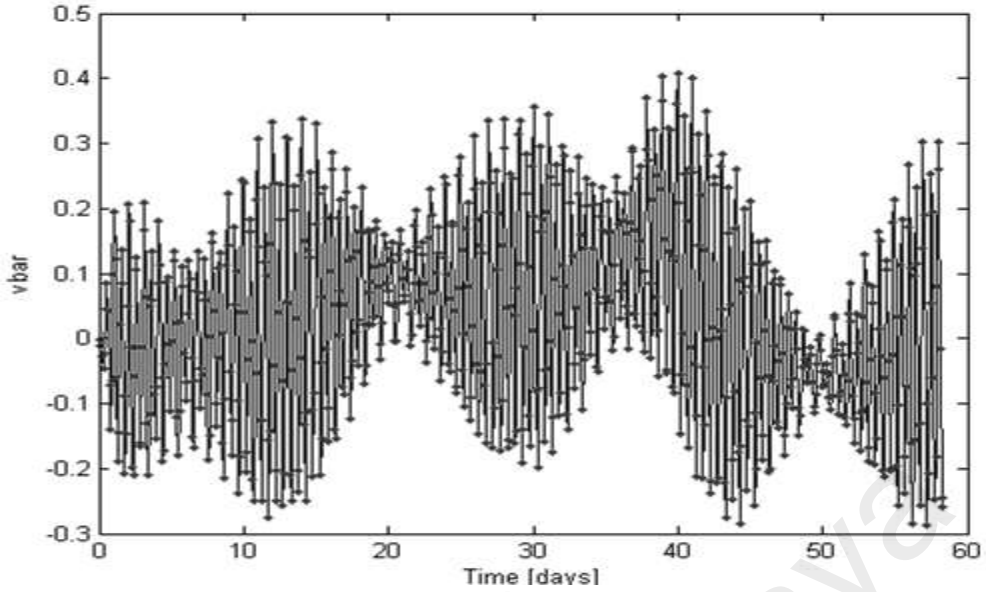

(d)

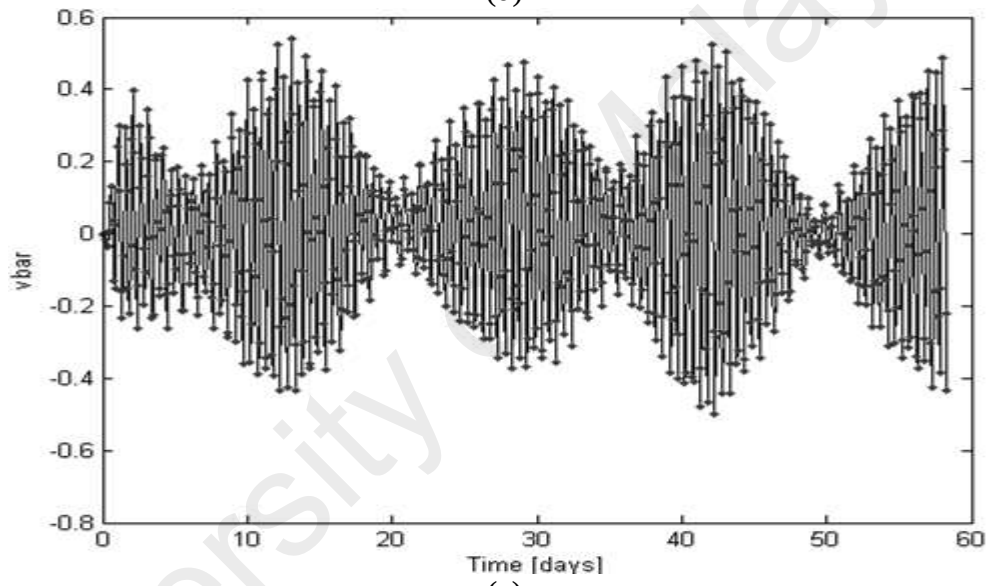

(e)

Figure 4.18 Variation of tidal flow speed at five grid points in zone-IV shown in (a), (b), (c), (d) and (e) respectively (a, b, c, d, and e represents five measuring points in Zone-IV).

4.8.2 Selected sites

Discussion in section 4.8.1 testifies that zone-I and zone-II are suitable region for extracting tidal stream energy in the Straits of Malacca. Whereas, the zone-III, and zone-IV receives insufficient tidal flow speeds. Therefore, site for harnessing tidal stream energy must be chosen in zone-I and zone-II.

Vicinity of selected sites to land should provide easy access to electrical grid and cities. Thus, based on above analysis three sites were identified suitable for harnessing tidal stream energy (Figure 3.6 and 4.13). The three sites are near the coastal waters of following cities:

1) Pangkor Island,

2) Malacca City coastline and

3) Port Klang

These sites provide sufficient tidal flow speed required for operation of tidal current turbines. In addition have appropriate sea depth for installation and maintenance of tidal current turbine. Site near coastline of the Pangkor Island have depth of 35 m and receive peak tidal flow speed 1.3 m/s. Port Klang provide depth of 25 m and receive peak tidal flow speed of 1.4 m/s. Malacca coastline provides depth of 20 m and receives peak tidal flow speed of 1.7m/s.

4.9 Analysis of Tidal Stream Energy

4.9.1 Threshold energy

Tidal stream energy stored in the tidal flows is represented as power per unit cross-sectional area. Tidal current turbines are used to harness tidal stream energy. It is important to look at start-up speed (cut-in speed) of the tidal current turbines. Start-up-speed is defined as minimum speed at which tidal current turbines start to operate. Commercial tidal current turbines such as the SeaGen, OpenHydro and NP1000 have start-up speed of 0.7 m/s, 0.6 m/s and 0.5 m/s respectively. Thus site for installing tidal current turbine should have flow speed greater than the start-up speed for most duration in a day.

The tidal energy flux corresponding to start-up speed is called threshold energy. In this study regions that receive tidal stream power greater than 64 W/m^2 are considered of interest. Energy fluxes of 64 W/m^2 correspond to tidal flow of 0.5 m/s. Contour lines are drawn for regions with threshold energy enough to operate tidal stream converters (Figure 4.11 and 4.12).

4.9.2 Tidal energy flux in the Straits of Malacca

This section discusses distribution of tidal stream energy in the Straits of Malacca. The Straits of Malacca was classified into four zones for this analysis. Classification is based on latitude starting from 1.5°N to 8°N as shown in Table 4.3. Contour lines in Figure 4.11 and Figure 4.12 indicate the tidal stream energy corresponding to tidal flow speed throughout the Straits of Malacca. Useful tidal stream energy in the Straits of Malacca varies from 64 W/m^2 to 2516 W/m^2 (Figure 4.11 and Figure 4.12).

Flow in the Straits of Malacca is tidal in nature; tidal energy distribution varies from the spring to neap tidal period (Table 4.3). Stronger tidal flow occurs during the spring period and lowers during the neap periods. The zone-I is at southeast end of the Straits of Malacca. It receives peak tidal stream energy of 2516 W/m^2 corresponding to flow speed of 1.7 m/s. Tidal flow direction changes four times a day during two high and low tides. The zone-II receives peak tidal stream energy of 1406 W/m^2 corresponding to flow speed of 1.4 m/s. The Zone-III is centre of the Straits of Malacca and receives peak tidal stream energy of 176 W/m^2. The zone-III and IV are in the upper part of the Straits of Malacca. They receive much lower tidal stream energy compared to other zones. This is due to presence of lower flows in zone-III and IV. Therefore, zone I and zone II provide best tidal stream energy resource in the region. It was also observed that magnitude of flow is greater when flow is towards southeast

direction. Peak flow in zone-II is 1.2 m/s when flow direction is to the north-west. But peak flow reaches up to 1.4 m/s in zone II when flow direction is towards southeast. This may be because of narrowing effect of the Peninsular Malaysia and the Sumatra Island. Similar trend was observed in zone I. Results show the Straits of Malacca is suitable for extraction of tidal stream energy as shown in Table 4.3.

Table 4.3 Characteristics of four zone under investigation for tidal stream energy in the Straits of Malacca.

Latitude	Zone	Range in tidal flow speed (m/s)	Tidal stream energy (W/m^2)	Suitable zone for Tidal Stream Energy
1.5°N to 3°N	I	0.40 - 1.50	32.80 – 2516	√
3°N to 4.5°N	II	0.30 - 1.30	14.00 – 1406	√
4.5°N to 6° N	III	0.10 – 0.70	0.51 -176	X
6°N to 8°N	IV	0.10 - 0.50	0.51 – 64	X

Tidal stream energy resources were identified in the present study. Amount of tidal energy varies in magnitude at these sites. Identified sites are ranked taking into account available tidal speed and sea depth (Table 4.4). Sites better suited for installation of tidal stream turbine were given higher grade. Malacca city coastline receives grade-A tidal stream resources. Port Klang and Pangkor Island have significant tidal stream energy and are grade-B resources. All these sites provide threshold tidal stream energy and sea-depth suitable for extraction of tidal stream energy.

Table 4.4 List of site selected for extracting tidal stream energy in the Straits of Malacca. Their appropriateness are suggested based on considerations of available power, flow speed and sea-depth.

Site for Tidal Current Turbine installation	Tidal stream energy (W/m^2)	Average sea-depth (m)	Grade of resource available at site.
Pangkor Island	1406	35	B
Port Klang	1406	25	B
Malacca city coastline	2516	25	A

4.9.3 Assessment of Power Potential

4.9.3.1 Available and extractable Power from Single Turbine

Pangkor Island, Malacca City coastline and Port Klang are three potential sites for extracting tidal stream energy. A comparative study was undertaken on performance of two tidal current turbines at these sites (Table 4.5). Performance of the OpenHydro and Gorlov turbine were compared at the three sites. Gorlov and Open Hydro represent vertical axis and horizontal axis turbine groups respectively. This investigation would provide insight into performance of these two group of turbines.

Gorlov turbine is vertical axis with 2.5 m height, 1m diameter, rated power 1.5 Kw at 1.5 m/s. Openhydro is horizontal axis turbine with 6 m diamter rated power 250 Kw at 2 m/s. This investigation on performance of tidal current turbine considered three parameters namely the availability energy, electric output (E_e), and capacity factors (C_f). Separate calculations were made for each of the three sites. Results are given in table 4.5.

A single Gorlov turbine extracts 28% of the available power from tidal current at all three sites. It is able to extract 28% of the available power because the Gorlov turbine has rated speed of 1.5 m/s, and the Straits of Malacca provides this flow speed at selected sites. Annual available power to Gorlov turbine from tidal flow streams is 13140 Kwh. All of this available power cannot be extracted due to design, mechanical, electrical, transmission, and other losses. A single Gorlov turbine produces 3922 Kwh, 3746.85 Kwh, and 3586.55 Kwh power annually at Malacca city coastline, Port Klang, and Pangkor Island respectively.

A single Open Hydro on the other hand can extract only 2.5% of the available tidal stream energy at three sites. This is mainly because Open Hydro turbines are designed to work efficiently in higher flows in the range of 1.5 m/s to 2.5 m/s. Whereas the Gorlov turbine are rated to work efficiently at 1.5 m/s. A single Open Hydro turbine produces 49.30 Mwh, 42.65 Mwh, and 52.90 Mwh power annually at Malacca city coastline, Port Klang, and Pangkor Island respectively. Thus this investigation found that the Gorlov turbine performs efficiently while OpenHydro under-performs in the Straits of Malacca. Therefore, Gorlov turbines are better suited for energy extraction in the Straits of Malacca.

Table 4.5 Annual estimate of extractable and available power for single Gorlov and Openhydro tidal current turbine at selected sites.

Sites	Gorlov turbine			OpenHydro		
	E(t) (Kwh)	E_e *(Kwh)*	C_f	*E(t) (Mwh)*	E_e *(Mwh)*	C_f
Malacca city	13140	3922.00	29.84%	2190	49.30	2.25%
Port Klang	13140	3746.85	28.51%	2190	42.65	1.94%
Pangkor Island	13140	3586.55	27.29%	2190	52.90	2.42%

4.9.3.2 Available and extractable Power from Tidal Farm

The installation of tidal current turbine farm is proposed to maximize the extractable energy in the Straits of Malacca. This study also estimates the annual electricity that can be generated using tidal farms in the Straits of Malacca. As discussed in chapter 3 section 3.11.3.2, this study considers three configuration of tidal farm. This study considered tidal farms with 50, 100, and 500 units of tidal current turbines in order to simplify the process of computing power potential.

Farm layout: A minimum water depth of 15 m is required for the proposed marine current turbine farm. As can be seen in Figure 4.10 a large part in the Straits of Malacca has suitable depth greater than 15 m. Based on the diameter, lateral spacing and downstream spacing between tidal stream turbines were determined. According to the

'Assessment of Tidal Energy Resource: Marine Renewable Energy Guides', the suggested lateral spacing (the distance measured between axis of rotation of adjacent turbines) is 2.5D (Blunden & Bahaj, 2007; Legrand, 2009). On the other hand, the suggested downstream spacing is 20D. Figure 3.18 shows part of the layout of the marine current turbine farm.

OpenHydro tidal current turbines are less efficient since they can only extract 2.9% of the available energy. Therefore, this study considers the Gorlov turbine for computing annual electricity from tidal farm. As discussed in previous sub-section, a single Gorlov turbine produces 3922 Kwh, 3746.85 Kwh, and 3586.55 Kwh electricity-annually at Malacca city coastline, Port Klang, and Pangkor Island respectively. This study made simple assumptions that performance of single device when installed in farm configuration is not affected when proper spacing is given between consecutive rows. Therefore, a tidal farm with *N* number of tidal current turbine would produce *N* time electricity of single device. Table 4.6 list the annual output from various configuration of tidal farm at three identified sites.

Table 4.6 Annual extractable power for tidal farm configurations of Gorlov turbine with 50, 100, and 500 units, at the selected sites.

Site	Annual electricity $E(t)$,E_e in *Mwh*, from Single Tidal Current Turbine		Annual electricity $E(t)$ in *Mwh*, for various Tidal Farm configuration at selected sites		
			50(*N*)	100(*N*)	500(*N*)
	E(*t*)	E_e			
Malacca city	13.140	3.922	196.10	392.20	19610
Port Klang	13.140	3.746	187.30	374.60	18730
Pangkor Island	13.140	3.586	179.30	358.60	17930

Power output: Available and extractable powers were calculated for the variation in the flow speed from flood tide to neap tide. For transmission efficiency and generator efficiency, an average efficiency of 0.9 was used (Belloni & Willden, 2011; Legrand, 2009). These values are also suggested by the 'Assessment of Tidal Energy Resource:

Marine Renewable Energy Guides'. As a result, the power coefficient (C_T) of 0.36 was used.

A farm size of 500 unit can produce 19610 Mwh, 18730 Mwh, and 17930 Mwh of electricity annually at Malacca city coastline, Port Klang, and Pangkor Island respectively. Similarly a conservative 100 unit of tidal current turbine in a farm can extract annually 392.20 Mwh, 374.60 Mwh, and 358.60 Mwh of electricity annually at Malacca city coastline, Port Klang, and Pangkor Island respectively. Further a small 50 unit size of tidal farm can extract 196.10 Mwh, 187.30 Mwh, and 179.30 Mwh of electricity annually at Malacca city coastline, Port Klang, and Pangkor Island respectively.

Significance of the extractable power from tidal farm becomes clear when a comparison is made with the peak demand for electricity in Peninsular Malaysia. As recorded on June 2012, the peak demand for electricity in the Peninsular Malaysia was about 16GW (Tang, 2008). Thus tidal stream energy can contribute significant amount of electricity to the Malaysia's electricity demands.

4.10 Summary

This chapter discussed result from this work. Discussion showed that numerical model validated satisfactorily with measurement and previous research works. Bathymetry of the Straits of Malacca ranges from few meters to more than 100 m. In depth discussion on bathymetry clearly indicates west coast of Malaysia provides suitable depth for installing tidal current turbines. Further tidal flow in the Straits of Malacca varies from one region to other. Southern and central part of the Straits receives peak flow more than 1.5 m/s, whereas northern part receives lower flows. Therefore, central and southern region of the Straits have desirable flow speed. This study divided the Straits into four even zones. In each zone five grid points were selected for analysing results of

tidal flow. This study identified three sites for harnessing tidal stream energy, based on above investigation. The three sites are off the coast of Malacca City; Port Klang; and Pangkor Island. The selected sites provide suitable flow speed and sea depth. Further this study gathered information on distribution of tidal stream energy using energy flux equation.

Investigation estimated annual available and extractable power at three selected sites. The calculation used design specification of Gorlov and OpenHydro tidal current turbine. Since these two turbines are representative of two class of commercial converters. Results show that annual extractable tidal power from single Gorlov turbine off the coast of Malacca City; port Klang; and Pangkor Island are 3922, 3746.85, and 3586.55 Kwh respectively. Annual extractable power from single OpenHydro turbine at selected sites of Malacca city; Port Klang; and Pangkor Island are 49.30, 42.65, and 52.90 Mwh respectively. In addition a farm configuration consisting of 500 unit of Gorlov turbine can extract 19610, 18730, and 17930 Mwh of electricity annually at Malacca city coastline, Port Klang, and Pangkor Island respectively. Results indicate that the Straits of Malacca is suitable for extracting tidal stream energy. This study successfully combination of numerical and theoretical method, and satellite data for investigating tidal stream energy resource.

CHAPTER 5

CONCLUSION

5.1 Summary

This study successfully used combination of numerical model, analytical method and satellite data to investigate tidal stream energy in the Straits of Malacca. At selected sites, the Straits of Malacca provides suitable flow speed and sea depth for operating tidal current turbine.

Following are major finding from this study:

- The Straits of Malacca receives semi-diurnal tide, with tidal flow ranging from 0.1 m/s to 1.7 m/s at various parts. Southern and central region of the Straits of Malacca receives peak tidal flow above 1.5 m/s, whereas the northern part receives lower flow with peak of 0.7 m/s.
- This study identified three sites in the Straits of Malacca for extracting tidal stream energy. The three sites are *(i)* Malacca City coastline; *(ii)* port Klang; and *(iii)* Pangkor Island with tidal stream energy density of 2516, 1406, and 1406 W/m^2.
- Annual extractable tidal power from single Gorlov turbine off the coast of Malacca City; port Klang; and Pangkor Island are 3922, 3746.85, and 3586.55 Kwh respectively. Annual extractable power from single OpenHydro turbine at selected sites of Malacca city; Port Klang; and Pangkor Island are 49.30, 42.65, and 52.90 Mwh respectively.
- Straits of Malacca provide suitable sea depth in the range of 15 to 60 m along coastline of Peninsular Malaysia.

- In addition a farm configuration consisting of 500 unit of Gorlov turbine can extract 19610, 18730, and 17930 Mwh of electricity annually at Malacca city coastline, Port Klang, and Pangkor Island respectively.

This study used numerical model to investigate distribution of tidal flow speed and sea depth in the Straits. Later, model results were used to select sites with higher concentration of tidal energy. The model results agree satisfactorily with measurements and previous research works. Results show three sites in the Straits have desired tidal stream energy potential. Investigation further analysed power potential of the selected sites. Analytical methods were used to calculate available and extractable tidal stream power. This study considered two scenarios for estimating available and extractable power. First case considered design specifications of two tidal current turbines for computing their performance at three sites. Annual extractable power was estimated for single tidal current turbine at three selected sites. Second scenario considered tidal farm configuration of 50, 100, and 500 unit of tidal current turbine in the Straits of Malacca.

5.2 Tidal Flow Speed in the Straits of Malacca

This study determined speed tidal flow in the Straits of Malacca as its first objective. In this regard, the investigation prepared a numerical model for the Straits of Malacca. Numerical model used the Princeton Ocean Model (POM) for estimating speed of tidal flow. Then this study calibrated and validated numerical model using observation data from tidal station and satellite. The validation of model used observation data for speed and elevation of tide from the National Hydrographic Centre, Malaysia. Another set of validation used data from previous research works of Wyrtki (1961), Keller and Richards (1967), and Rizal et al. (2012). Model output showed excellent agreement with both observation and published data.

Tidal flow speed at twenty points for 60 day duration was analysed (Figure 4.15). Result shows speed of tidal flow in the Straits of Malacca varies from 0.1 to 1.7 m/s for a Spring-Neap tidal cycle (Figure 4.16-4.19). The Straits of Malacca receives semi-diurnal tide. Knowledge of distribution of sea depth and tidal flow was important for selecting site and assessing power potential. Moving ahead site with higher flow speed and suitable depth were selected for extraction of tidal stream energy. This study successfully determined speed of tidal flow in the Straits of Malacca.

5.3 Site Selected for Extracting Tidal Stream Energy

Sites for extracting tidal stream energy needs to fulfil criteria of the sea depth and flow speed. This study used high resolution satellite data to investigate bathymetry (sea depth) throughout the Straits of Malacca. Further results of numerical model helped to investigate distribution of tidal flow. Previous research works propose suitable depth for selecting site in the range of 15 to 60 m. Research studies consider acceptable flow speed of around 1 m/s for extracting tidal stream energy.

This study divided the Straits of Malacca into four zones in order to investigate speed of tidal stream (Figure 4.15). This investigation selected five measuring points for analysing tidal flow velocity. Numerical model covered fours spring-neap cycle providing tidal flow speeds for 60 days. Analysis found zone-I and zone-II provide suitable flow speed and sea depth for installing tidal current turbines (Figure 4.15).

Satellite data was filtered for various ranges to investigate sea depth. This study considered three set of sea depth range for analysis of satellite data i.e. 15-1500 m, 15-100 m and 15-60 m (Figure 4.8-4.11). Sea depth on west coast of Malaysia was found to be suitable, ranging from 15 to 60 m (Figure 4.10, 4.11). Further this study analysed flow speed and tidal energy flux in region which provide suitable sea depth (Figure 4.12-4.13). Region too far into ocean were neglected, since it is infeasible and

economically inefficient. Investigation found peak tidal flow reaches above 1.5 m/s in central and southern part of the Straits (Zone-1 and Zone-II, Figure 4.15). Whereas the northern parts of the Straits receive lower flows with peak ranging from 0.5 to 0.8 m/s. This study selected sites near major coastal city which provided suitable sea depth and tidal flow velocity.

Sites off the coast of Malacca city, Port Klang and Pangkor Island are found to be economical for extracting tidal stream energy (Table 4.3-4.4). They provide suitable sea depth and desired threshold speed for installing and operating tidal current turbines (Table 4.3-4.4). Further this study looked at available and extractable power at these three sites under various considerations.

5.4 Available and Extractable Tidal Stream Energy

Tidal current turbines convert the kinetic energy from tidal stream into useful electricity. Due to design consideration of tidal current turbine it is not possible to extract all the available kinetic energy from free flowing tidal streams. Amount of power generated by tidal current turbine from the available power is called extractable power. This study investigated and estimated available and extractable energy at the selected sites. Two scenarios were considered for estimating available and extractable tidal stream energy. First scenario considered design of two turbines from major classes of commercial tidal current turbines. Second scenario considered hypothetical tidal farm for estimating extractable tidal stream energy.

Performance of Open Hydo and Gorlov turbines were investigated. Golorv turbine is 2.5 m height, and 1 m diameter, vertical axis turbine. On the other hand Open Hydro is 10 m diameter horizontal axis turbine. Investigation found that open hydro turbine have larger available power because of larger cross sectional area in comparison with Gorlov. This study calculated the annual power output from single turbine based on tidal flow

speed and energy flux. A single Gorlov turbine produces 3922 Kwh, 3746.85 Kwh, and 3586.55 Kwh power annually at Malacca city coastline, Port Klang, and Pangkor Island respectively (Table 4.5). A single Open Hydro turbine produces 49.30 Mwh, 42.65 Mwh, and 52.90 Mwh power annually at Malacca city coastline, Port Klang, and Pangkor Island respectively (Table 4.5).

Investigation found Open Hydro under-performs at all three sites. Open Hydro performs with capacity factor of 2.5% at the site, which implies it can only extract 2.5% of the available power from tidal streams. On the other hand the Gorlov turbine performs satisfactorily at all three sites. Gorlov turbine performs with capacity factor of 28%, which implies it converts 28% of tidal stream energy into useful electricity. This study estimates annual power output from tidal stream energy for single tidal current turbine at selected sites. Tidal farm with 500 units in the Straits of Malacca would generate 19610, 18730, and 17930 Mwh of electricity annually at Malacca city coastline, Port Klang, and Pangkor Island respectively. Further this analysis also found mini-tidal current turbine like the Gorlov turbine performs better than big commercial turbines such as Open Hydro.

5.5 Conclusion

Tidal stream energy is renewable and sustainable source of electricity. This study successfully investigated tidal stream energy resources in the Straits of Malacca. First validated numerical model was used to obtain speed of tidal flow in the Straits of Malacca. Carefully this study eliminated region which receive low tidal flow and have higher sea depth. Selected region receives significant flow speed with peak flow speed reaching up to 1.7 m/s. Investigation identified three sites for extracting tidal stream energy in the Straits. The three sites being off the Coast of Pangkor Island, Port Klang and Malacca city. The study found significant power can be generated from the selected

sites using tidal current turbines (Table 4.4). Site near coastline of the Pangkor Island have average depth of 35 m and receive peak tidal energy flux 1406 W/m2. Port Klang provide average depth of 25 m and receive 1406 W/m^2 of peak tidal energy flux. Malacca coastline provides depth of average 20 m and receives 2516 W/m^2 of peak tidal energy flux.

Tidal farm in the Straits of Malacca would generate 19610, 18730, and 17930 Mwh of electricity annually at the three selected sites i.e. Malacca city coastline, Port Klang, and Pangkor Island respectively.Study made a comparative study between the Gorlov and Open Hydro tidal current turbine. The Gorlov turbine performs efficiently over the Open Hydro. Annual power output of a single Gorlov turbine was found to be 3500 kWh. While a single Open Hydro turbine gave annual power output of 45 Mwh. Open hydro turbine gave high power output over the Gorlov turbine because of larger swept blade area and higher rated power output. However, look into the capacity factor indicates that Gorlov turbine efficiently harness tidal stream energy in the Straits of Malacca. The Gorlov turbine converts 28% of the available tidal stream energy into electricity. On the other hand the Open hydro converts only 2.5 % of the available tidal stream energy into electricity. This study computed speed of tidal flow, selected site, and estimated power output for harnessing tidal stream energy.

5.6 Benefit and Limitation of the Study

This study successfully used combination of numerical model, analytical method and satellite data to investigate tidal stream energy in the Straits of Malacca. It is impractical to physically survey whole of the Straits of Malacca. This investigation used freely available satellite data and numerical code. Thus methodology use in present study reduces amount of capital cost. Field measurement requires help from boatman, survey vessel, labour, tripod frame and engineers. Normally, field measurement costs RM

40,000 (11,000 USD) for making single point measurement into ocean using the Acoustic Doppler Current Profiler (ADCP). A huge capital would be required, if field experiment would have been conducted to investigate whole of the Straits. Thus it is economical to use numerical model instead of field measurement.

A high resolution satellite data was used to investigate sea depth and topography of the Straits of Malacca. Numerical model was used for modelling speed of tidal flow, for this high resolution computation grid was used. Numerical model was validated and calibrated using observation data from tidal stations. However, running high resolution numerical model required high performing computer time. In addition, the three selected sites still require localized surveys for precise measurement. Nevertheless, this study helped to converge and focused area of interest to carry out field measurements. For future study it is suggested to carry out field measurement at selected sites for investigating type of bathymetry, local flow, and prototype testing of tidal current turbine.

REFERENCES

Adcock, T., Draper, S., Houslsby, G., Borthwick, A., & Serhadliglu, S. (2013). The available power from tidal stream turbines in the Pentland Firth. *Proceedings of the Royal Society A: Mathematical, Physical and Engineering Science, 469*, 2157.

Addis, P., Cau, A., Massuti, E., Merella, P., Sinopoli, M., & Andaloro, F. (2006). Spatial and temporal changes in the assemblage structure of fishes associated to fish aggregation devices in the Western Mediterranean. *Aquatic Living Resources, 19*(2), 149-160. doi: Doi 10.1051/Alr:2006018

Ali, R., Daut, I., & Taib, S. (2012). A review on existing and future energy sources for electrical power generation in Malaysia. *Renewable and Sustainable Energy Reviews, 16*(6), 4047-4055.

Alidadi, M., & Calisal, S. (2014). A numerical method for calculation of power output from ducted vertical axis hydro-current turbines. *Computers & Fluids, 105*, 76-81.

Amante, C., & Eakins, B. Arc-minute global relief model: procedures, data sources and analysis (ETOPO1). *NOAA, National Geophysical Data Center, Boulder, Colorado, USA*.

Amante, C., & Eakins, B. W. (2009). *ETOPO1 1 arc-minute global relief model: procedures, data sources and analysis*: US Department of Commerce, National Oceanic and Atmospheric Administration, National Environmental Satellite, Data, and Information Service, National Geophysical Data Center, Marine Geology and Geophysics Division.

Arany, L., Bhattacharya, S., Macdonald, J., & Hogan, S. J. (2014). Simplified critical mudline bending moment spectra of offshore wind turbine support structures. *Wind Energy*.

Assessment of Energy Production Potential from Tidal Streams in the United States. (2011). USA: Georgia Tech Research Corporation.

Bahaj, A. S. (2011). Generating electricity from the oceans. *Renewable & Sustainable Energy Reviews, 15*(7), 3399-3416. doi: DOI 10.1016/j.rser.2011.04.032

Bahaj, A. S. (2013). Marine current energy conversion: the dawn of a new era in electricity production. *Philosophical Transactions of the Royal Society A: Mathematical,Physical and Engineering Sciences, 371*(1985). doi: 10.1098/rsta.2012.0500

Bahaj, A. S., & Myers, L. (2004). Analytical estimates of the energy yield potential from the Alderney Race (Channel Islands) using marine current energy

converters. *Renewable Energy, 29*(12), 1931-1945. doi: DOI 10.1016/j.renene.2004.02.013

Bala, G., Krishna, S., Narayanappa, D., Cao, L., Caldeira, K., & Nemani, R. (2013). An estimate of equilibrium sensitivity of global terrestrial carbon cycle using NCAR CCSM4. *Climate dynamics, 40*(7-8), 1671-1686.

Barbarelli, S., Florio, G., Amelio, M., Scornaienchi, N., Cutrupi, A., & Zupone, G. L. (2014). Design procedure of an innovative turbine with rotors rotating in opposite directions for the exploitation of the tidal currents. *Energy, 77*, 254-264.

Belloni, C. S., & Willden, R. H. (2011). *Flow field and performance analysis of bidirectional and open-centre ducted tidal turbines.* Paper presented at the 9th European Wave and Tidal Energy Conference.

Besio, G., & Losada, M. A. (2008). Sediment transport patterns at Trafalgar offshore windfarm. *Ocean Engineering, 35*(7), 653-665. doi: DOI 10.1016/j.oceaneng.2008.01.002

Blumberg, A. F., & Mellor, G. L. (1983). Diagnostic and Prognostic Numerical Circulation Studies of the South-Atlantic Bight. *Journal of Geophysical Research-Oceans and Atmospheres, 88*(Nc8), 4579-4592. doi: Doi 10.1029/Jc088ic08p04579

Blunden, L., & Bahaj, A. (2006). Initial evaluation of tidal stream energy resources at Portland Bill, UK. *Renewable Energy, 31*(2), 121-132.

Blunden, L., & Bahaj, A. (2007). Tidal energy resource assessment for tidal stream generators. *Proceedings of the Institution of Mechanical Engineers, Part A: Journal of Power and Energy, 221*(2), 137-146.

Blunden, L., Bahaj, A., & Aziz, N. (2013). Tidal current power for Indonesia? An initial resource estimation for the Alas Strait. *Renewable Energy, 49*, 137-142.

Boersma, J., & Terwindt, J. (1981). Neap–spring tide sequences of intertidal shoal deposits in a mesotidal estuary. *Sedimentology, 28*(2), 151-170.

Brans, C., & Dicke, R. H. (1961). Mach's principle and a relativistic theory of gravitation. *Physical Review, 124*(3), 925.

Brink, K. (1991). Coastal-trapped waves and wind-driven currents over the continental shelf. *Annual Review of Fluid Mechanics, 23*(1), 389-412.

Bryden, I., Couch, S., Owen, A., & Melville, G. (2007). Tidal current resource assessment. *Proceedings of the Institution of Mechanical Engineers, Part A: Journal of Power and Energy, 221*(2), 125-135.

Bryden, I., Grinsted, T., & Melville, G. (2004). Assessing the potential of a simple tidal channel to deliver useful energy. *Applied Ocean Research, 26*(5), 198-204.

Bryden, I. G., & Couch, S. J. (2006). ME1—marine energy extraction: tidal resource analysis. *Renewable Energy, 31*(2), 133-139. doi: http://dx.doi.org/10.1016/j.renene.2005.08.012

Chen, H., Malanotte-Rizzoli, P., Koh, T.-Y., & Song, G. (2014). The relative importance of the wind-driven and tidal circulations in Malacca Strait. *Continental Shelf Research, 88*, 92-102.

Chen, W. B., Liu, W. C., & Hsu, M. H. (2013a). Modeling assessment of tidal current energy at Kinmen Island, Taiwan. *Renewable Energy, 50*(0), 1073-1082. doi: http://dx.doi.org/10.1016/j.renene.2012.08.080

Chen, W. B., Liu, W. C., & Hsu, M. H. (2013b). Modeling Evaluation of Tidal Stream Energy and the Impacts of Energy Extraction on Hydrodynamics in the Taiwan Strait. *Energies, 6*(4), 2191-2203.

Chen, Y., Lin, B., & Lin, J. (2014). Modelling tidal current energy extraction in large area using a three-dimensional estuary model. *Computers & Geosciences, 72*, 76-83.

Chong, H., & Lam, W. (2013). Ocean renewable energy in Malaysia: The potential of the Straits of Malacca. *Renewable and Sustainable Energy Reviews, 23*, 169-178.

Christodoulidis, D., Smith, D., Williamson, R., & Klosko, S. (1988). Observed tidal braking in the Earth/Moon/Sun system. *Journal of Geophysical Research: Solid Earth (1978–2012), 93*(B6), 6216-6236.

Chua, T.-E. (1979). *Site selection, structural design, construction, management and production of floating cage culture system in Malaysia.* Paper presented at the Proceedings of the International Workshop on Pen Cage Culture of Fish, 11-12 February 1979, Tigbauan, Iloilo, Philippines (pp. 65-80). Tigbauan, Iloilo, Philippines: Aquaculture Department, Southeast Asian Fisheries Development Center; International Development Research Centre.

Coiro, D., Nicolosi, F., De Marco, A., Melone, S., & Montella, F. (2005). *Dynamic behavior of novel vertical axis tidal current turbine: numerical and experimental investigations.* Paper presented at the The Fifteenth International Offshore and Polar Engineering Conference.

Connolly, D., Lund, H., Mathiesen, B. V., & Leahy, M. (2011). The first step towards a 100% renewable energy-system for Ireland. *Applied Energy, 88*(2), 502-507. doi: http://dx.doi.org/10.1016/j.apenergy.2010.03.006

Dadswell, M. J., Rulifson, R. A., & Daborn, G. R. (1986). Potential impact of large-scale tidal power developments in the upper Bay of Fundy on fisheries resources of the Northwest Atlantic. *Fisheries, 11*(4), 26-35.

Defne, Z., Haas, K. A., & Fritz, H. M. (2011a). GIS based multi-criteria assessment of tidal stream power potential: A case study for Georgia, USA. *Renewable & Sustainable Energy Reviews, 15*(5), 2310-2321. doi: DOI 10.1016/j.rser.2011.02.005

Defne, Z., Haas, K. A., & Fritz, H. M. (2011b). Numerical modeling of tidal currents and the effects of power extraction on estuarine hydrodynamics along the Georgia coast, USA. *Renewable Energy, 36*(12), 3461-3471. doi: DOI 10.1016/j.renene.2011.05.027

Douglas, C., Harrison, G., & Chick, J. (2008). Life cycle assessment of the Seagen marine current turbine. *Proceedings of the Institution of Mechanical Engineers, Part M: Journal of Engineering for the Maritime Environment, 222*(1), 1-12.

Draper, S., Adcock, T. A. A., Borthwick, A. G. L., & Houlsby, G. T. (2014). Estimate of the tidal stream power resource of the Pentland Firth. *Renewable Energy, 63*(0), 650-657. doi: http://dx.doi.org/10.1016/j.renene.2013.10.015

Dushaw, B. D., Egbert, G. D., Worcester, P. F., Cornuelle, B. D., Howe, B. M., & Metzger, K. (1997). A TOPEX/POSEIDON global tidal model (TPXO.2) and barotropic tidal currents determined from long-range acoustic transmissions. *Progress in Oceanography, 40*(1-4), 337-367. doi: Doi 10.1016/S0079-6611(98)00008-1

Esteban, M., & Leary, D. (2012). Current developments and future prospects of offshore wind and ocean energy. *Applied Energy, 90*(1), 128-136.

Ezer, T., Arango, H., & Shchepetkin, A. F. (2002). Developments in terrain-following ocean models: intercomparisons of numerical aspects. *Ocean Modelling, 4*(3-4), 249-267. doi: Pii S1463-5003(02)00003-3

Fernandez-Rodriguez, E., Stallard, T., & Stansby, P. (2014). Experimental study of extreme thrust on a tidal stream rotor due to turbulent flow and with opposing waves. *Journal of Fluids and Structures*.

Fraenkel, P. (2002). Power from marine currents. *Proceedings of the Institution of Mechanical Engineers, Part A: Journal of Power and Energy, 216*(1), 1-14.

Fraenkel, P. (2007). Marine current turbines: pioneering the development of marine kinetic energy converters. *Proceedings of the Institution of Mechanical Engineers, Part A: Journal of Power and Energy, 221*(2), 159-169.

Fraenkel, P. L. (2006). Tidal current energy technologies. *Ibis, 148*(s1), 145-151.

Frau, J. P. (1993). Tidal energy: promising projects: La Rance, a successful industrial-scale experiment. *Energy Conversion, IEEE Transactions on, 8*(3), 552-558.

Garrett, C., & Cummins, P. (2005). The power potential of tidal currents in channels. *Proceedings of the Royal Society a-Mathematical Physical and Engineering Sciences, 461*(2060), 2563-2572. doi: DOI 10.1098/rspa.2005.1494

Garrett, C., & Cummins, P. (2007). The efficiency of a turbine in a tidal channel. *Journal of Fluid Mechanics, 588*, 243-251. doi: Doi 10.1017/S0022112007007781

Garrett, C., & Cummins, P. (2008). Limits to tidal current power. *Renewable Energy, 33*(11), 2485-2490. doi: DOI 10.1016/j.renene.2008.02.009

Garrett, C., & Cunnins, P. (2005). *The power potential of tidal currents in channels.* Paper presented at the Proceedings of the Royal Society a-Mathematical Physical and Engineering Sciences.

Gillett, N. P., Arora, V. K., Zickfeld, K., Marshall, S. J., & Merryfield, W. J. (2011). Ongoing climate change following a complete cessation of carbon dioxide emissions. *Nature Geoscience, 4*(2), 83-87.

Gorlov, A., & Rogers, K. (1997). Helical turbine as undersea power source. Results of first stage experiments involve harnessing energy from slow undersea currents for marine applications. *Sea Technology, 38*(12), 39-43.

Grabbe, M., Lalander, E., Lundin, S., & Leijon, M. (2009). A review of the tidal current energy resource in Norway. *Renewable and Sustainable Energy Reviews, 13*(8), 1898-1909.

Halpern, B. S., Longo, C., Hardy, D., McLeod, K. L., Samhouri, J. F., Katona, S. K., . . . Ranelletti, M. (2012). An index to assess the health and benefits of the global ocean. *Nature, 488*(7413), 615-620.

Hammar, L., Ehnberg, J., Mavume, A., Francisco, F., & Molander, S. (2012). Simplified site-screening method for micro tidal current turbines applied in Mozambique. *Renewable Energy, 44*, 414-422.

Hassan, H. F., El-Shafie, A., & Karim, O. A. (2012). Tidal current turbines glance at the past and look into future prospects in Malaysia. *Renewable and Sustainable Energy Reviews, 16*(8), 5707-5717.

Iyser, A., Couch, S., Harrison, G., & Wallace, A. (2013). Variability and phasing of tidal current energy around the United Kingdom. *Renewable Energy, 51*, 343-357.

Jing, F., Sheng, Q., & Zhang, L. (2014). Experimental research on tidal current vertical axis turbine with variable-pitch blades. *Ocean Engineering, 88*, 228-241.

Keenan, G., Sparling, C., Williams, H., & Fortune, F. (2011). SeaGen Envionmental Monitoring Programme Final Report. Edinburgh,UK: Royal Haskoning.

Keller, G. H., & Richards, A. F. (1967). Sediments of the Malacca Strait, Southeast Asia. *Journal of Sedimentary Research, 37*(1).

Khan, M. J., Bhuyan, G., Iqbal, M. T., & Quaicoe, J. E. (2009). Hydrokinetic energy conversion systems and assessment of horizontal and vertical axis turbines for river and tidal applications: A technology status review. *Applied Energy, 86*(10), 1823-1835. doi: http://dx.doi.org/10.1016/j.apenergy.2009.02.017

Kim, G., Lee, M. E., Lee, K. S., Park, J. S., Jeong, W. M., Kang, S. K., . . . Kim, H. (2012). An overview of ocean renewable energy resources in Korea. *Renewable & Sustainable Energy Reviews, 16*(4), 2278-2288. doi: DOI 10.1016/j.rser.2012.01.040

Kirschwink, J. L. (1997). Magnetoreception - Homing in on vertebrates. *Nature, 390*(6658), 339-340. doi: Doi 10.1038/36986

Kofoed, J. P., Frigaard, P., Friis-Madsen, E., & Sørensen, H. C. (2006). Prototype testing of the wave energy converter wave dragon. *Renewable energy, 31*(2), 181-189.

Koh, S., & Lim, Y. (2008). *Malaysia, Preliminary investigation of the potential of harnessing tidal energy for electricity generation in.* Paper presented at the 2008 IEEE/Pres Transmission and Distribution Conference and Exposition.

Kong, F. K., Zhu, Y. W., & Li, Y. T. (2014). Structural Analysis of Horizontal Tidal Current Turbine Main Shaft. *Key Engineering Materials, 572*, 32-35.

Koo, C. H., Mohammad, A. W., Suja', F., & Meor Talib, M. Z. (2012). Review of the effect of selected physicochemical factors on membrane fouling propensity based on fouling indices. *Desalination, 287*(0), 167-177. doi: http://dx.doi.org/10.1016/j.desal.2011.11.003

Kvale, E. P. (2006). The origin of neap–spring tidal cycles. *Marine Geology, 235*(1), 5-18.

Lam, W., Bhatia, A., Cao, Y., Roy, C. B., Chen, L., Chu, Y. J., . . . Ng, K. W. (2013, 6th June). *Opportubities and challenges of Marine Current Energy in The Straits of Malacca.* Paper presented at the proceedings of 1st Malaysian Ocean Renewable Energy Symposium, Putrajaya.

Langhamer, O., Wilhelmsson, D., & Engstrom, J. (2009). Artificial reef effect and fouling impacts on offshore wave power foundations and buoys - a pilot study. *Estuarine Coastal and Shelf Science, 82*(3), 426-432. doi: DOI 10.1016/j.ecss.2009.02.009

Legrand, C. (2009). *Assessment of Tidal Energy Resource: Marine Renewable Energy Guides*: European Marine Energy Centre.

Leijon, M., Danielsson, O., Eriksson, M., Thorburn, K., Bernhoff, H., Isberg, J., . . . Ågren, O. (2006). An electrical approach to wave energy conversion. *Renewable Energy, 31*(9), 1309-1319.

Li, Y., & Calisal, S. M. (2010). Three-dimensional effects and arm effects on modeling a vertical axis tidal current turbine. *Renewable energy, 35*(10), 2325-2334.

Li, Y., Karri, N., & Wang, Q. (2014). Three-dimensional numerical analysis on blade response of a vertical-axis tidal current turbine under operational conditions. *Journal of Renewable and Sustainable Energy, 6*(4), 043123.

Masden, E. A., Haydon, D. T., Fox, A. D., Furness, R. W., Bullman, R., & Desholm, M. (2009). Barriers to movement: impacts of wind farms on migrating birds. *Ices Journal of Marine Science, 66*(4), 746-753. doi: DOI 10.1093/icesjms/fsp031

Matheson, D., & Thomson, S. (1973). Geological implications of valley rebound. *Canadian Journal of Earth Sciences, 10*(6), 961-978.

Mellor, G. (2004). Users guide for a three-dimensional, primitive equation, numerical ocean model. Princeton University, Princeton, NJ 08 544-0710: Program in the Atmospheric and Oceanic Sciences.

Mellor, G., Oey, L., & Ezer, T. (1998). Sigma coordinate pressure gradient errors and the seamount problem. *Journal of Atmospheric and Oceanic Technology, 15*(5), 1122-1131.

Mitigation, C. C. (2011). IPCC special report on renewable energy sources and climate change mitigation.

Myers, L., & Bahaj, A. (2012). An experimental investigation simulating flow effects in first generation marine current energy converter arrays. *Renewable Energy, 37*(1), 28-36.

Myers, L., & Bahaj, A. S. (2005). Simulated electrical power potential harnessed by marine current turbine arrays in the Alderney Race. *Renewable Energy, 30*(11), 1713-1731. doi: DOI 10.1016/j.renene.2005.02.008

Myers, L., Keogh, B., & Bahaj, A. (2011). *Experimental investigation of inter-array wake properties in early tidal turbine arrays.* Paper presented at the OCEANS 2011.

Myers, L. E., & Bahaj, A. S. (2010). Experimental analysis of the flow field around horizontal axis tidal turbines by use of scale mesh disk rotor simulators. *Ocean Engineering, 37*(2-3), 218-227. doi: DOI 10.1016/j.oceaneng.2009.11.004

National-Hydrographic-Centre. (2012). *JADUAL PASANG SURUT*.

Negro, V., López-Gutiérrez, J.-S., Esteban, M. D., & Matutano, C. (2014). Uncertainties in the design of support structures and foundations for offshore wind turbines. *Renewable Energy, 63*, 125-132.

Polagye, B. (2010a). *Environmental effects of tidal energy.* Paper presented at the Renewable Ocean Energy and the Marine Environment, FL.

Polagye, B. (2010b). *Environmental effects of tidal energy development* Paper presented at the A scientific workshop, Seattle, Washington.

Ponta, F., & Shankar Dutt, G. (2000). An improved vertical-axis water-current turbine incorporating a channelling device. *Renewable Energy, 20*(2), 223-241.

Ramos, V., Carballo, R., Álvarez, M., Sánchez, M., & Iglesias, G. (2014). A port towards energy self-sufficiency using tidal stream power. *Energy, 71*(0), 432-444.

Rashid, A. (2012). Status and potentials of tidal in-stream energy resources in the southern coasts of Iran: A case study. *Renewable and Sustainable Energy Reviews, 16*(9), 6668-6677. doi: http://dx.doi.org/10.1016/j.rser.2012.08.010

Redden, A. (2010). *Tidal energy developments in Canada making progress and looking forward.* Paper presented at the Renewable Ocean energy and the Marine environment, Palm Beach Gardens,FL.

Rizal, S., Damm, P., Wahid, M. A., Sundermann, J., Ilhamsyah, Y., Iskandar, T., & Muhammad. (2012). General Circulation in the Malacca Strait and Andaman Sea: A numerical model study. *American Journal of Environmental Science,, 8*(5), 479-488. doi: doi:10.3844/ajessp.2012.479.488

Rizal, S., Setiawan, I., Iskandar, T., Ilhamsyah, Y., Wahid, M. A., & Musman, M. (2010). Currents Simulation in the Malacca Straits by Using Three-Dimensional Numerical Model. *Sains Malaysiana, 39*(4), 519-524.

Rourke, F. O., Boyle, F., & Reynolds, A. (2010). Marine current energy devices: Current status and possible future applications in Ireland. *Renewable and Sustainable Energy Reviews, 14*(3), 1026-1036. doi: http://dx.doi.org/10.1016/j.rser.2009.11.012

Saharuddin, A. H., Ali, A., Lokman, M. H., & Salihin, W. (2012, 21-24 May 2012). *Recent development and management of artificial reefs (ARs) in Malaysia.* Paper presented at the OCEANS, 2012 - Yeosu.

Sakmani, A., Lam, W., Hashim, R., & Chong, H. (2013). Site selection for tidal turbine installation in the Straits of Malacca. *Renewable and Sustainable Energy Reviews, 21*, 590-602.

Sanz-Casado, E., Garcia-Zorita, J. C., Serrano-López, A. E., Larsen, B., & Ingwersen, P. (2013). Renewable energy research 1995–2009: a case study of wind power research in EU, Spain, Germany and Denmark. *Scientometrics, 95*(1), 197-224.

Sarma, N., Biswas, A., & Misra, R. (2014). Experimental and computational evaluation of Savonius hydrokinetic turbine for low velocity condition with comparison to Savonius wind turbine at the same input power. *Energy Conversion and Management, 83*, 88-98.

Schwartz, M. (2006). *Encyclopedia of coastal science*: Springer.

Scruggs, J., & Jacob, P. (2009). Harvesting ocean wave energy. *Science, 323*(5918), 1176-1178.

Shi, W., Park, H., Han, J., Na, S., & Kim, C. (2013). A study on the effect of different modeling parameters on the dynamic response of a jacket-type offshore wind turbine in the Korean Southwest Sea. *Renewable Energy, 58*, 50-59.

Small, A. A., Cook, G. K., & Brown, M. J. (2014). *The Geotechnical Challenges of Tidal Turbine Projects.* Paper presented at the ASME 2014 33rd International Conference on Ocean, Offshore and Arctic Engineering.

Smith, P. F. (2013). *Architecture in a Climate of Change*: Routledge.

Tang, C. F. (2008). A re-examination of the relationship between electricity consumption and economic growth in Malaysia. *Energy Policy, 36*(8), 3077-3085. doi: http://dx.doi.org/10.1016/j.enpol.2008.04.026

Vennell, R. (2010). Tuning turbines in a tidal channel. *Journal of Fluid Mechanics, 663*, 253-267. doi: Doi 10.1017/S0022112010003502

Vennell, R. (2011a). Estimating the power potential of tidal currents and the impact of power extraction on flow speeds. *Renewable Energy, 36*(12), 3558-3565. doi: DOI 10.1016/j.renene.2011.05.011

Vennell, R. (2011b). Tuning tidal turbines in-concert to maximise farm efficiency. *Journal of Fluid Mechanics, 671*, 587-604. doi: Doi 10.1017/S0022112010006191

Vennell, R. (2012a). The energetics of large tidal turbine arrays. *Renewable Energy, 48*, 210-219.

Vennell, R. (2012b). Realizing the potential of tidal currents and the efficiency of turbine farms in a channel. *Renewable Energy, 47*, 95-102. doi: DOI 10.1016/j.renene.2012.03.036

Vennell, R. (2013). Exceeding the Betz limit with tidal turbines. *Renewable Energy, 55*, 277-285. doi: DOI 10.1016/j.renene.2012.12.016

Walters, R. A., Tarbotton, M. R., & Hiles, C. E. (2013). Estimation of tidal power potential. *Renewable Energy, 51*, 255-262.

Wang, S., Yuan, P., Li, D., & Jiao, Y. (2011). An overview of ocean renewable energy in China. *Renewable and Sustainable Energy Reviews, 15*(1), 91-111.

Wilhelmsson, D., & Malm, T. (2008). Fouling assemblages on offshore wind power plants and adjacent substrata. *Estuarine Coastal and Shelf Science, 79*(3), 459-466. doi: DOI 10.1016/j.ecss.2008.04.020

Williamson, B. J., Blondel, P., Armstrong, E., Bell, P. S., Hall, C., Waggitt, J. J., & Scott, B. E. (2015). A Self-Contained Subsea Platform for Acoustic Monitoring of the Environment Around Marine Renewable Energy Devices–Field Deployments at Wave and Tidal Energy Sites in Orkney, Scotland.

Work, P. A., Haas, K. A., Defne, Z., & Gay, T. (2013). Tidal stream energy site assessment via three-dimensional model and measurements. *Applied Energy, 102*(0), 510-519. doi: http://dx.doi.org/10.1016/j.apenergy.2012.08.040

Wyrtki, K. (1961). Physical Oceanography of the Southeast Asian waters. UC San Diego: Scripps Institution of Oceanography.

Yang, Z., Wang, T., & Copping, A. E. (2013). Modeling tidal stream energy extraction and its effects on transport processes in a tidal channel and bay system using a three-dimensional coastal ocean model. *Renewable Energy, 50*, 605-613. doi: 10.1016/j.renene.2012.07.024

Yin, L. L., Lo, K. H., & Wang, S. S. (2014). *Structural Dynamics and Load Analysis of Large Offshore Wind Turbines in Western Gulf of Mexico Shallow Water.* Paper presented at the ASME 2014 33rd International Conference on Ocean, Offshore and Arctic Engineering.

LIST OF PUBLICATIONS AND PAPERS PRESENTED

Lam, W. H., & Roy, C. B. (2014). Insights into the Ocean Health Index for marine renewable energy. *Renewable and Sustainable Energy Reviews*. (Q1)(ISI Cited).

CB Roy**,** KW Ng, WH Lam, R Hashim (2013), Potential Site for Tidal Current Turbine (TCT) in West Coast of Peninsula Malaysia: A Case Study of Pangkor Island, *Malaysian Journal of Science* 32 (SCS Sp Issue): 317-324. (SCOPUS-Cited Publication).

Roy, C. B., & Lam, W. (2013). Harnessing Tidal Stream Energy In Southeast Asia. Paper presented at the *IEEE International Conference on Renewable Energy and Sustainable Energy ICRESE13*., Coimbatore.

Wei-Haur Lam, Aalisha Bhatiaa, Yuhe Cao, Chandra Bhushan Roy, Long Chen, Yung-Jeh Chu, Cindy Soon, Xin-Le Lim, Kai-Wern Ng (2013) Opportunities and challenges of marine current energy in the Straits of Malacca, *1st Malaysian Ocean Renewable Energy Symposium, Maritime Centre, Putrajaya*, 6 June 2013. (Non-ISI/Non-SCOPUS Cited Publication)

APPENDICES

Appendix A: Source of POM model

Princeton Ocean Model used in this study was downloaded from following link which is supported by Princeton University:

Home Page: http://www.ccpo.odu.edu/POMWEB/

Download code: http://www.ccpo.odu.edu/POMWEB/userinfo.htm

In addition to above links user can also download other versions of POM code based on the requirement:

POM-Wave Model:

http://www.aos.princeton.edu/WWWPUBLIC/PROFS/pom_codes/nearshorepom/

POM-MPI (Parallel Version):

http://www.aos.princeton.edu/WWWPUBLIC/PROFS/DownloadCodes.html

POM used netCDF data format for input and output files. It can be generated by using netCDF library available from Unidata (http://www.unidata.ucar.edu/software/netcdf/).

Following Visualization Tools were used to explore input and output results:

- MATLAB based visualization using Matlan-2012b to read and write netCDF data format. POM model takes input in netCDF file format set by researchers.
- ncView (net).
- ArcView.

Appendix B: Source of Satellite Data

This study used numerous open source data sources for obtaining satellite data. Satellite data was used to create numerical bathymetry for the Straits of Malacca.

Further, sea surface temperature (SST), salinity, heat radiation, tidal elevation, and tidal period were used to create initial and boundary condition file for running the POM model.

Satellite data were obtained from the links given in table A1:

Table A1: Download links for obtaining satellite data

Variable	Download Link
Bathymetry (sea bed topography)	http://maps.ngdc.noaa.gov/viewers/wcs-client/
Oceanic data (SSS,SST, ρ, radiation. etc)	http://iridl.ldeo.columbia.edu/
Surface Wind	http://apps.ecmwf.int/datasets/data/interim_full_daily/
Tide	http://volkov.oce.orst.edu/tides/